ESA 6th Advanced Training Course on Radar Polarimetry

UNDERSTANDING 3D SAR TOMOGRAPHY

Stefano Tebaldini
Politecnico di Milano

Laurent Ferro-Famil
*Université de Rennes 1, Centre **d'Etudes** Spatiales de la Biosphère*

ESA UNCLASSIFIED – For ESA Official Use Only

Synthetic Aperture Radar Imaging

Synthetic Aperture Radar (SAR) technology has increasingly been shaping spaceborne remote sensing in the last years

1978-1995 *SEASAT, ERS-1/2, RADARSAT, SIR-C/X, J-ERS-1*

2000 *SRTM*

2002 *ENVISAT*

2006 *ALOS*

2007 *CSK-1, CSK-2, TSX, RADARSAT-2*

2008 *CSK-3*

2010 *CSK-4, TDX*

2014 *ALOS-2, SENTINEL-1A*

2016 *SENTINEL-1B, GAOFEN-3*

2018 *SAOCOM-1A*

SAOCOM-1B, CSG-1-2

SENTINEL-1C

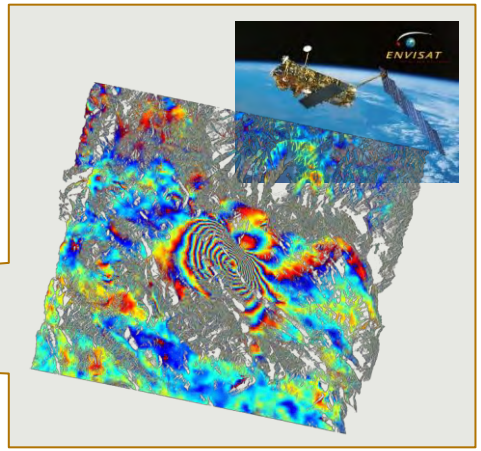

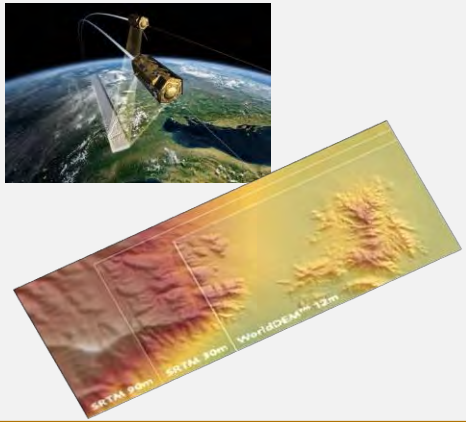

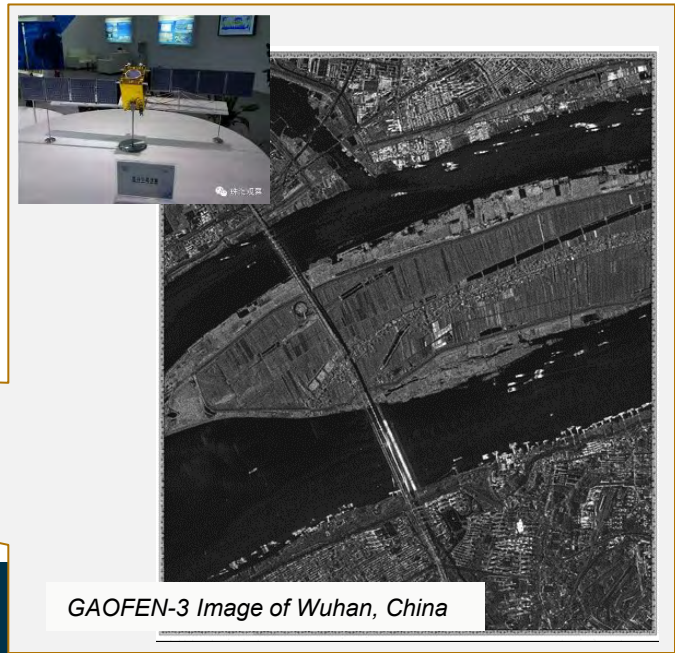

GAOFEN-3 Image of Wuhan, China

Synthetic Aperture Radar Imaging

SAR systems employ a RADAR sensor flown onboard a satellite platform to synthesize an antenna aperture as long as several kilometers

- Accurate measurement of Radar echoes backscattered from the targets as the system is flown along the satellite trajectory
- Image formation by Digital Processing techniques

⇒ The result is a high resolution **two-dimensional** map of the imaged scene

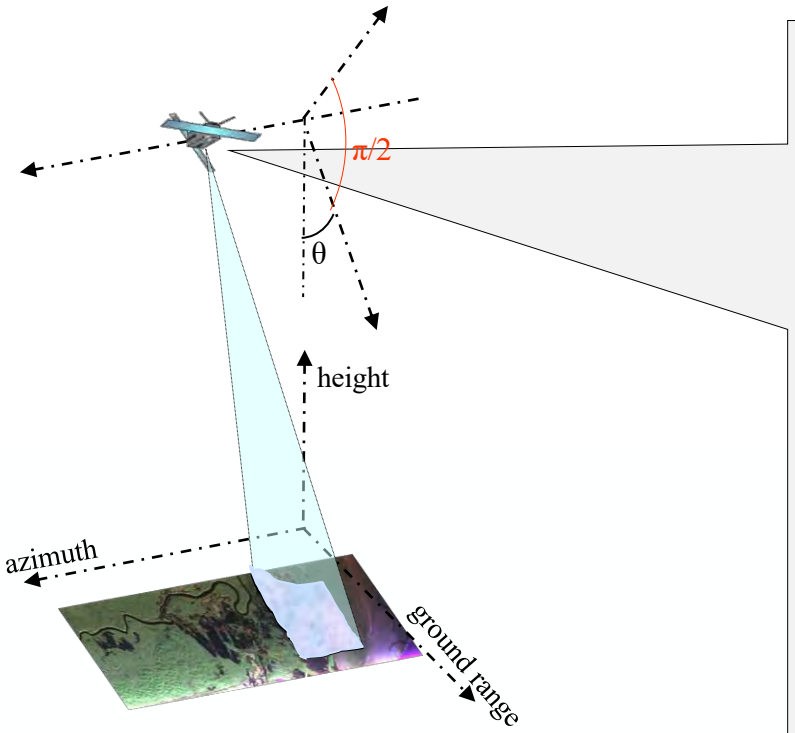

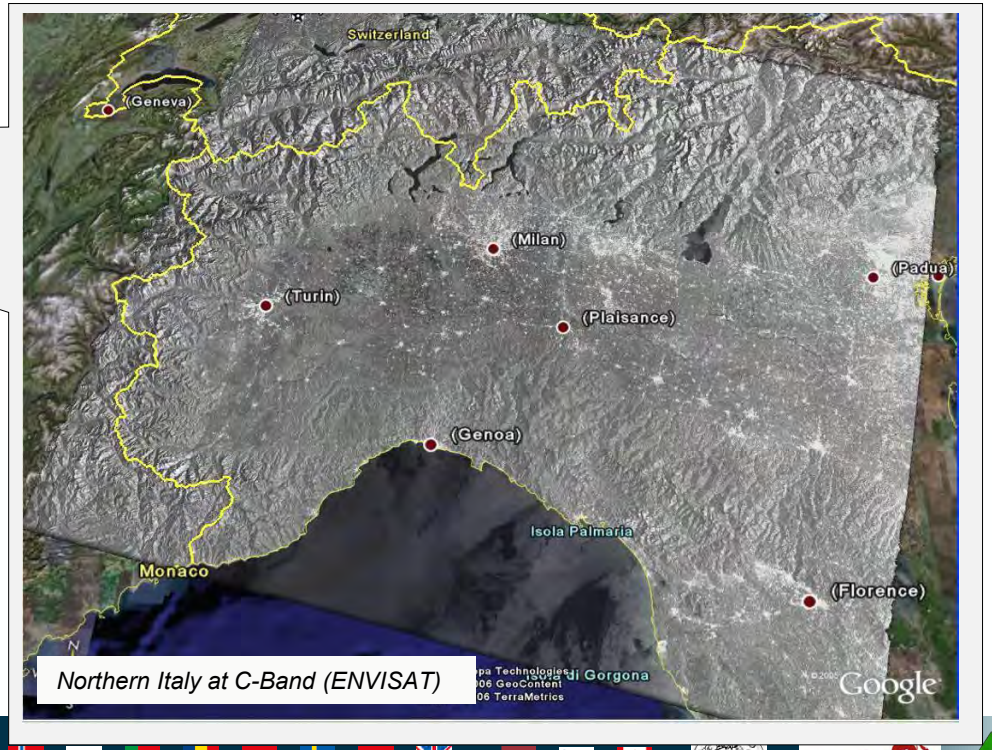

Northern Italy at C-Band (ENVISAT)

Synthetic Aperture Radar Imaging

Key features:

- Microwaves penetrate through rain and clouds ⇔ *visibility in all weather conditions*
- Aperture Synthesis ⇔ *fine spatial resolution*
- Phase preserving ⇔ *millimeter accuracy about distance variations*

⇨ Spaceborne SARs provide *accurate* and *continuous* information about the Earth's surface and its evolution over time

Topographic mapping

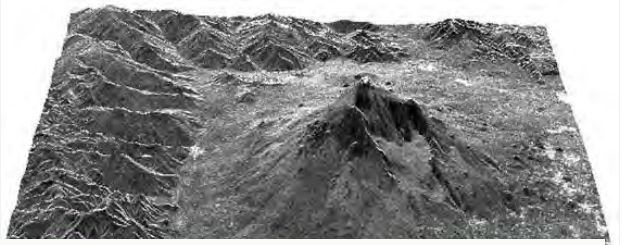

DEM of Mount Etna, Sicily, derived from ERS-1 (ESA)

Land mapping

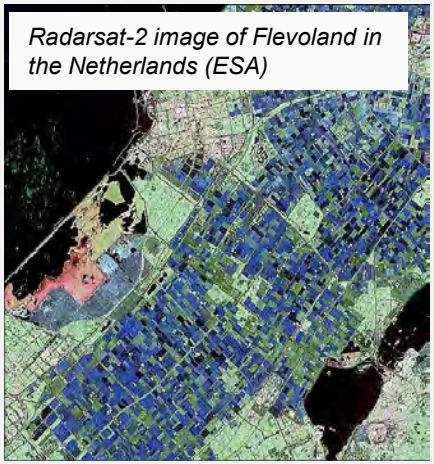

Radarsat-2 image of Flevoland in the Netherlands (ESA)

Change detection

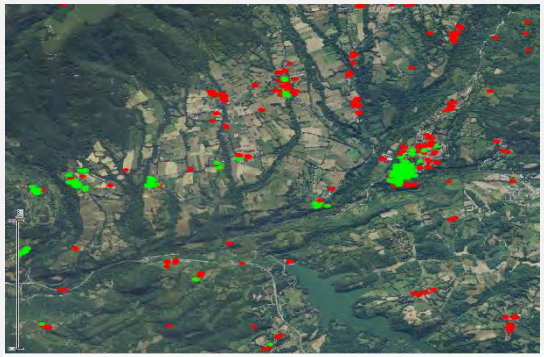

Post-earthquake change detection map in Amatrice, Italy, derived from Sentinel-1A (PoliMi)

Deformation monitoring

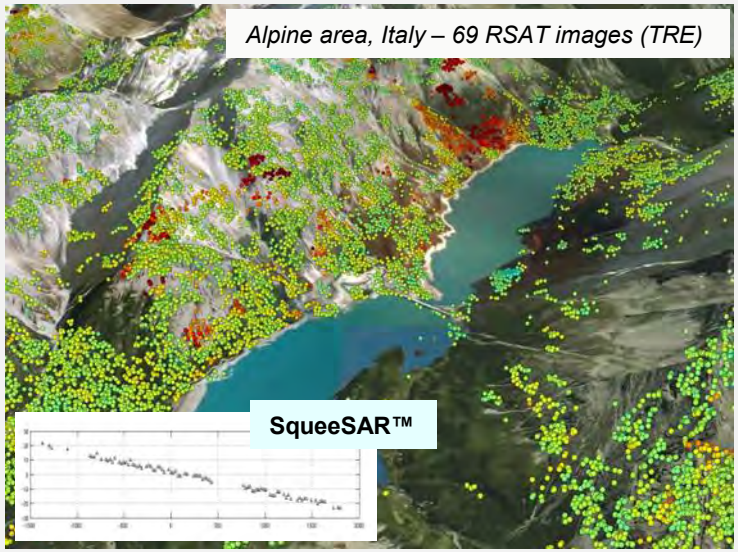

Alpine area, Italy – 69 RSAT images (TRE)

Synthetic Aperture Radar Imaging

Another key feature:

- Microwaves **penetrate** into natural media, like forests, snow, ice, sand ⇔ *sensitivity to the three-dimensional structure of illuminated media*

⇒ A single pixel within a SAR image is actually a mixture of different scattering mechanisms distributed over height

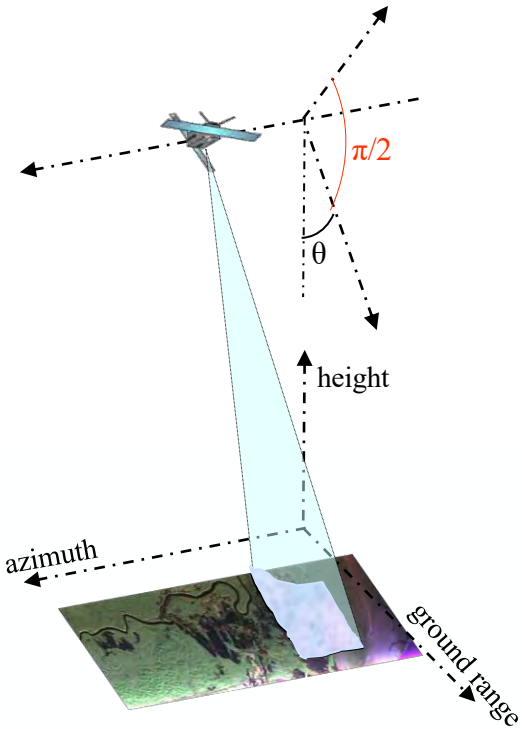

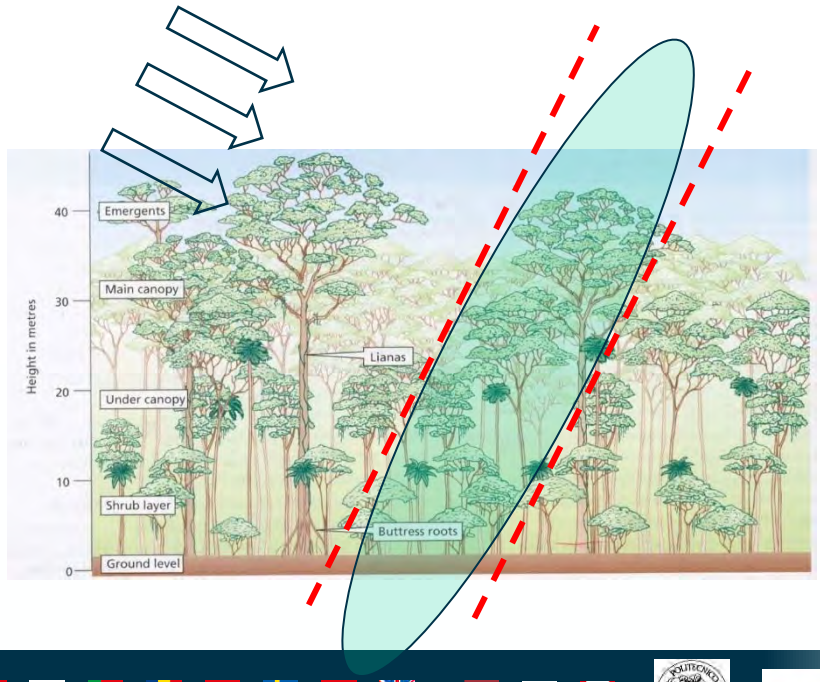

Tomographic SAR Imaging

TomoSAR systems employ a RADAR sensor flown along **multiple** trajectories

- Image formation by Digital Processing techniques

⇒ ***Three dimensional representation*** of Radar intensity at a given wavelength

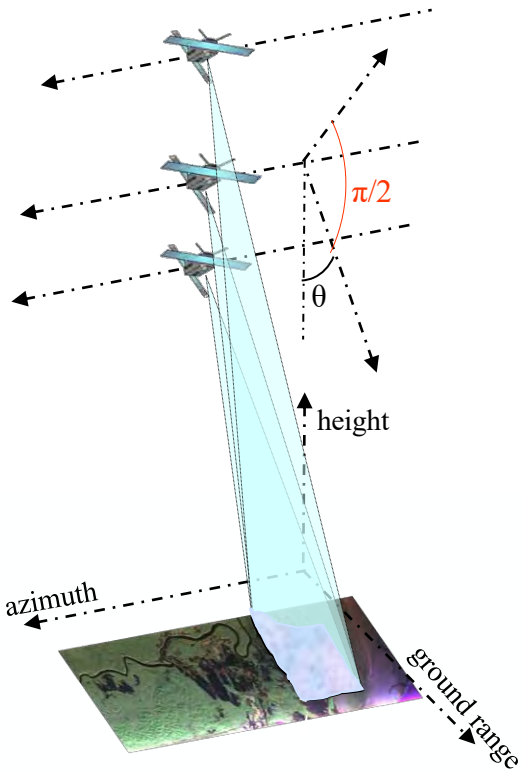

SAR produces pixels

TomoSAR produces voxels !!!

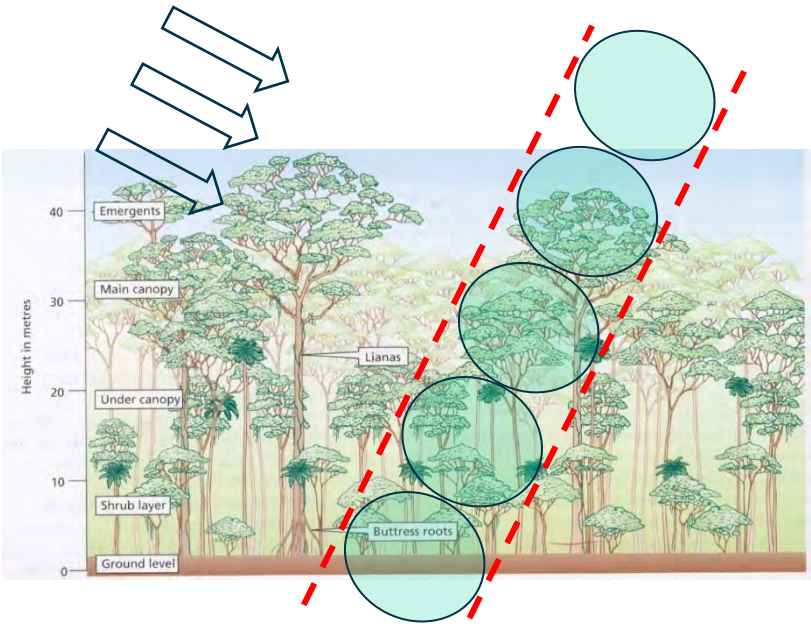

Tomographic SAR Imaging

TomoSAR systems employ a RADAR sensor flown along **multiple** trajectories

- Image formation by Digital Processing techniques

⇒ ***Three dimensional representation*** of Radar intensity at a given wavelength

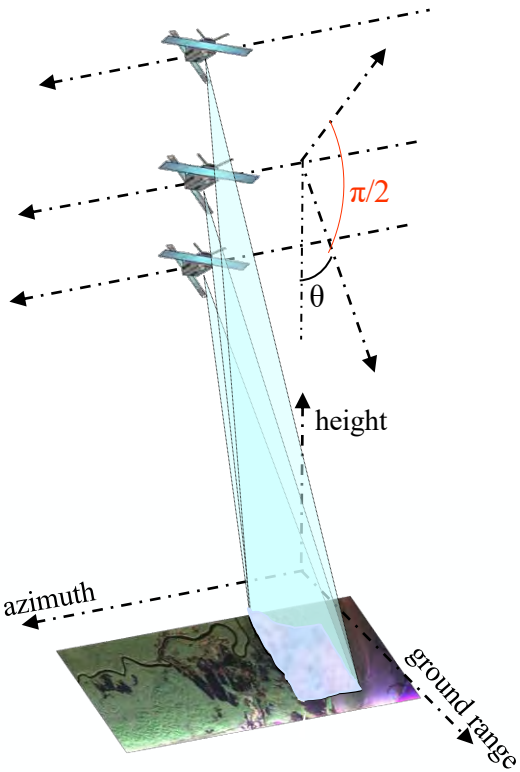

SAR produces pixels

TomoSAR produces voxels !!!

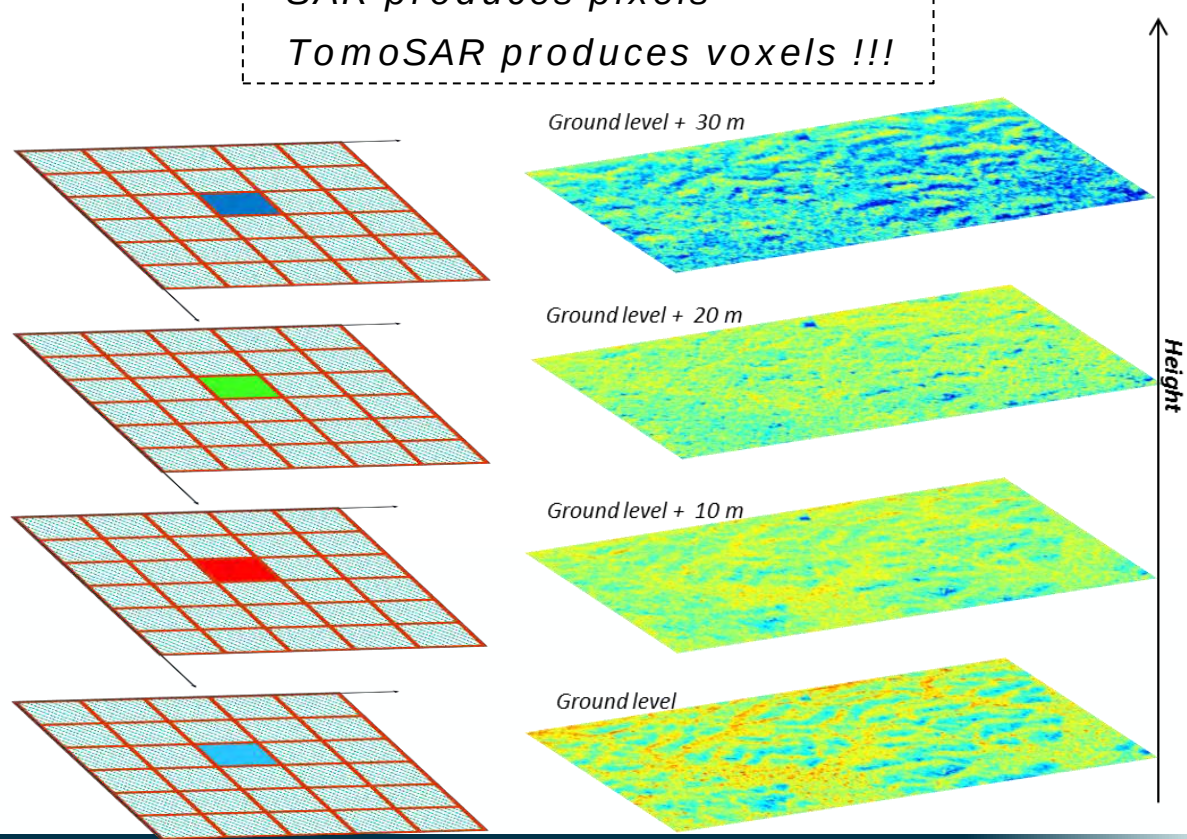

Tomographic SAR Imaging

TomoSAR systems employ a RADAR sensor flown along **multiple** trajectories

- Image formation by Digital Processing techniques

⇒ ***Three dimensional representation*** of Radar intensity at a given wavelength

SAR produces pixels

TomoSAR produces voxels !!!

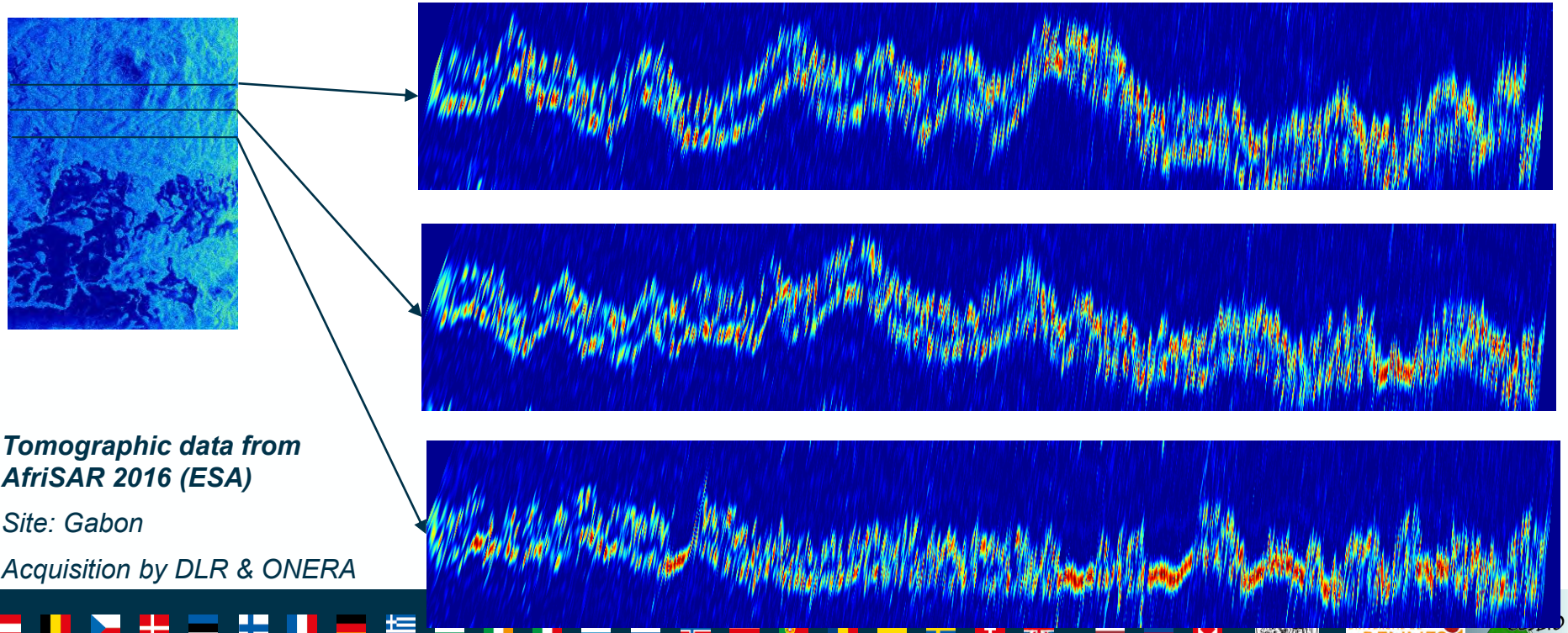

Tomographic data from AfriSAR 2016 (ESA)

Site: Gabon

Acquisition by DLR & ONERA

Tomographic SAR Imaging

***Forest scenarios**: separation of backscatter from different heights within the vegetation*

- ⇒ *Improved forest biomass retrieval*
- ⇒ *Sub-canopy terrain topography*
- ⇒ *Forest height*

The Paracou forest (French Guiana) at P-Band

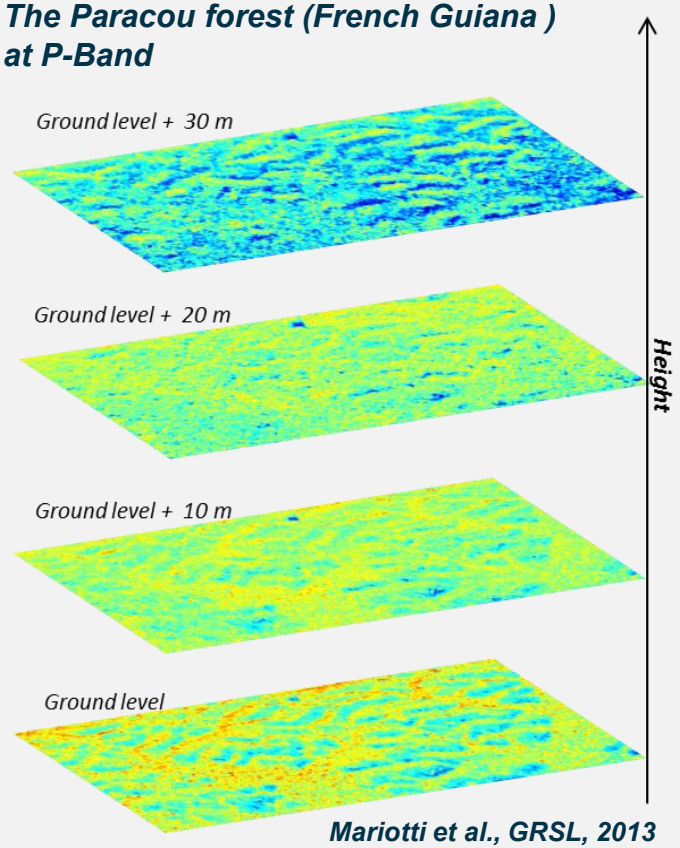

Mariotti et al., GRSL, 2013

Improved forest biomass retrieval

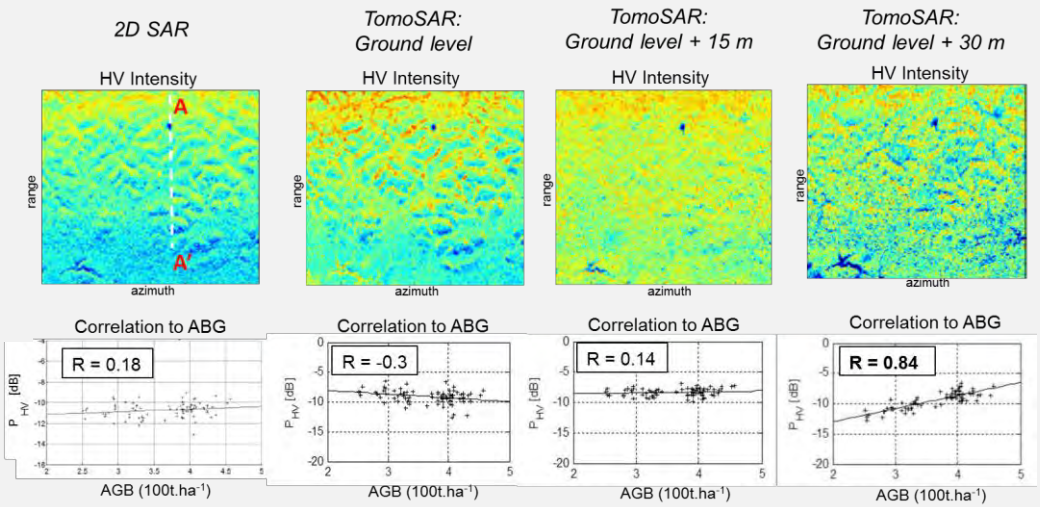

Ho Tong Minh et al., TGRS, 2014

Sub-canopy terrain topography

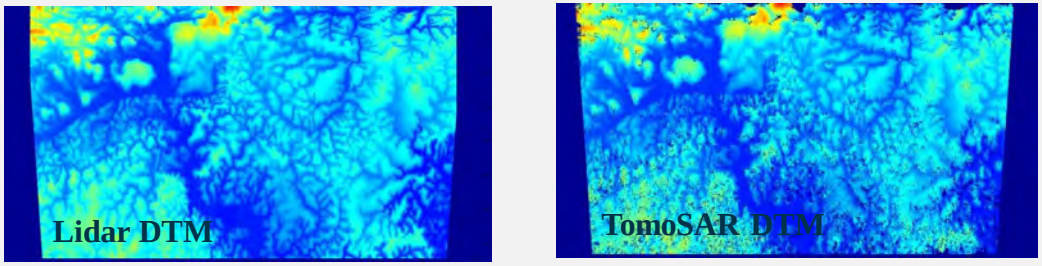

Tomographic SAR Imaging

***Glaciers**: inside view of the glacier volume*

- ⇒ *Bedrock detection up to 50 m below the ice surface*
- ⇒ *Detection of internal structures (crevasses, firn layering)*

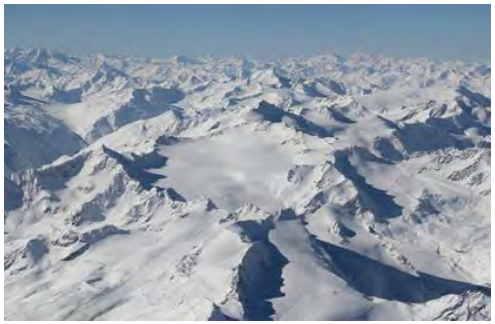

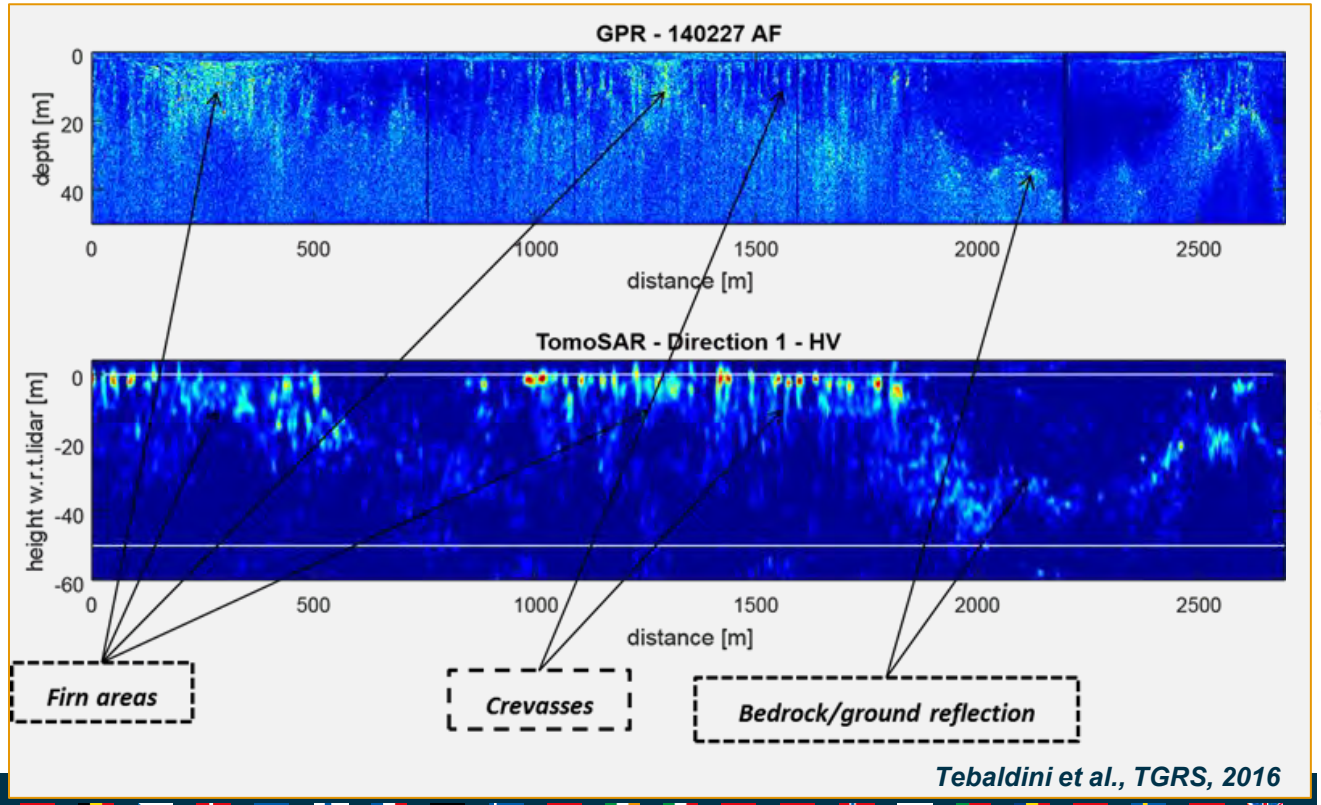

Tebaldini et al., TGRS, 2016

The Mittelbergferner (Austria) at L-Band

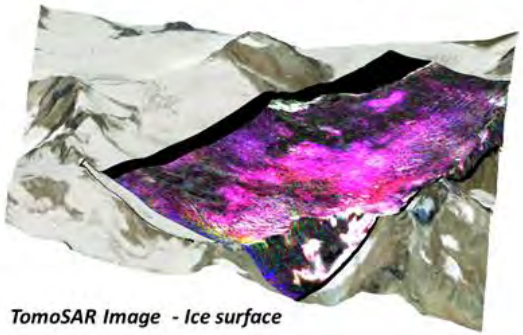

TomoSAR Image - Ice surface

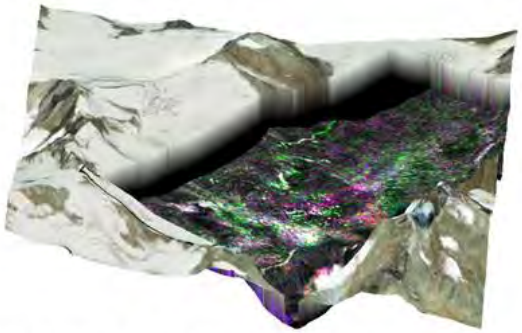

TomoSAR Image - 25 m below the Ice surface

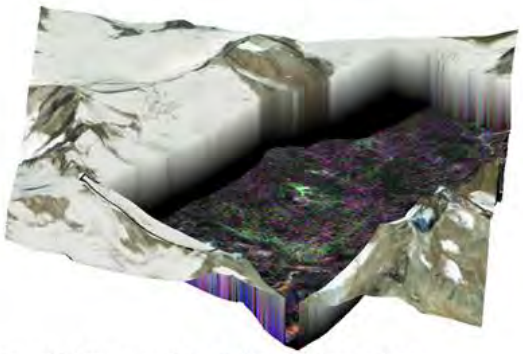

TomoSAR Image - 50 m below the Ice surface

Tomographic SAR Imaging

***Snow**: fine structure of snowpack layering*

⇒ *Total Snow depth*

⇒ *Refractive index*

⇒ *Internal layering*

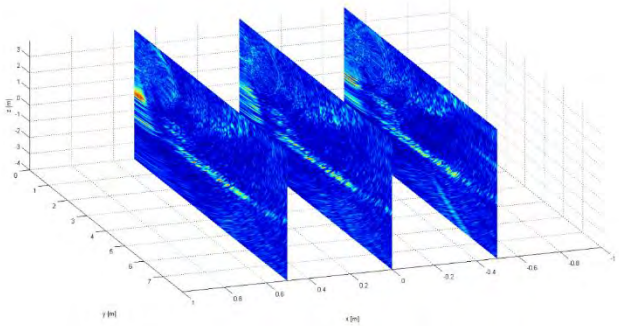

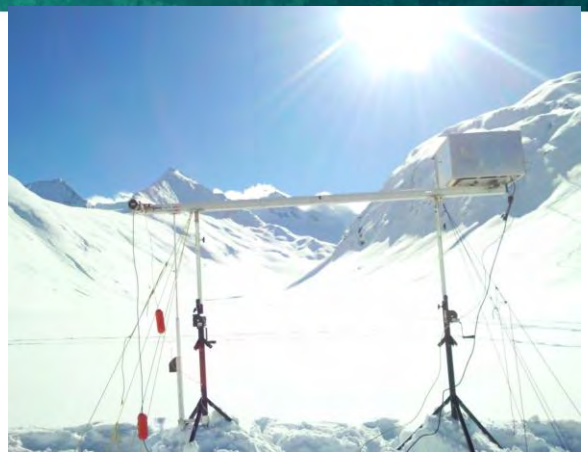

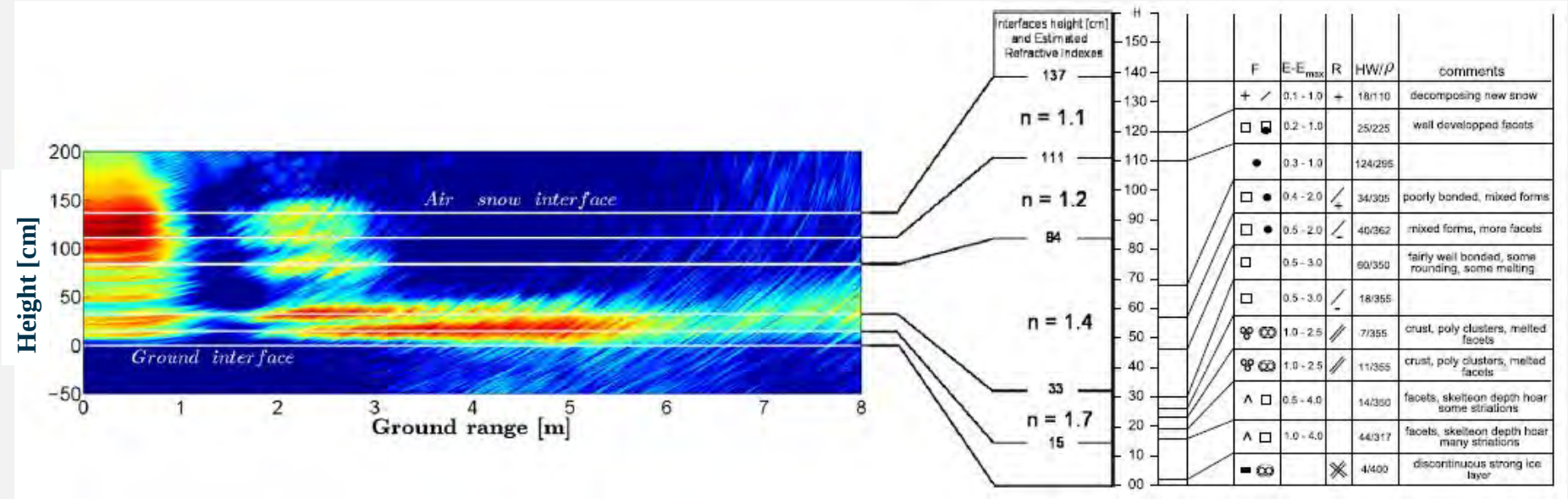

Rekioua et al., Comptes Rendus Physique , 2017

ESA 6th Advanced Training Course on Radar Polarimetry
UNDERSTANDING 3D SAR TOMOGRAPHY
Stefano Tebaldini
Politecnico di Milano
Laurent Ferro-Famil
Université de Rennes 1, Centre d'Etudes Spatiales de la Biosphère

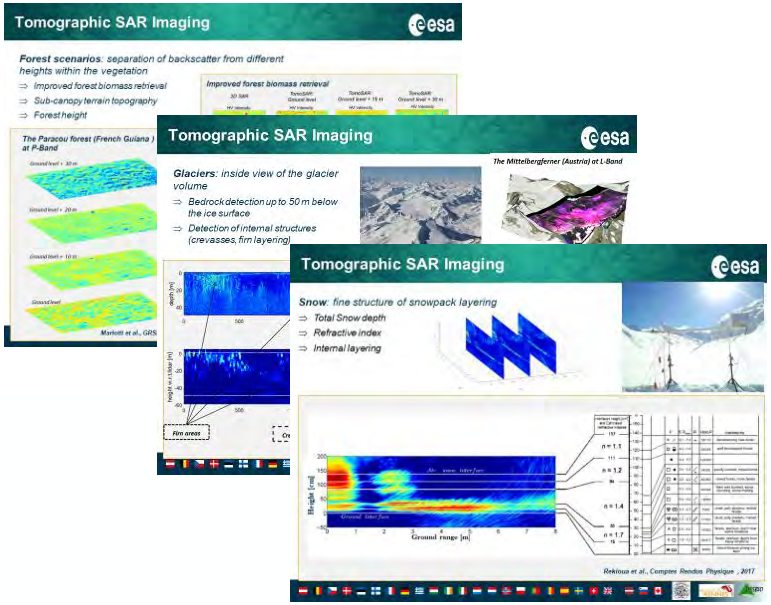
Tomographic SAR Imaging
Forest scenarios: separation of backscatter from different heights within the vegetation
⇒ Improved forest biomass retrieval
⇒ Sub-canopy terrain topography
⇒ Forest height
Improved forest biomass retrieval
The Paracou forest (French Guiana) at P-Band
Marlotti et al., GRS
Tomographic SAR Imaging
Glaciers: inside view of the glacier volume
⇒ Bedrock detection up to 50 m below the ice surface
⇒ Detection of internal structures (crevasses, firn layering)
The Mittelbergferner (Austria) at L-Band
Firn areas
Tomographic SAR Imaging
Snow: fine structure of snowpack layering
⇒ Total Snow depth
⇒ Refractive index
⇒ Internal layering
Ground range [m]
Rekioua et al., Comptes Rendus Physique, 2017

Answer:
Yes (☺), with a little help from:

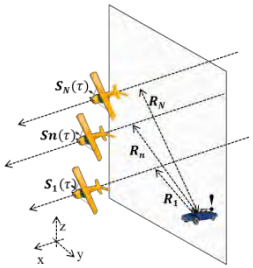

Geometry

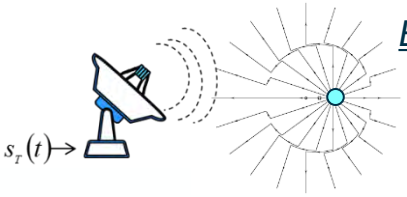

EM waves

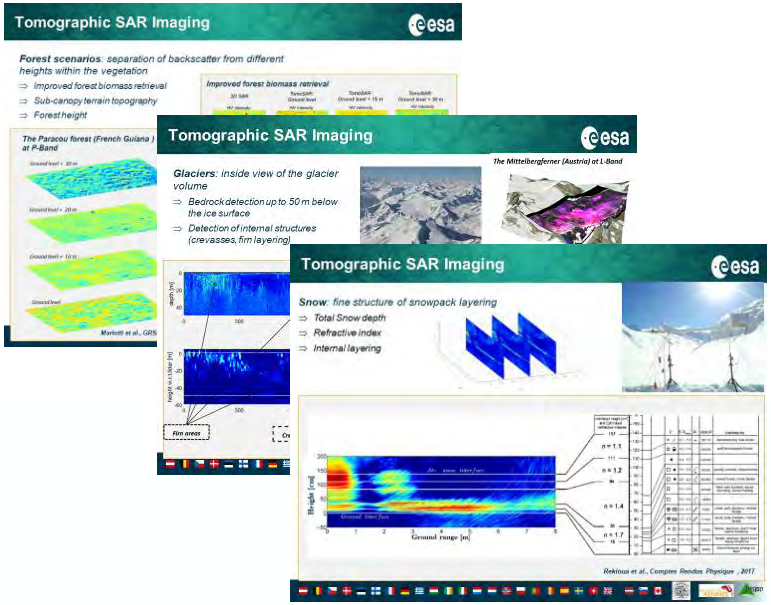

$$y_n(r,x) = \int s(r,x,v)\exp\left(-j\frac{4\pi}{\lambda r}b_n v\right)dv$$

Signal Processing

$$\mathbf{W} = E[\mathbf{y}\mathbf{y}^H] = \sum_{k=1}^{K}\mathbf{C}_k \otimes \mathbf{R}_k$$

Geometric principles of target localization

Localization in 1 D

RADAR (***Radio Detection And Ranging***) is a technology to detect and study far off targets by transmitting EM pulses at radiofrequency and observing the backscattered echoes

Transmission

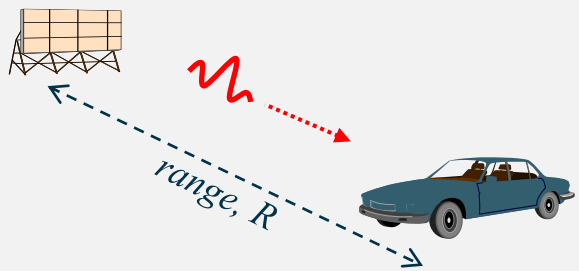

$$s_{Tx}(t) = s(t)$$

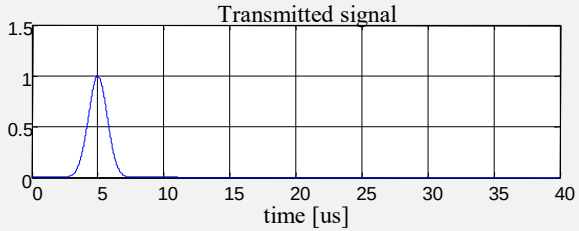

Reception

Signal delay

⇔

Sensor-to-target distance

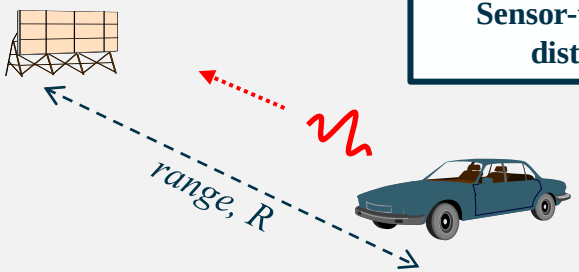

$$s_{Rx}(t) = s\left(t - \frac{2R}{c}\right)$$

r : sensor-to-target distance
c : speed of light

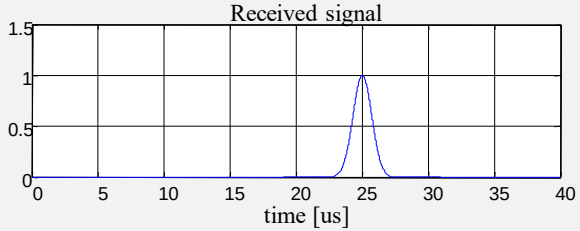

Localization in 1 D

Delay measurement ⇔ Localization on the surface of a sphere

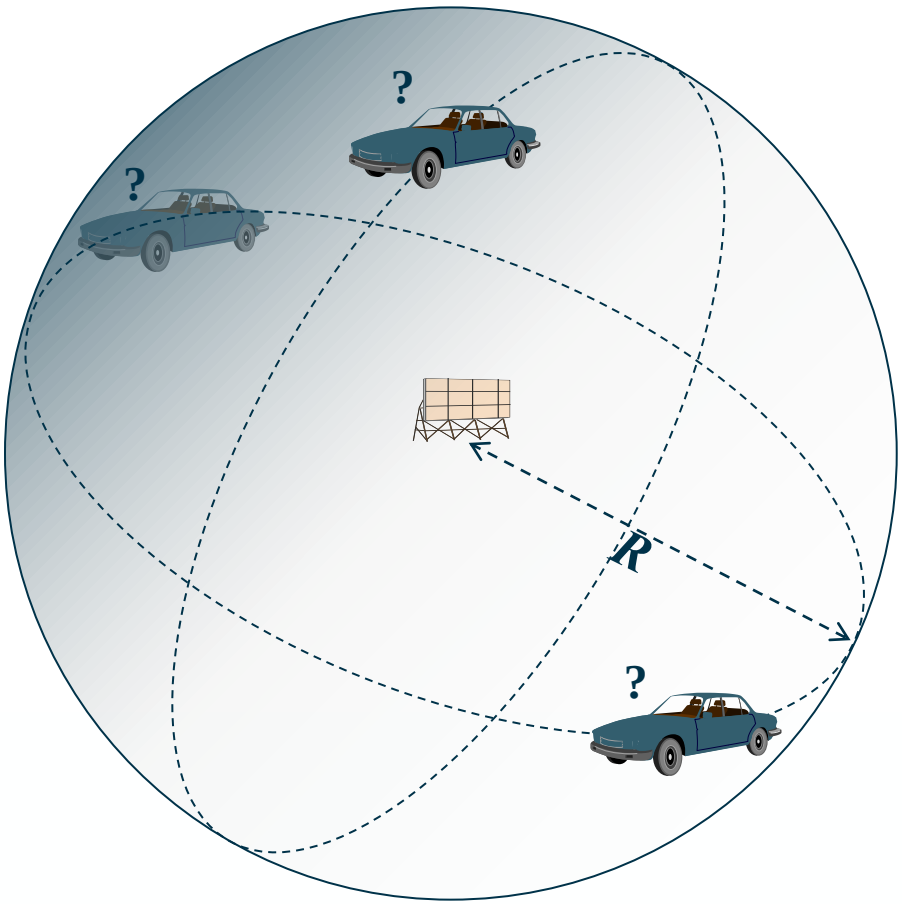

The target is bound to lie on a sphere

- o Centered on the RADAR
- o Of radius R

⇒ ***1D Localization***

Localization in 2D (SAR)

Flying a RADAR along a straight line = measuring the distance from the target to each point on the line

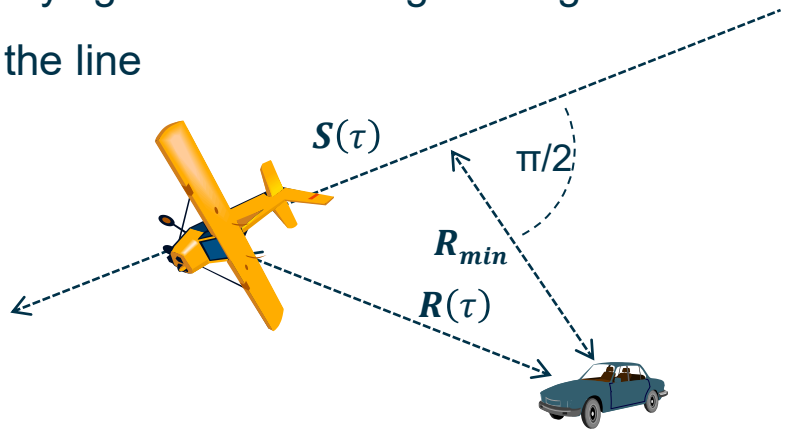

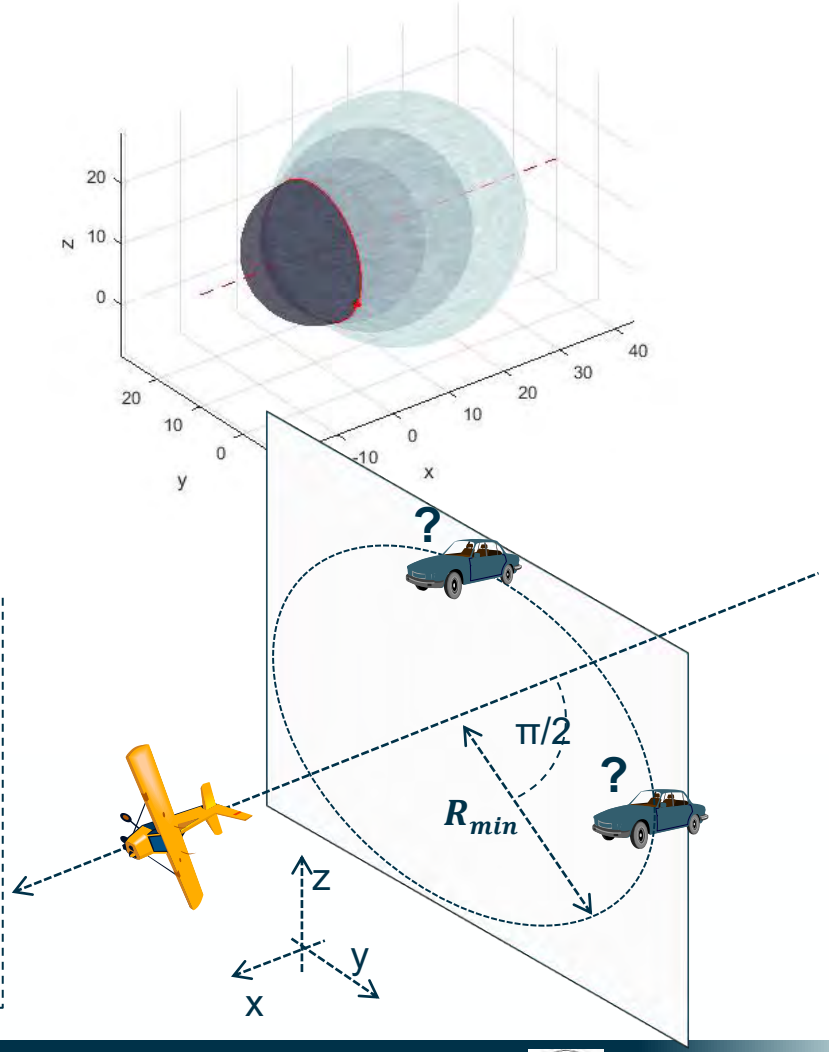

The target is bound to lie on the intersection of all the spheres:

- Centered in $S(\tau)$
- Of radius $R(\tau)$

$\Rightarrow$ The target is bound to lie on the circle:

- Centered on the trajectory
- Perpendicular to the trajectory (*yz* plane)
- Of radius R_{min}

$\Rightarrow$ 2D Localization

Localization in 3D (TomoSAR)

Flying a RADAR along multiple lines = measuring the distance from the target to multiple lines

The target is bound to lie on the circles:

- Centered on each trajectory
- Perpendicular to the trajectory ,
- Of radius $\boldsymbol{R_1} \ldots \boldsymbol{R_n} \ldots . \boldsymbol{R_N}$

⇒ Only 1 solution in the 3D space !

⇒ 3D localization

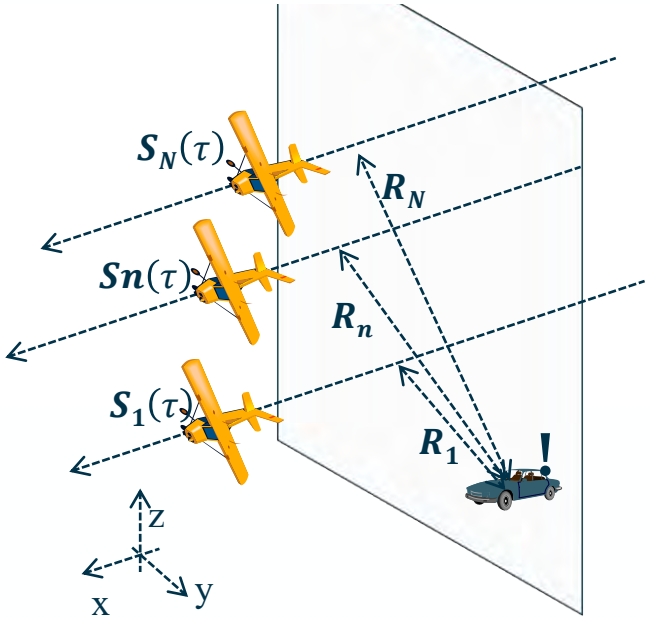

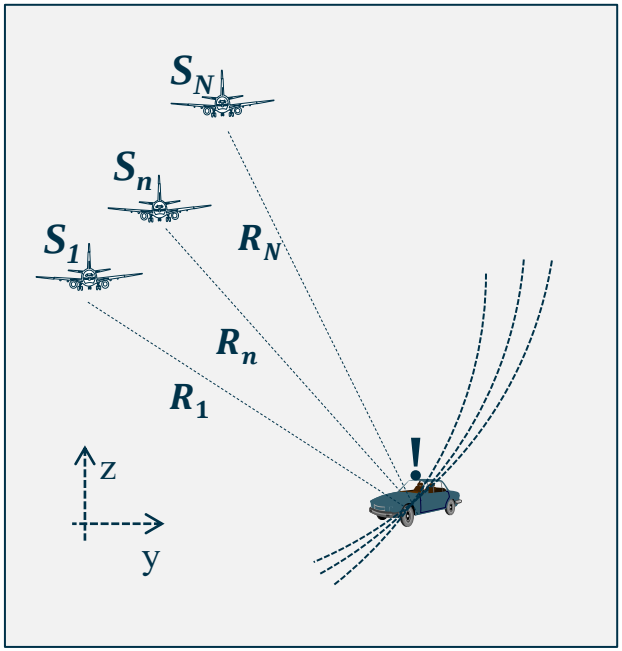

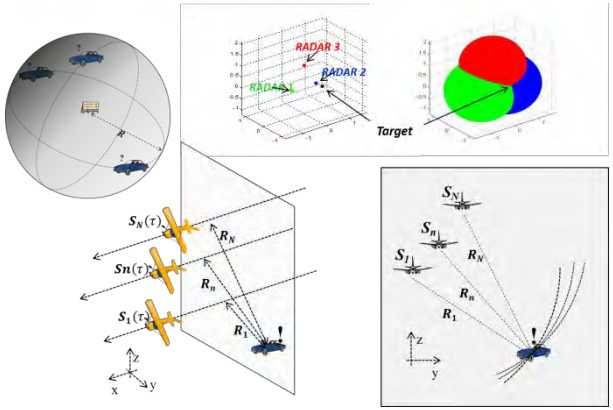

Geometry unveils the principle why flying multiple trajectories results in the capability to localize a target in the 3D space

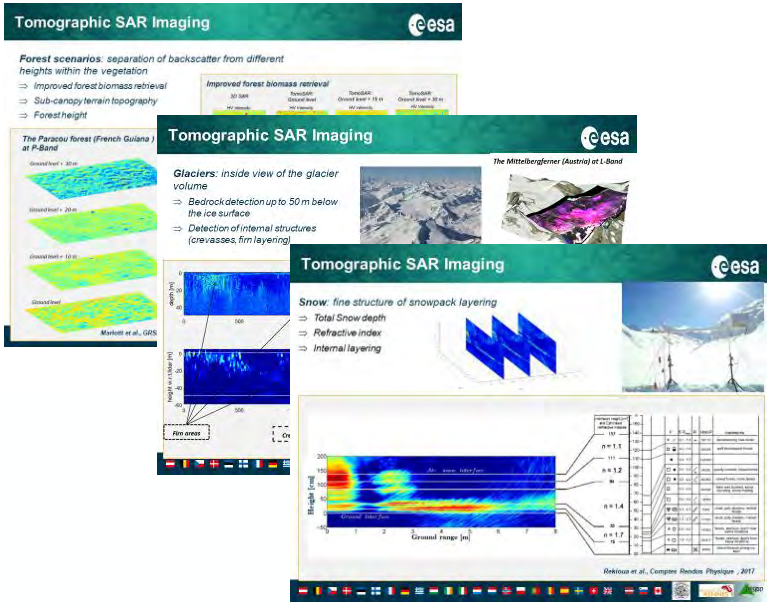

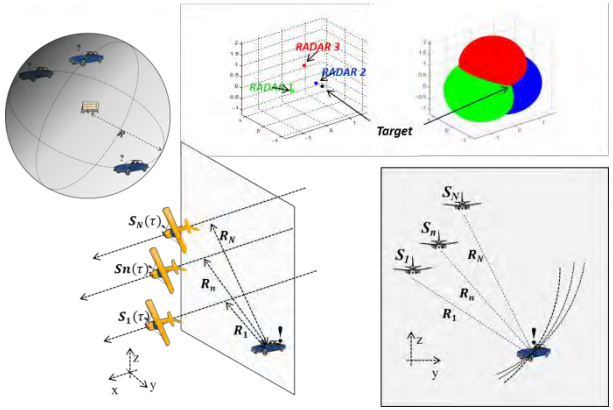

Geometry unveils the principle why flying multiple trajectories results in the capability to localize a target in the 3D space

Missing elements:

- *Resolution*
- *What if there are many targets ?!!!*

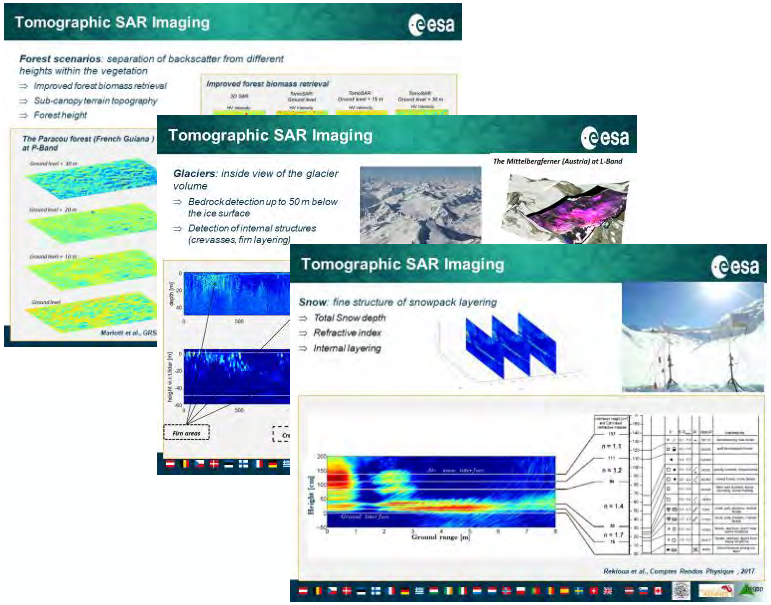

(Some) RADAR Signal processing

Radar signals

RADARs transmit and receive Radiofrequency (RF) pulses

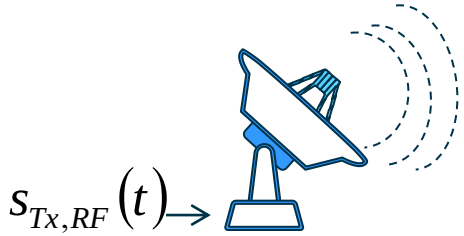

$$s_{Tx,RF}(t) = z(t) \cdot cos(2\pi f_0 t)$$

z(t) = baseband pulse
f_0 = carrier frequency

The received signal from a point target is a delayed version of the transmitted signal (amplitude factors omitted)

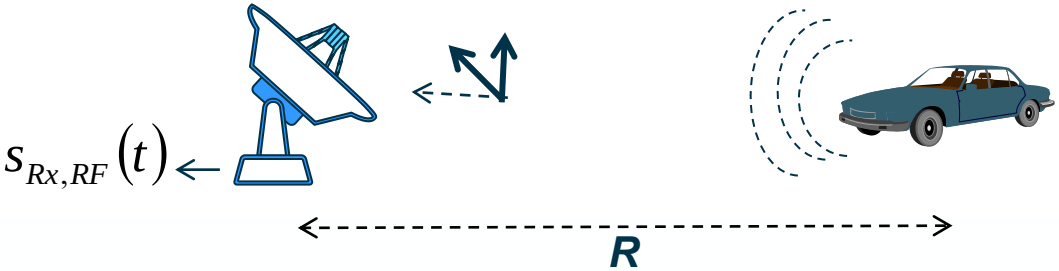

$$d = \frac{2R}{c}$$

$$s_{Rx,RF}(t) = s_{Tx,RF}(t-d) = z(t-d) \cdot cos\big(2\pi f_0 (t-d)\big)$$

Radar signals

The received RF signal is processed to form a complex signal

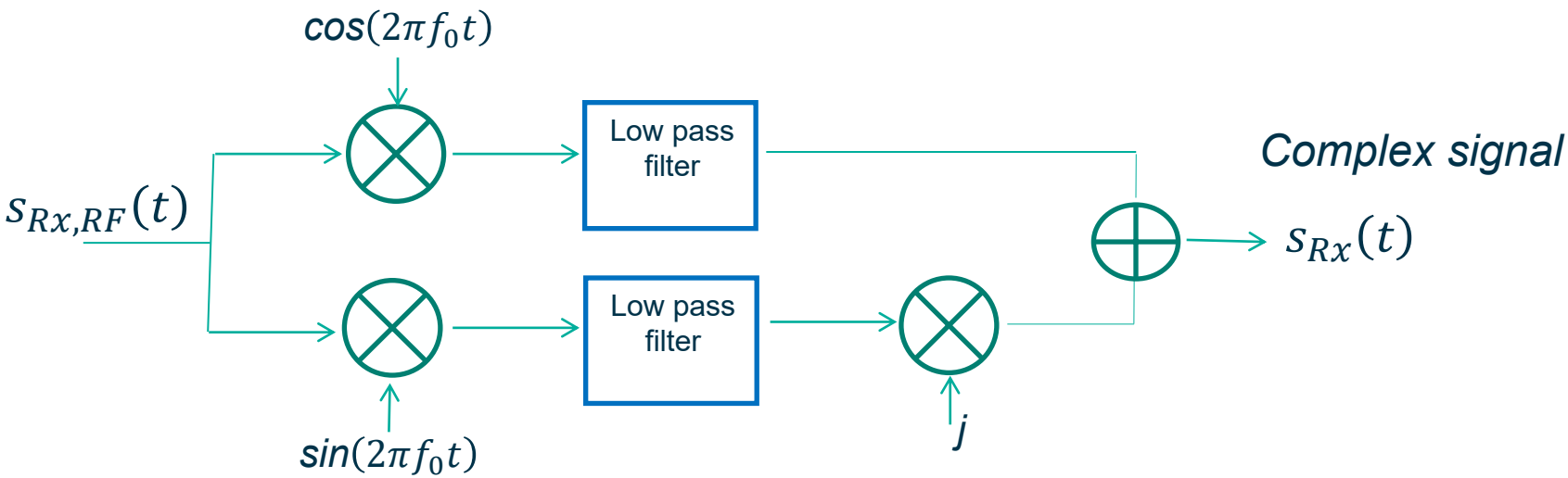

$$s_{Rx}(t) = z\left(t - \frac{2R}{c}\right) \cdot e^{-j\frac{4\pi}{\lambda}R}$$

Radar signals

The received RF signal is processed to form a complex signal

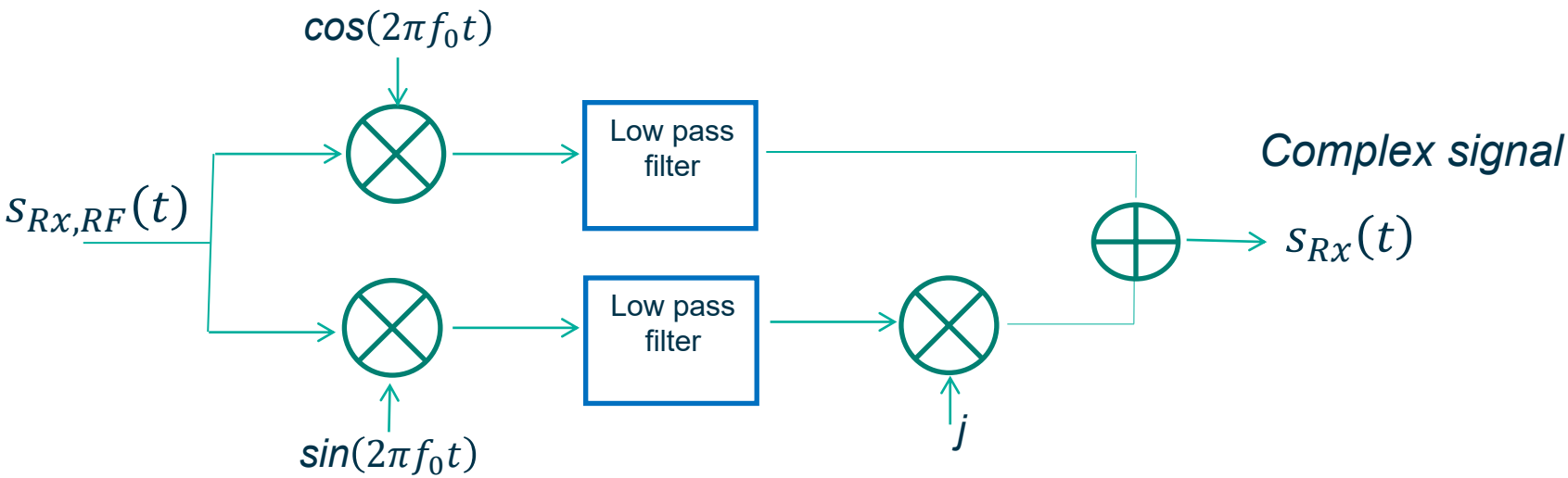

$$s_{Rx}(t) = z\left(t - \frac{2R}{c}\right) \cdot e^{-j\frac{4\pi}{\lambda}R}$$

Delayed pulse

Phase

Radar signals

The received RF signal is processed to form a complex signal

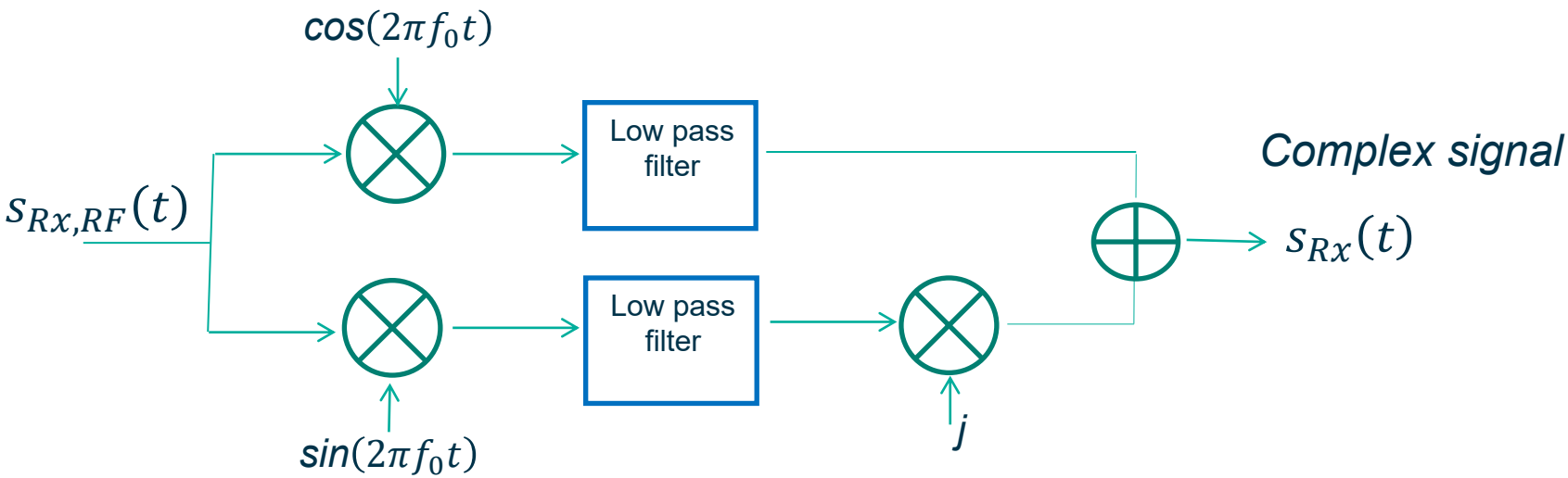

$$s_{Rx}(t) = z\left(t - \frac{2R}{c}\right) \cdot e^{-j\frac{4\pi}{\lambda}R}$$

Delayed pulse

Phase

Note: a complex signal is just a handy way to treat two signals at once!

$$Real(s_{Rx}(t)) = +z\left(t - \frac{2R}{c}\right) \cdot cos\left(\frac{4\pi}{\lambda}R\right)$$

$$Imag(s_{Rx}(t)) = -z\left(t - \frac{2R}{c}\right) \cdot sin\left(\frac{4\pi}{\lambda}R\right)$$

Localization in 1D – Range resolution

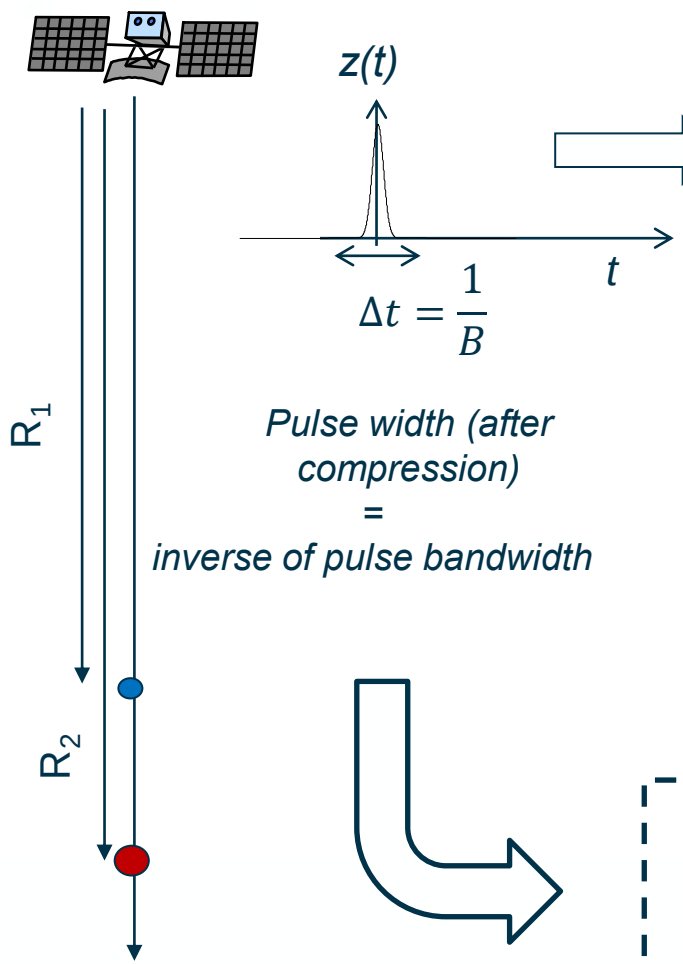

Pulse width (after compression)
=
inverse of pulse bandwidth

$$s_{Rx}(t) = A_1 z\left(t - \frac{2R_1}{c}\right) \cdot e^{-j\frac{4\pi}{\lambda}R_1} + A_2 z\left(t - \frac{2R_2}{c}\right) \cdot e^{-j\frac{4\pi}{\lambda}R_2}$$

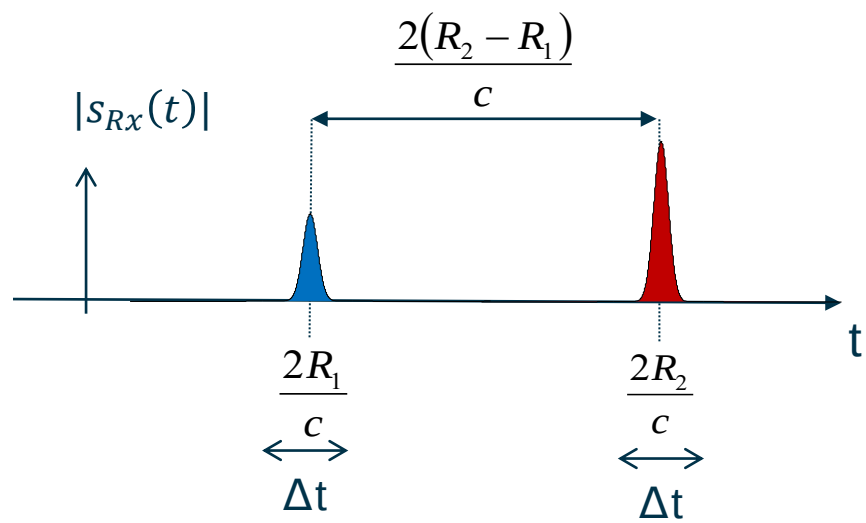

Two targets produce two distinct peaks as long as

$$|R_1 - R_2| \leq \Delta R = \frac{c}{2B}$$

(ΔR = range resolution)

Range resolution cell

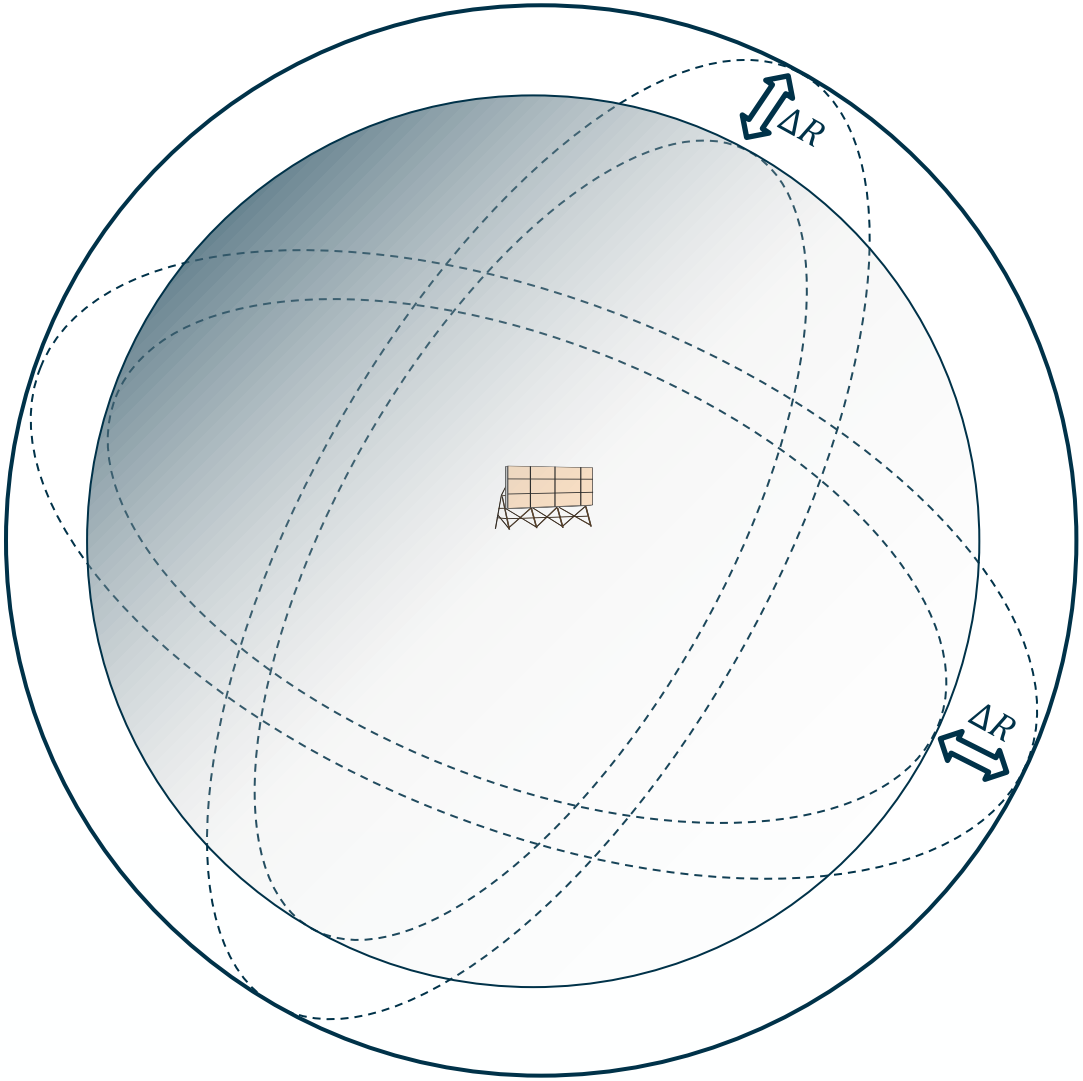

Range resolution cell
in the 3D space

Localization in 2D

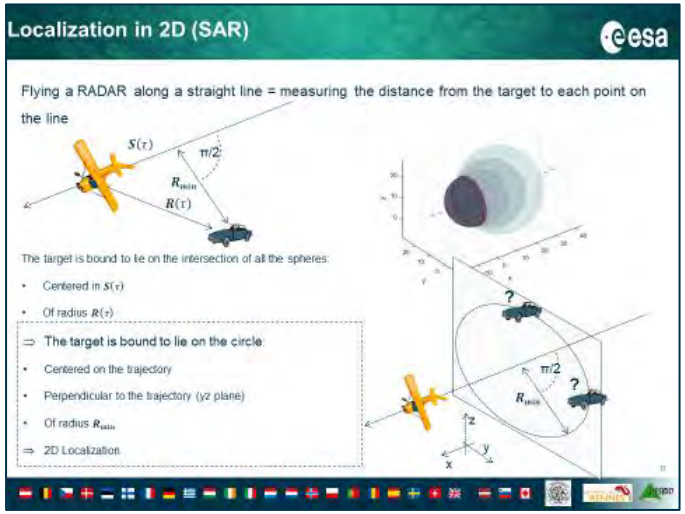

Moving a RADAR along a straight line = measuring the distance from the target to each point on the line

⇔ 2D Localization

How ?

Let's take a step back….

Direction of Arrival

Consider an array of *N* antennas, sequentially emitting a ***monochromatic wave***

Note: Monochromatic wave ⇔ no range resolution

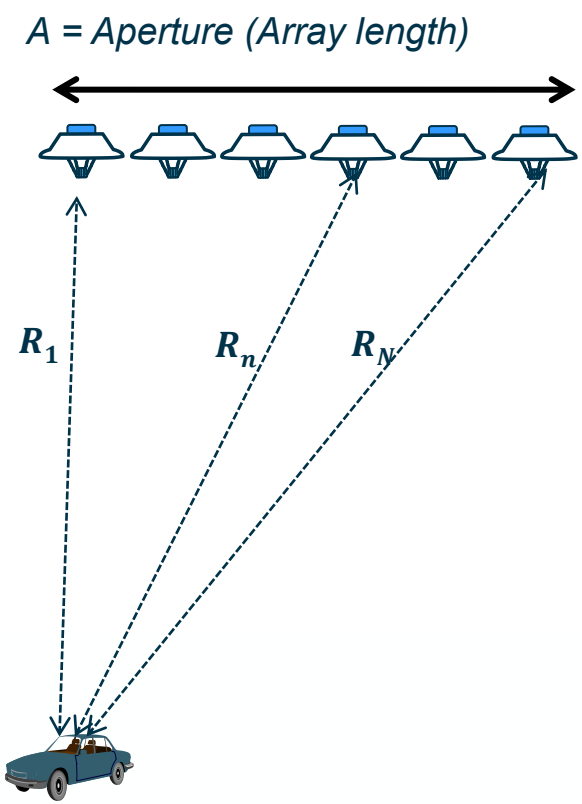

Transmitted signal

$$s_{Tx,RF}(t) = z(t) \cdot cos(2\pi f_0 t)$$

Received complex signal

$$s_{Rx}(n) = A_{car} \cdot e^{-j\frac{4\pi}{\lambda}R_n}$$

Direction of Arrival

Consider an array of *N* antennas, sequentially emitting a ***monochromatic wave***

Note: Monochromatic wave ⇔ no range resolution

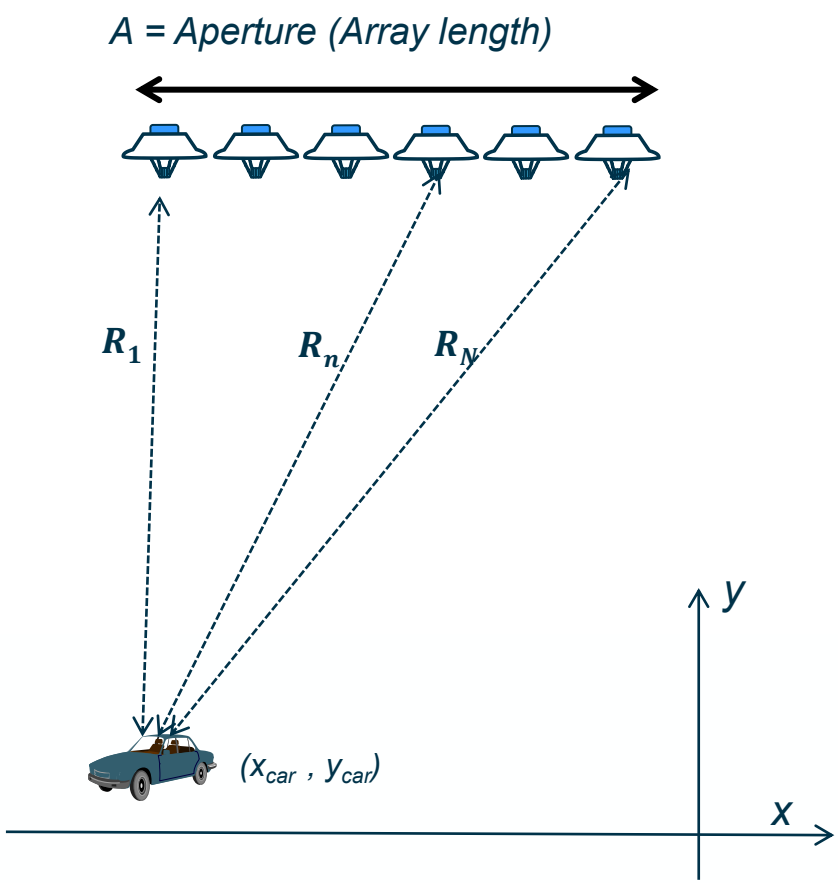

Transmitted signal

$$s_{Tx,RF}(t) = z(t) \cdot cos(2\pi f_0 t)$$

Received complex signal

$$s_{Rx}(n) = A_{car} \cdot e^{-j\frac{4\pi}{\lambda}R_n}$$

$$R_n = \sqrt{(x_n - x_{car})^2 + (y_{car})^2}$$

Direction of Arrival

Consider an array of *N* antennas, sequentially emitting a ***monochromatic wave***

Note: Monochromatic wave ⇔ no range resolution

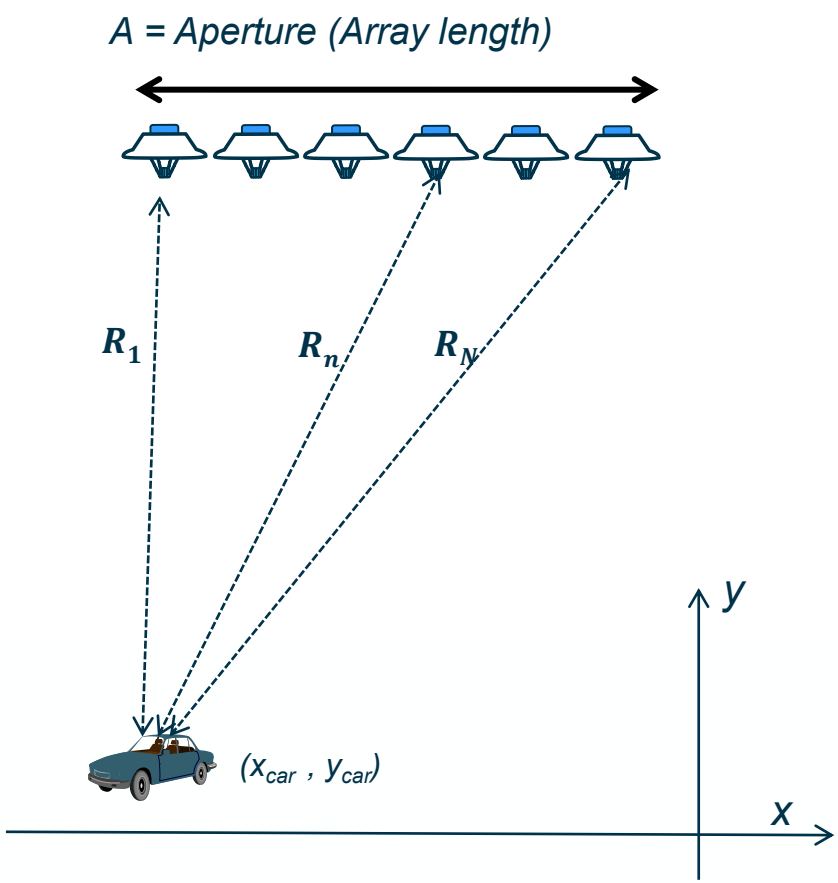

Transmitted signal

$$s_{Tx,RF}(t) = z(t) \cdot cos(2\pi f_0 t)$$

Received complex signal

$$s_{Rx}(n) = A_{car} \cdot e^{-j\frac{4\pi}{\lambda}R_n}$$

$$R_n \cong R_{car} + sin(\psi_{car}) \cdot (x_n - x_0)$$

Valid for $R_{car} >> A$

Direction of Arrival

Consider an array of *N* antennas, sequentially emitting a ***monochromatic wave***

Note: Monochromatic wave ⇔ no range resolution

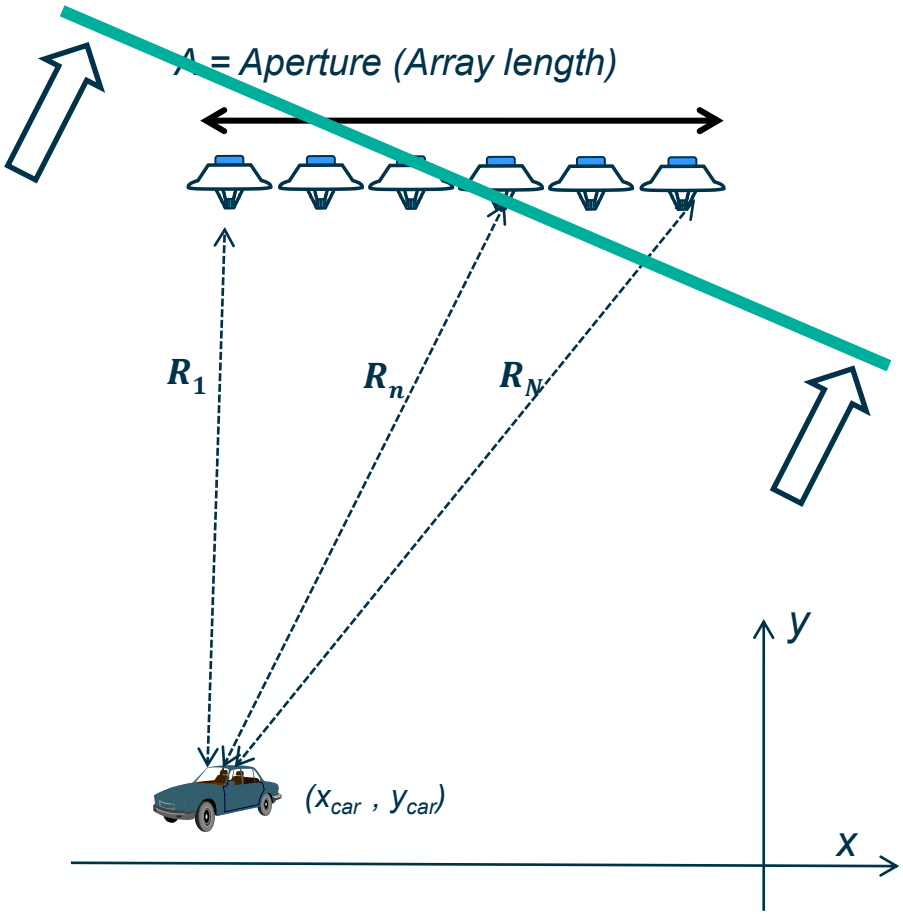

Transmitted signal

$$s_{Tx,RF}(t) = z(t) \cdot cos(2\pi f_0 t)$$

Received complex signal

$$s_{Rx}(n) = A_{car} \cdot e^{-j\frac{4\pi}{\lambda}R_n}$$

$$R_n \cong R_{car} + sin(\psi_{car}) \cdot (x_n - x_0)$$

Valid for $R_{car} >> A$

Equivalent to a planar wavefront from the car to the antenna array

Direction of Arrival

Plane wavefront approximation

$$R_n \cong R_{car} + sin(\psi_{car}) \cdot (x_n - x_0)$$

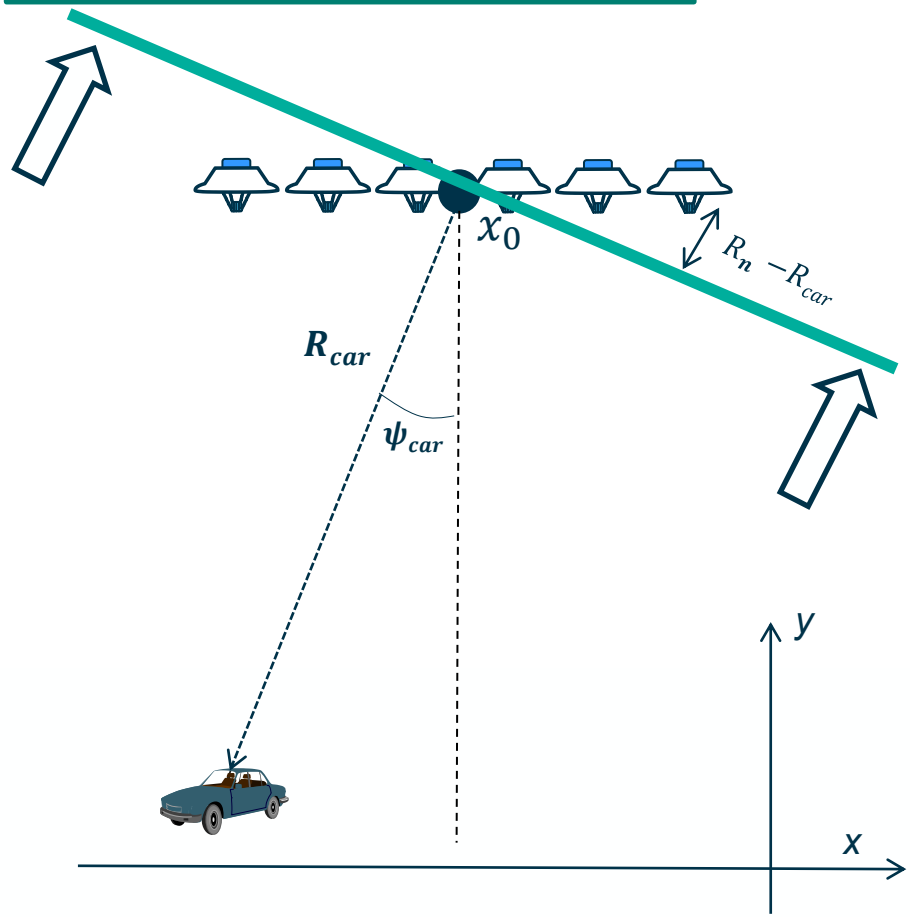

Received signal

$$s_{Rx}(n) \cong A_{car} e^{-j\frac{4\pi}{\lambda}R_{car}} \cdot e^{-j\frac{4\pi}{\lambda}sin(\psi_{car})\cdot x_n}$$

Complex sinusoid with spatial frequency

$$f_{car} = \frac{2}{\lambda} sin(\psi_{car})$$

The Direction of Arrival (DoA) of the wavefront impinging on the array can be found by measuring the spatial frequency along the array

Direction of Arrival

From space to spatial frequency ⇔ Discrete Fourier Transform

$$S_{Rx}(f_x) = \sum_n s_{Rx}(n) \cdot e^{-j2\pi f_x \cdot x_n}$$

One target

$$s_{Rx}(n) \cong A_{car} e^{-j\frac{4\pi}{\lambda}R_{car}} \cdot e^{-j\frac{4\pi}{\lambda}sin(\psi_{car})\cdot x_n}$$

$$S_{Rx}(f_x) = A_{car} e^{-j\frac{4\pi}{\lambda}R_{car}} h(f_x - f_{car})$$

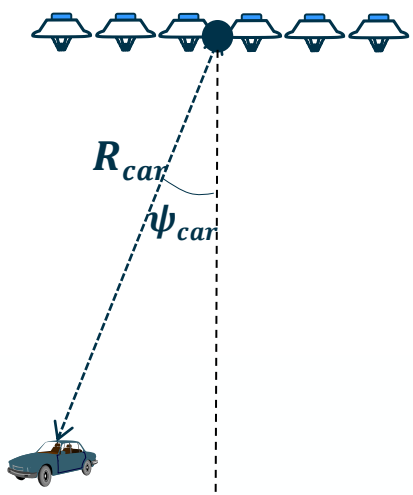

Frequency resolution $\Delta f = \frac{1}{A}$

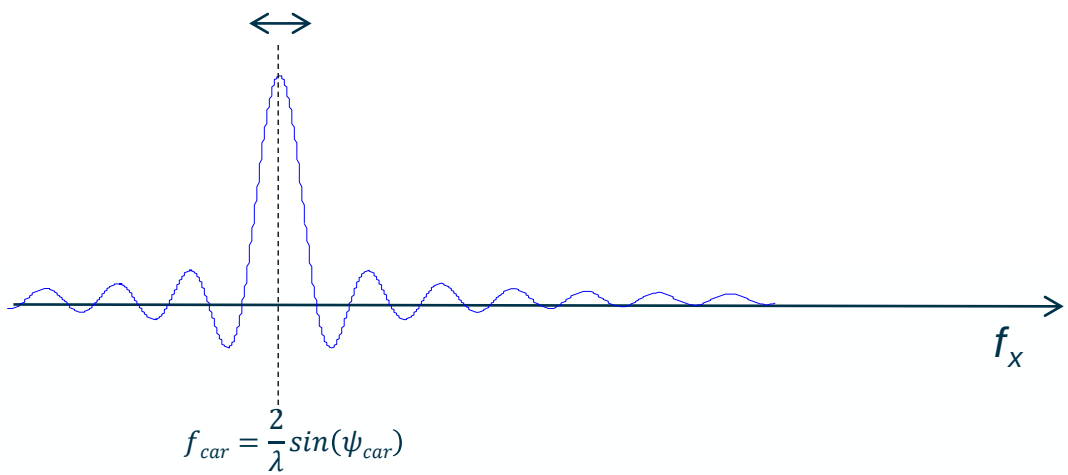

Direction of Arrival

Two targets

$$s_{Rx}(n) \cong A_{car} e^{-j\frac{4\pi}{\lambda}R_{car}} \cdot e^{-j\frac{4\pi}{\lambda}sin(\psi_{car})\cdot x_n} + A_{tree} e^{-j\frac{4\pi}{\lambda}R_{tree}} \cdot e^{-j\frac{4\pi}{\lambda}sin(\psi_{tree})\cdot x_n}$$

$$S_{Rx}(f_x) = A_{car} e^{-j\frac{4\pi}{\lambda}R_{car}} h(f_x - f_{car}) + A_{tree} e^{-j\frac{4\pi}{\lambda}R_{tree}} h(f_x - f_{tree})$$

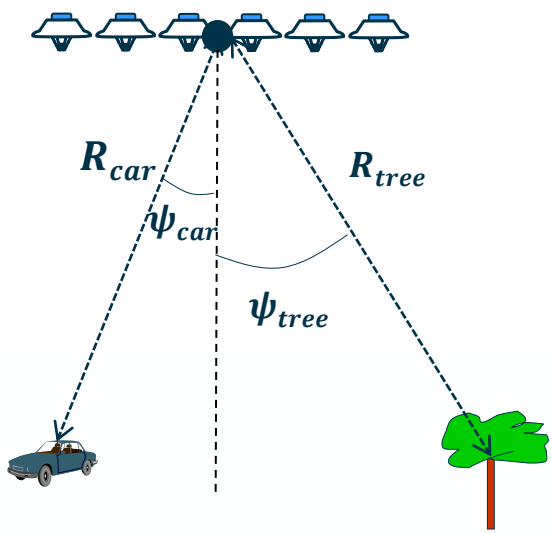

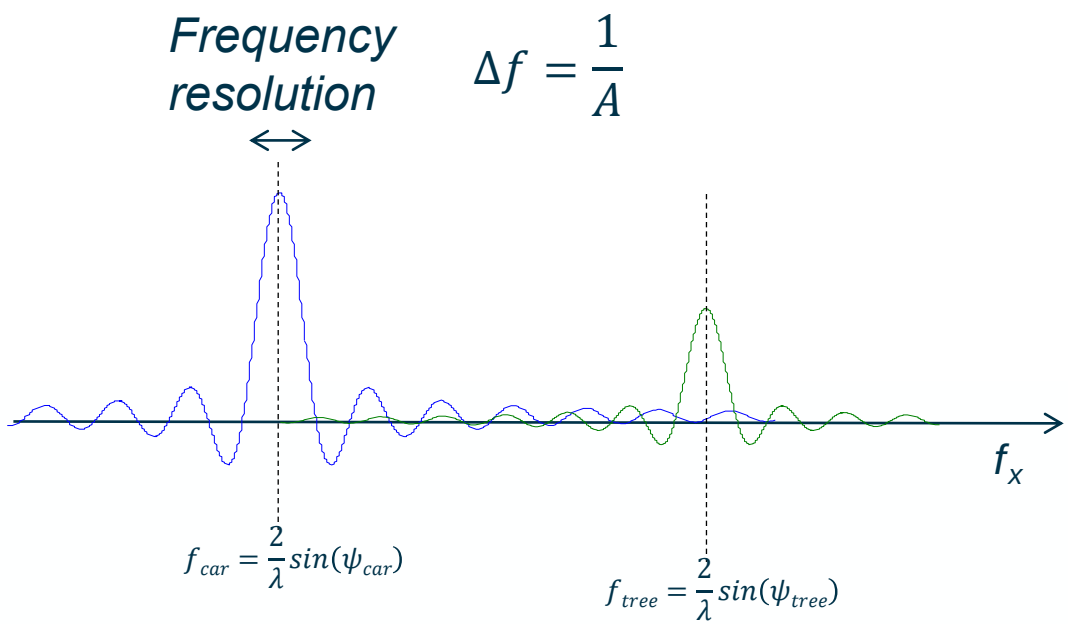

Direction of Arrival

From spatial frequency to angles

$$f_x = \frac{2}{\lambda} sin(\psi)$$

Angular resolution

$$\Delta\psi = \frac{\lambda}{2Acos(\psi)} \geq \frac{\lambda}{2A}$$

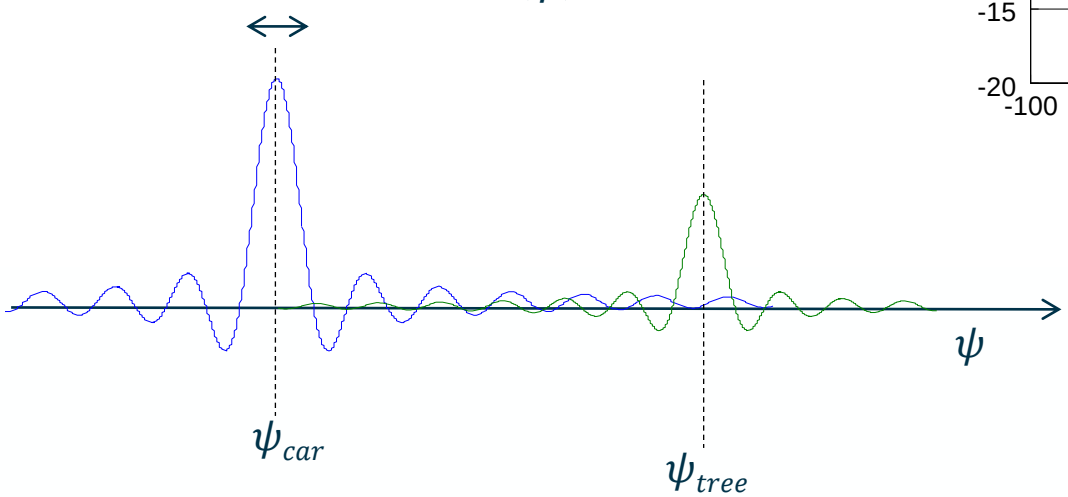

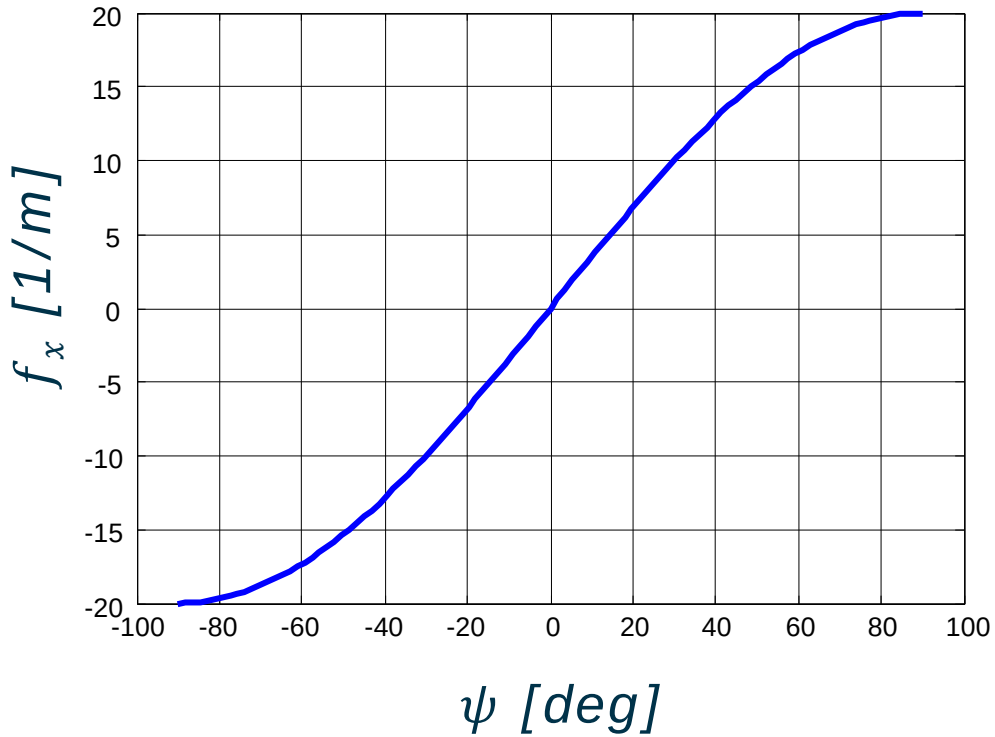

Localization in 2D

Bandwidth
⇔
Range resolution

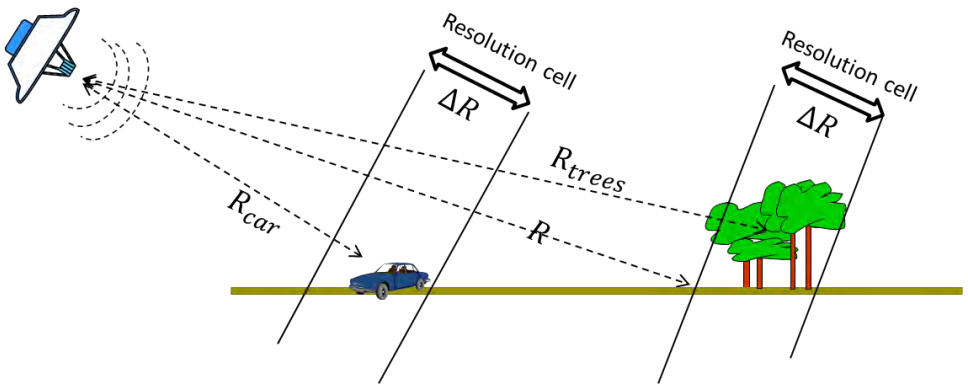

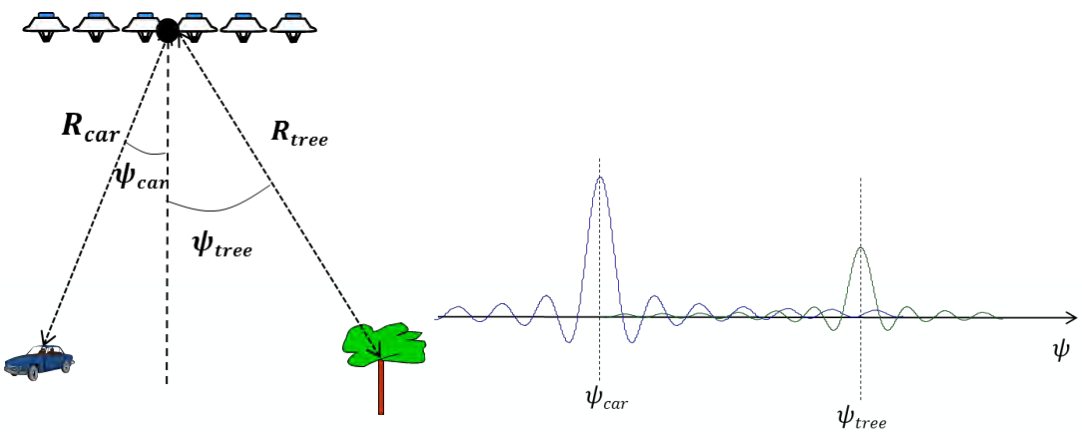

Antenna array emitting a monochromatic wave
⇔
Angular resolution

SAR Imaging

Flying a RADAR along a straight line = measuring the distance from the target to each point on the line

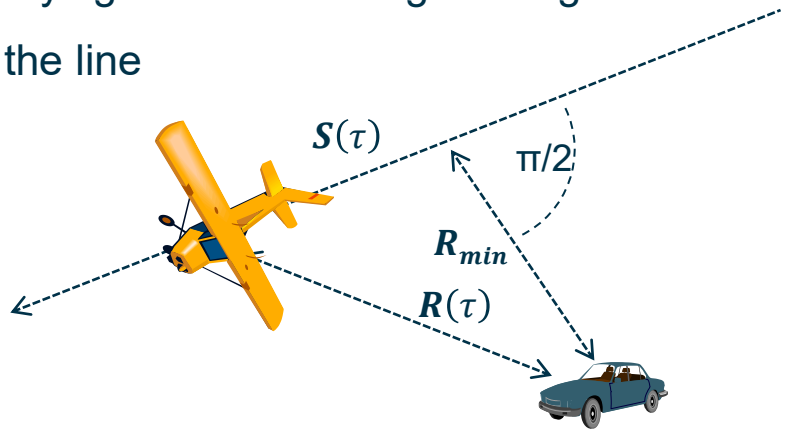

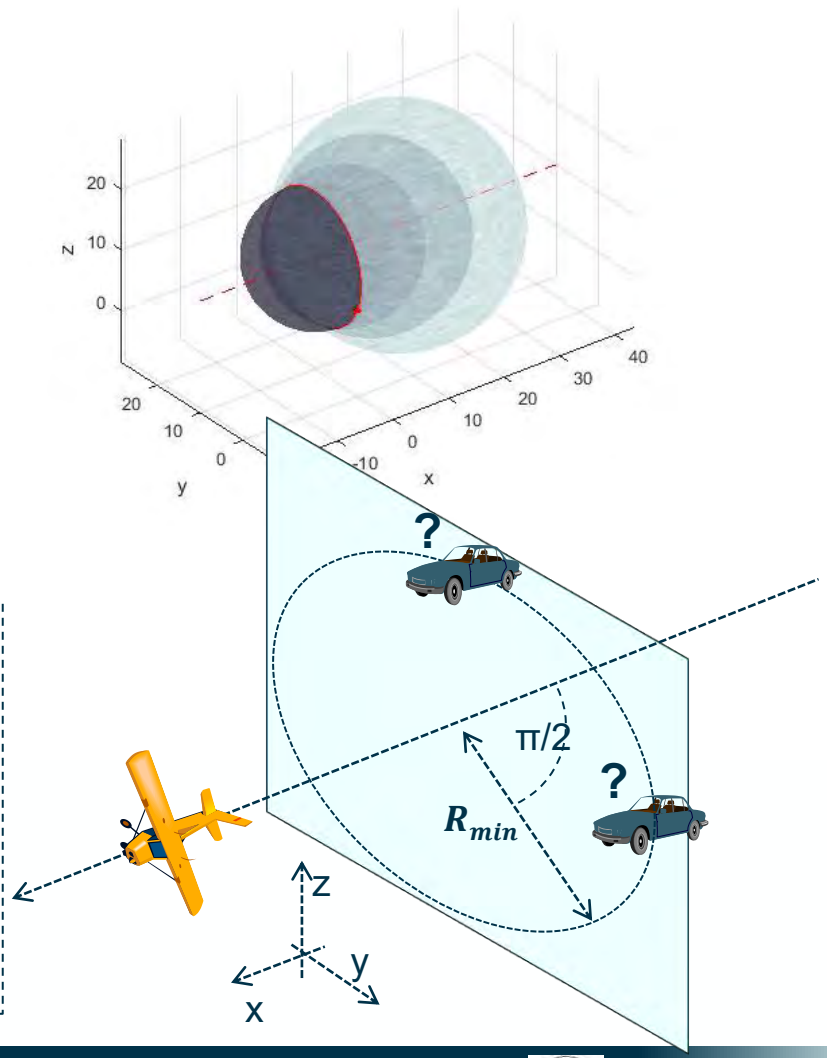

The target is bound to lie on the intersection of all the spheres:

- Centered in $S(\tau)$
- Of radius $R(\tau)$

⇒ The target is bound to lie on the circle:

- Centered on the trajectory
- Perpendicular to the trajectory (*yz* plane)
- Of radius R_{min}

⇒ 2D Localization

SAR Imaging

Synthetic Aperture Radars (SAR) employ a moving RADAR sensor, flown onboard a satellite or an aircraft, in order to synthesize an antenna as long as several kilometers

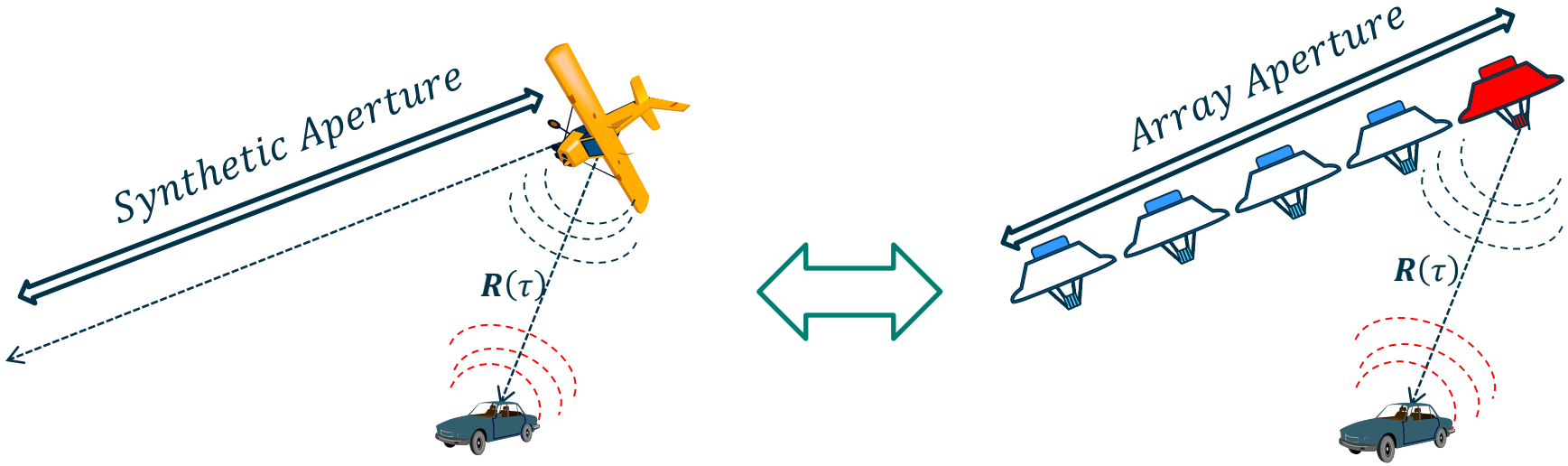

SAR Imaging

Synthetic Aperture Radars (SAR) employ a moving RADAR sensor, flown onboard a satellite or an aircraft, in order to synthesize an antenna as long as several kilometers

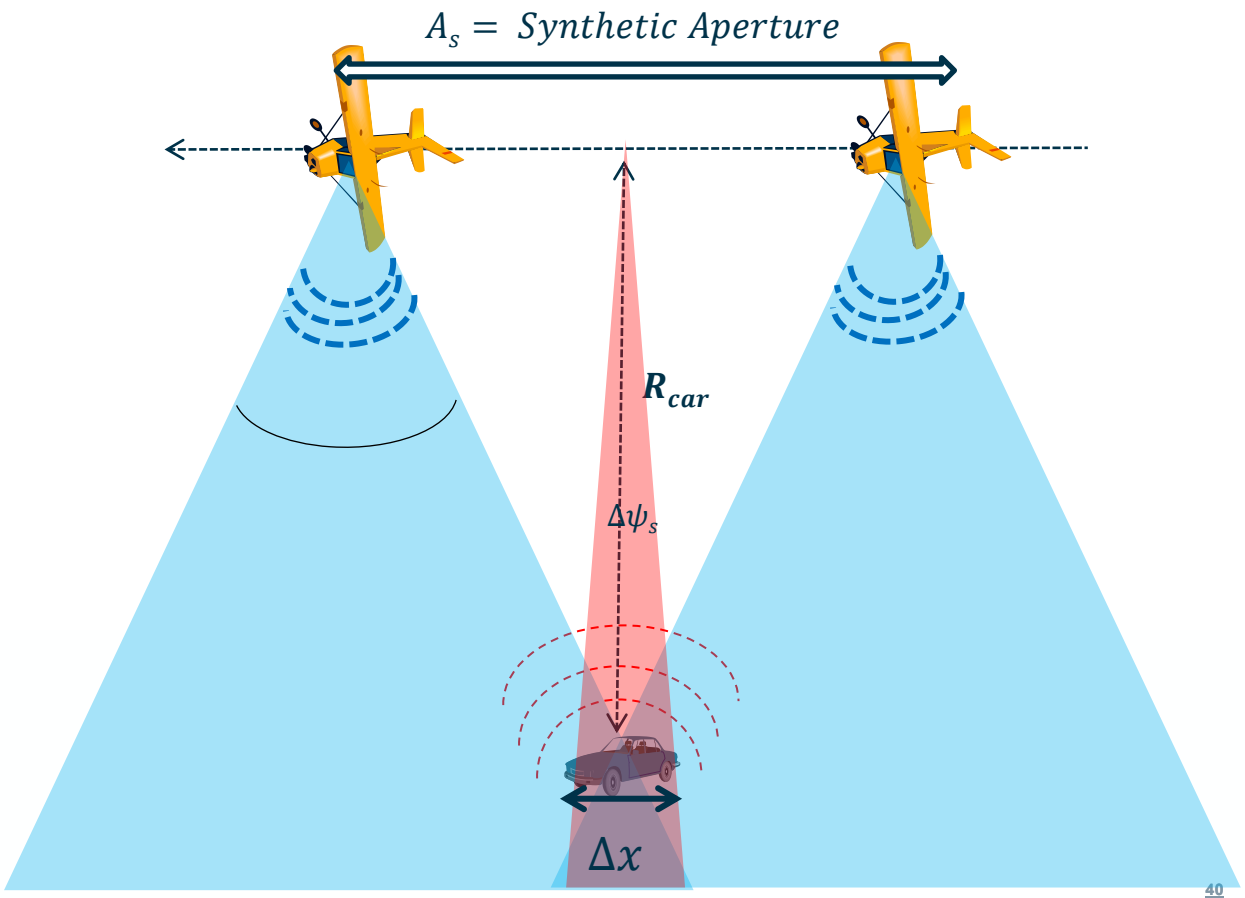

SAR Imaging

Synthetic Aperture Radars (SAR) employ a moving RADAR sensor, flown onboard a satellite or

a ...na as long as several kilometers

Result from array theory

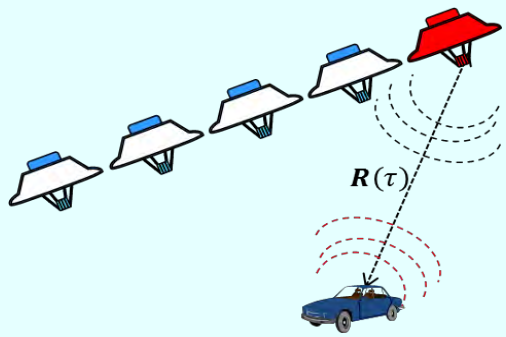

Aperture length translates to angular resolution according to

$$\Delta\psi_s \cong \frac{\lambda}{2A_s}$$

Angular resolution translates into horizontal resolution according to

$$\Delta x \cong \Delta\psi_s \cdot \boldsymbol{R_{min}}$$

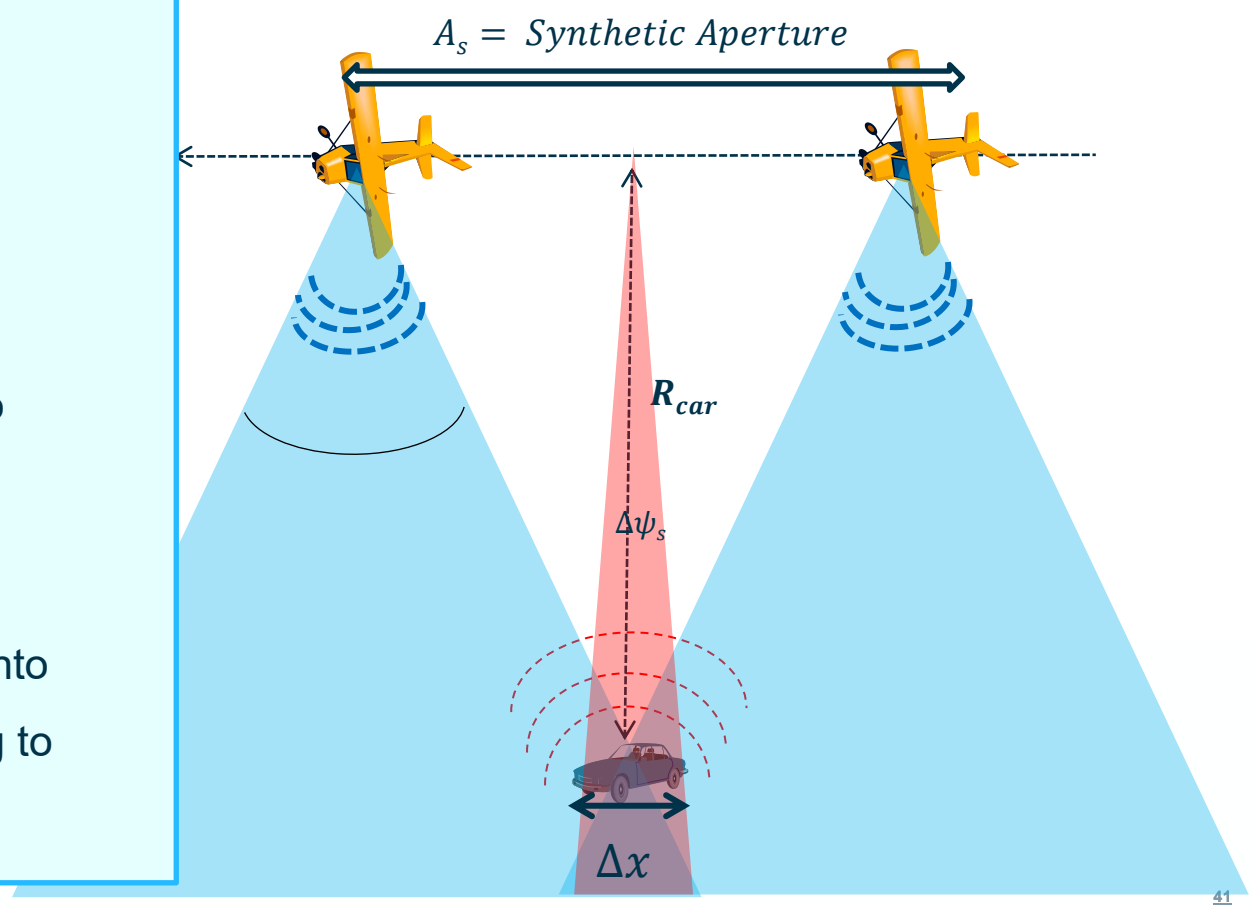

SAR Imaging

Flying a RADAR along a straight line = measuring the distance from the target to each point on the line

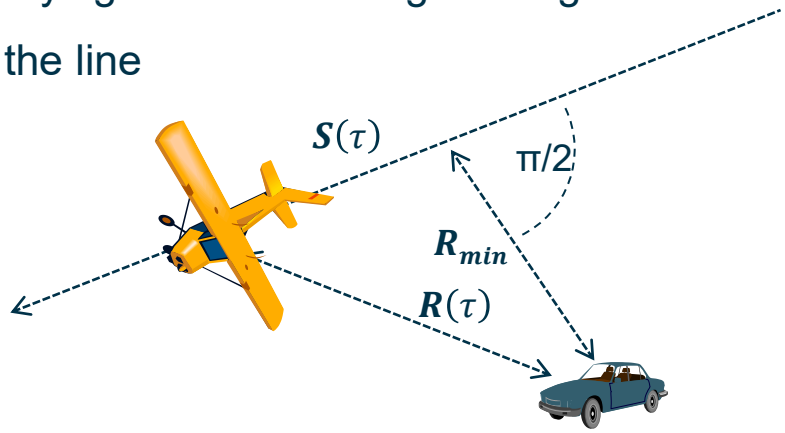

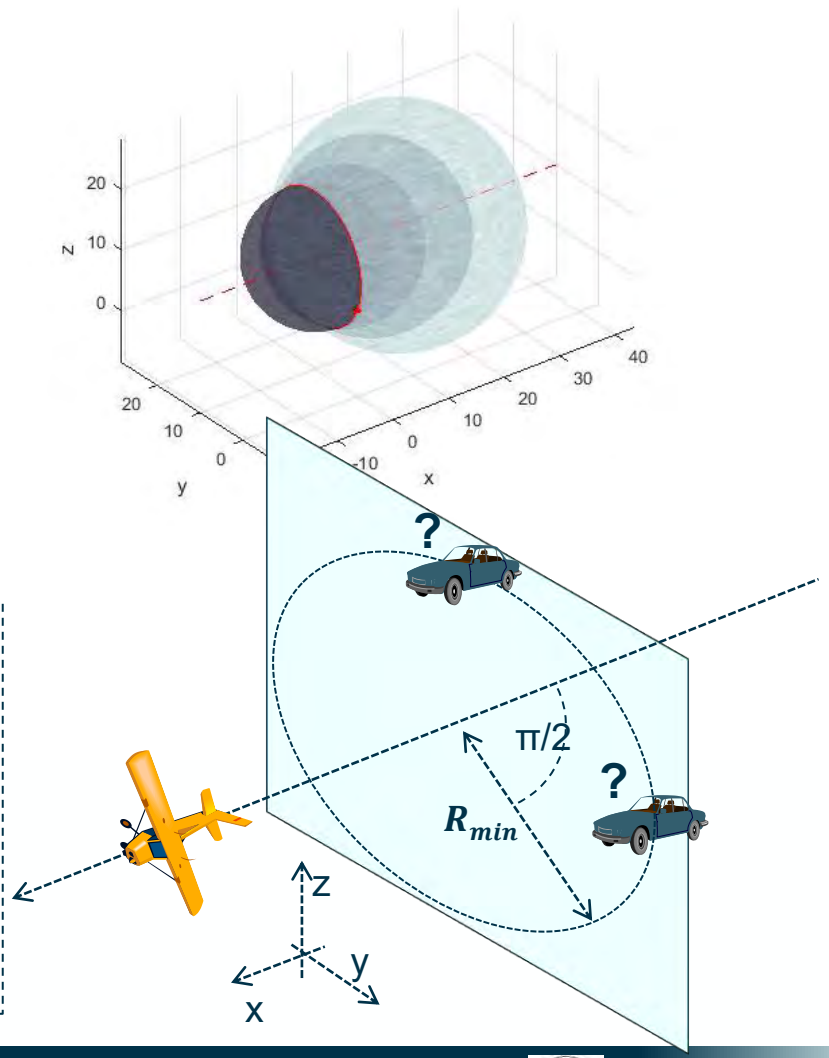

The target is bound to lie on the intersection of all the spheres:

- Centered in $S(\tau)$
- Of radius $R(\tau)$

⇒ The target is bound to lie on the circle:

- Centered on the trajectory
- Perpendicular to the trajectory (*yz* plane)
- Of radius R_{min}

⇒ 2D Localization

SAR Resolution Cell

⇒ The target is bound to lie in the region of space:

- o Centered on the trajectory
- o Perpendicular to the trajectory (*yz* plane)
- o Range thickness ΔR
- o Along-track thickness Δx

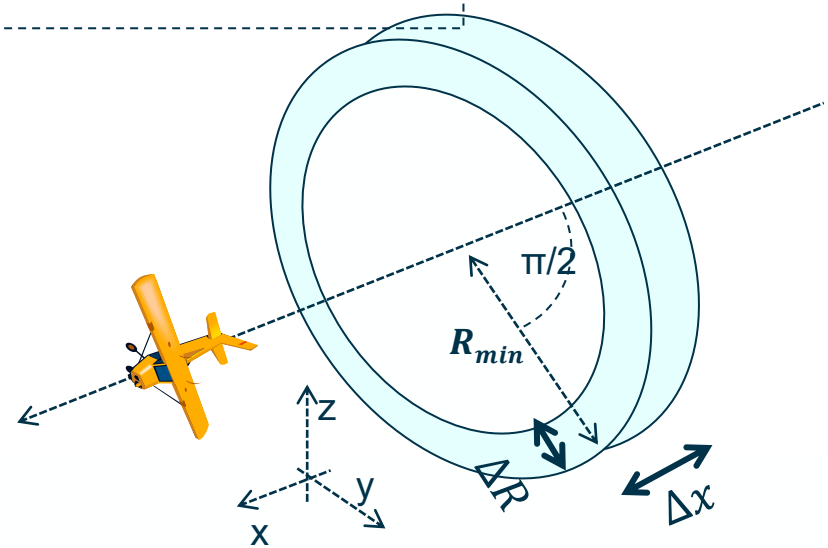

SAR jargon

- o R = (slant) range
- o x = azimuth

SAR Resolution Cell

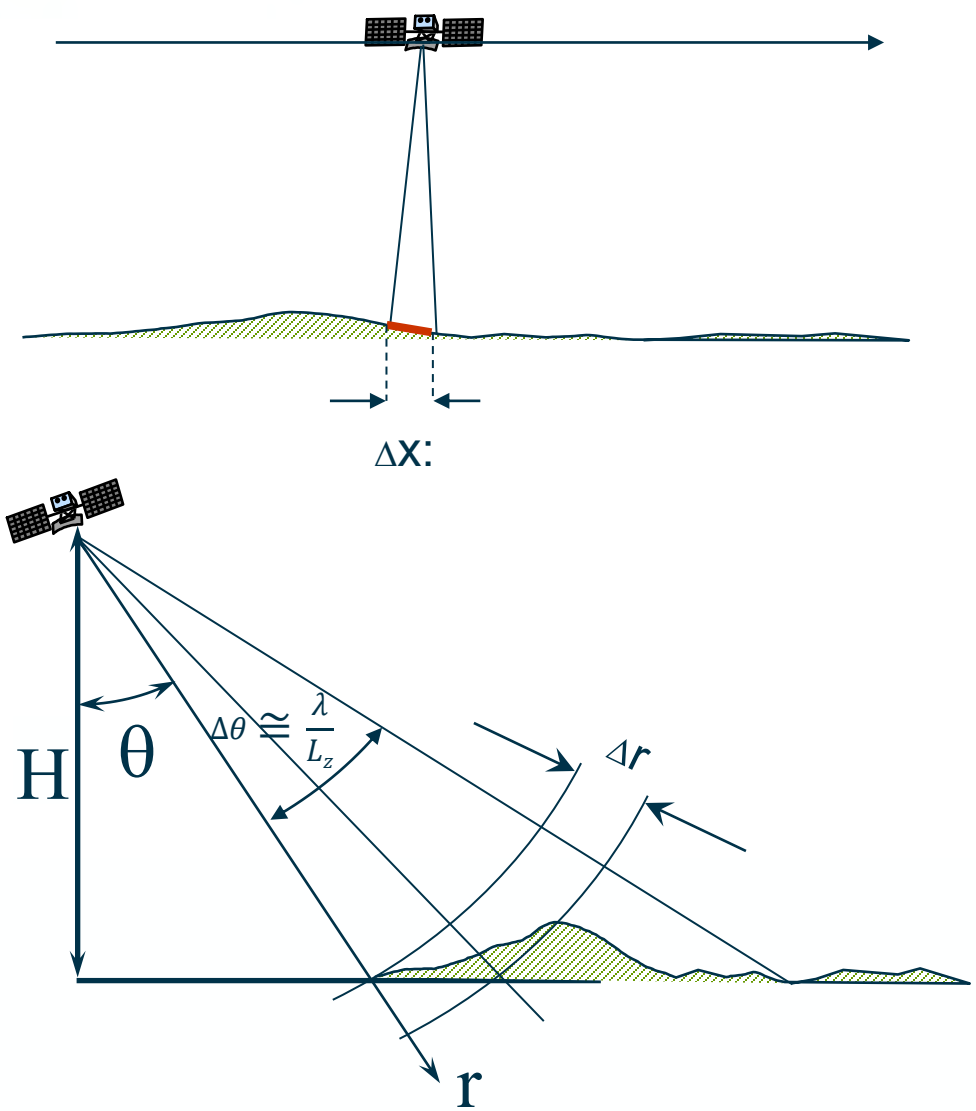

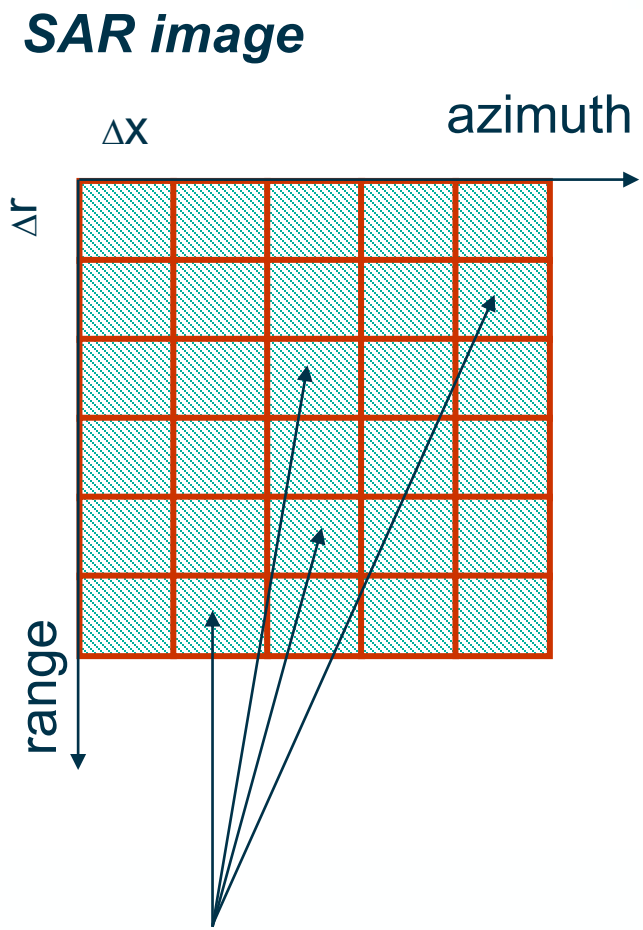

Each pixel is associated with a range/azimuth resolution cell

SAR Resolution Cell

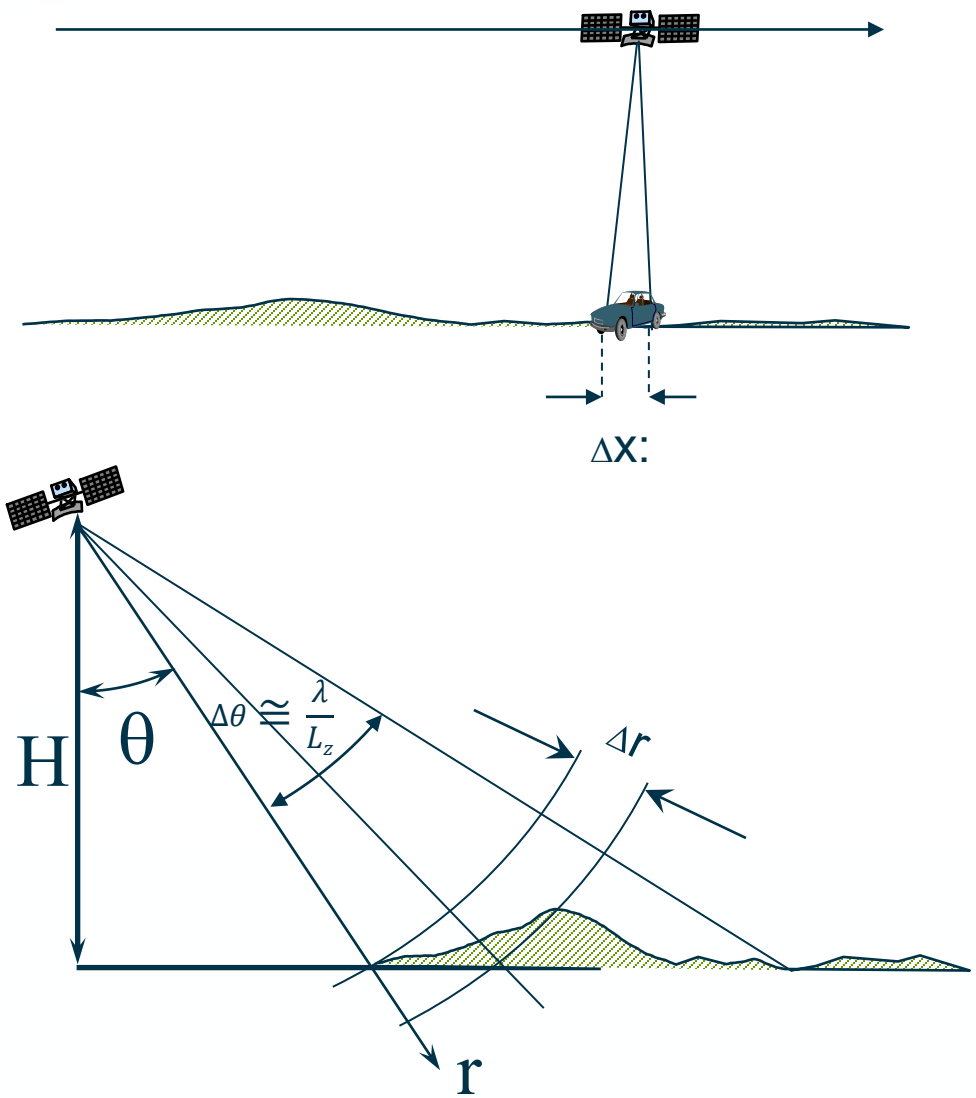

SAR image

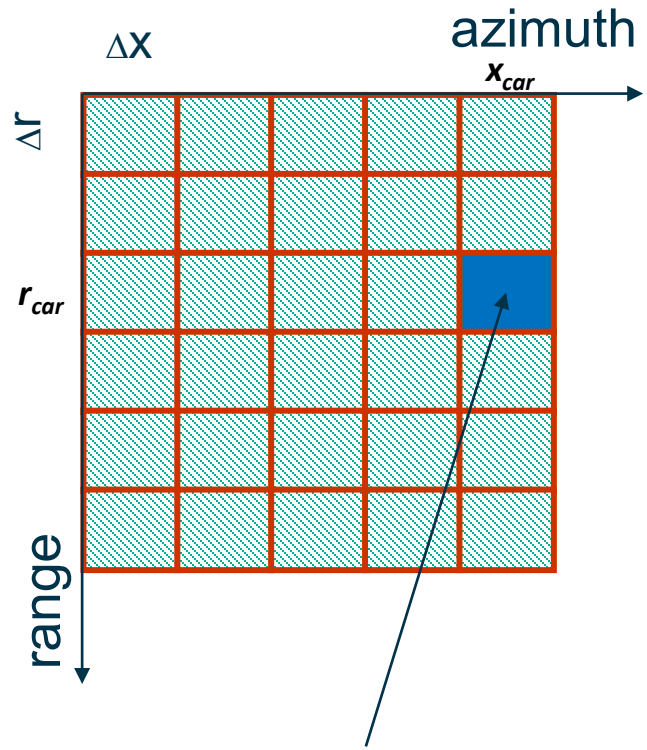

This pixel value corresponds to the target at position x_{car}, r_{car}

$$I(r_{car}, x_{car}) = A_{car} \cdot e^{-j\frac{4\pi}{\lambda} r_{car}}$$

SAR Resolution Cell

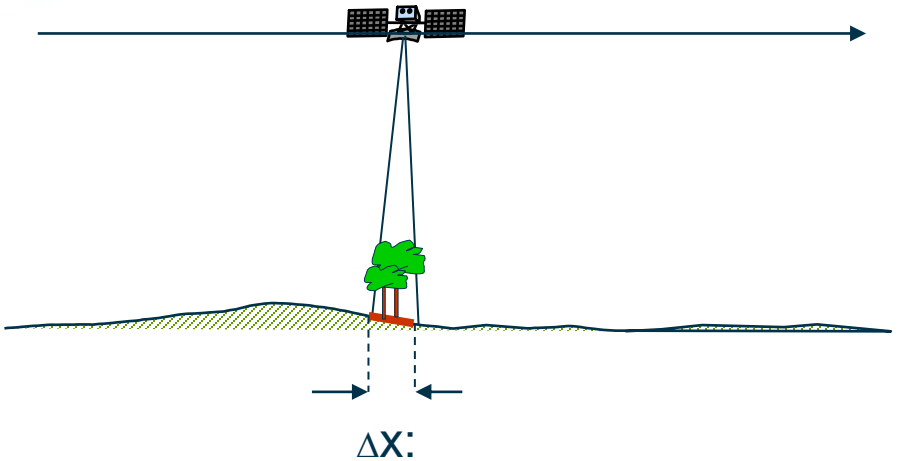

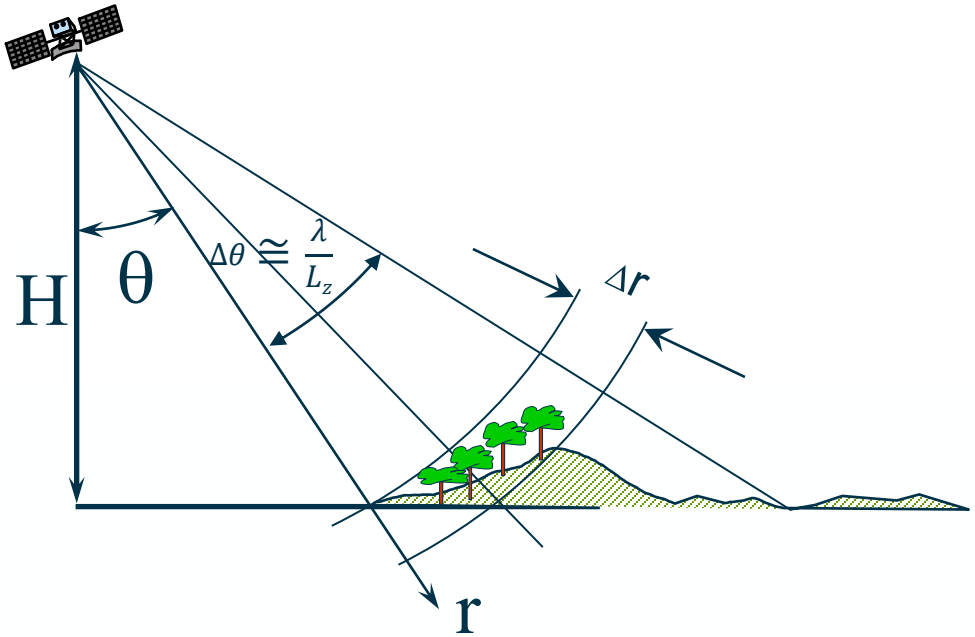

SAR image

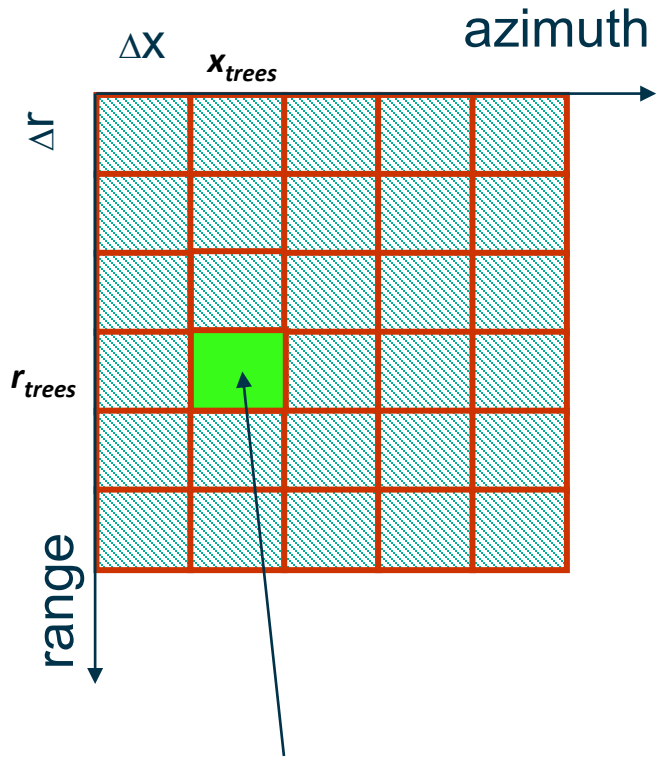

This pixel value is arises from all trees within the resolution cell

SAR Resolution Cell

$$I(r_{trees}, xtree_s) = \int A(x,y,z) \cdot e^{-j\frac{4\pi}{\lambda}R(x,y,z)} dxdydz$$

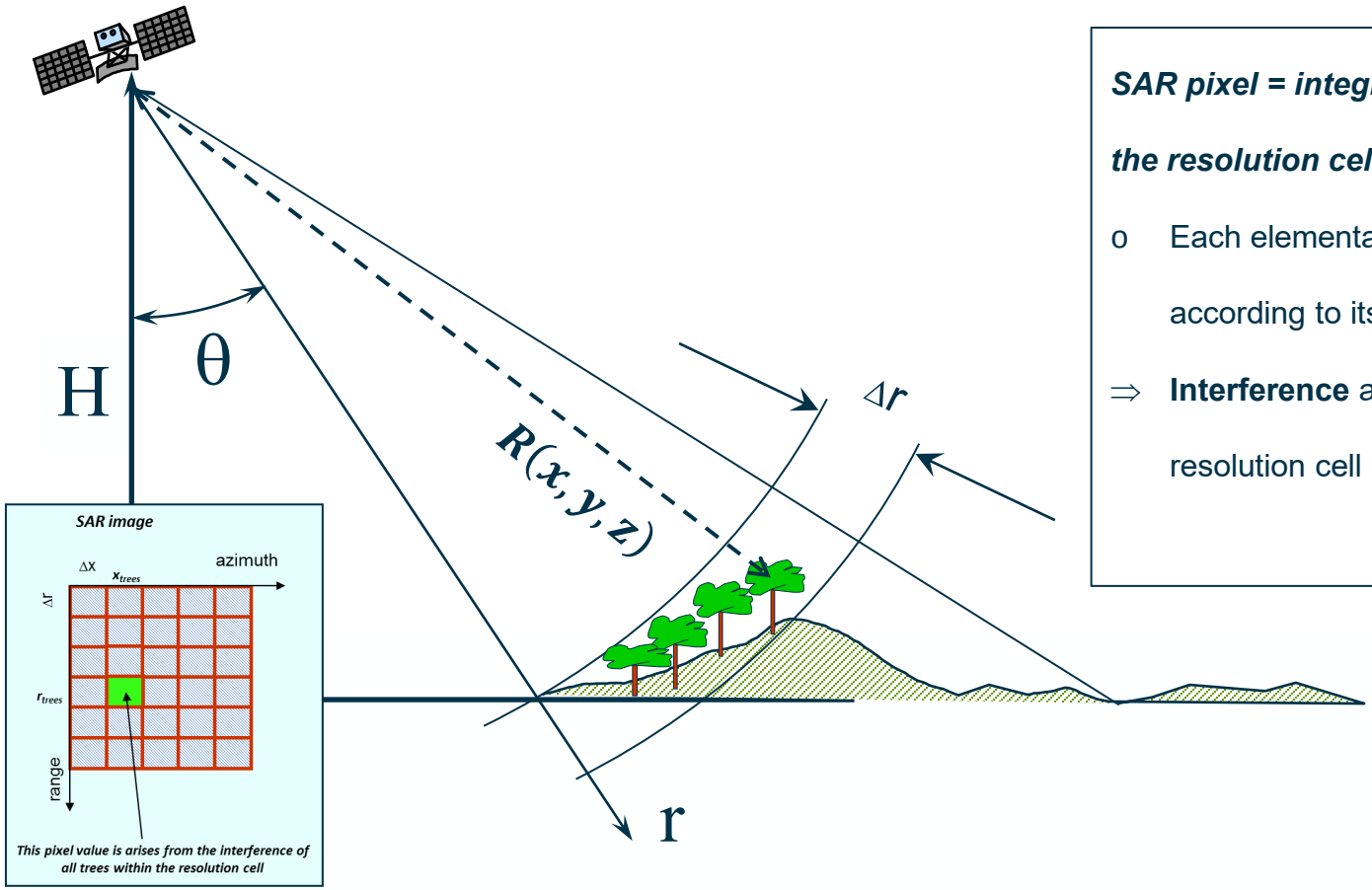

SAR pixel = integral of all contributions within the resolution cell

- o Each elementary scatterer is phase-rotated according to its distance from the Radar

⇒ **Interference** among all targets in the same resolution cell ⇔ ***Speckle***

Localization in 3D (TomoSAR)

Flying a RADAR along multiple lines = measuring the distance from the target to multiple lines

The target is bound to lie on the circles:

- Centered on each trajectory
- Perpendicular to the trajectory ,
- Of radius $\boldsymbol{R_1} \ldots \boldsymbol{R_n} \ldots . \boldsymbol{R_N}$

⇒ Only 1 solution in the 3D space !

⇒ 3D localization

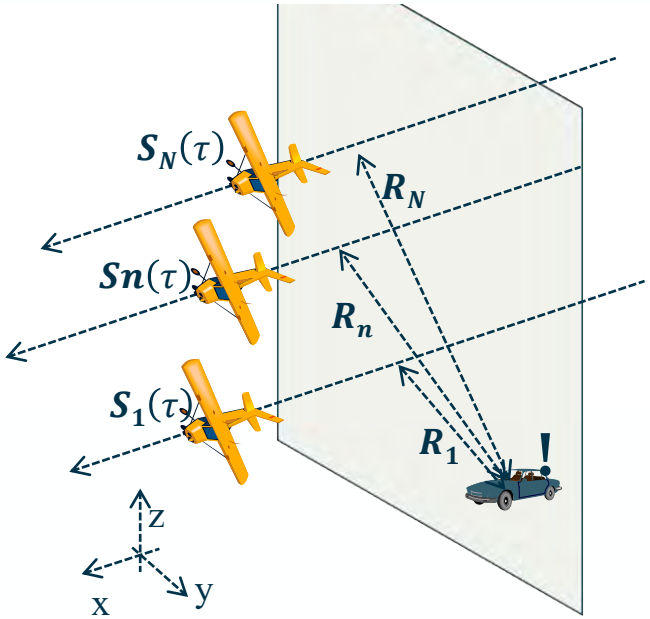

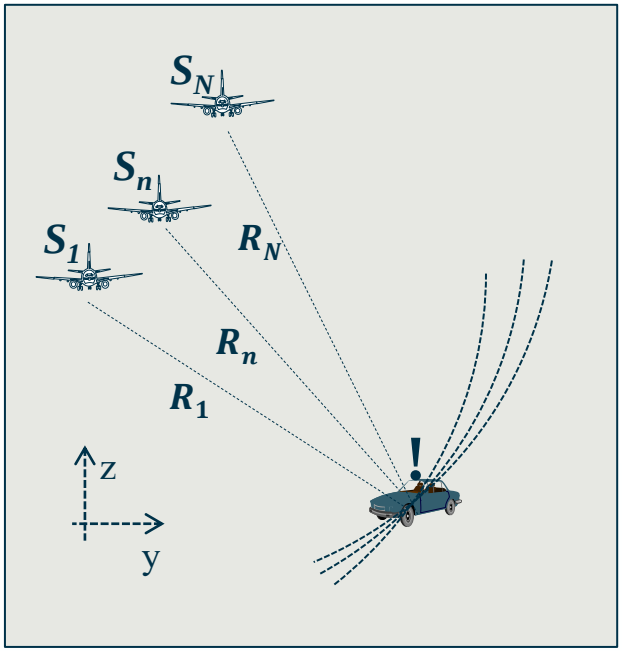

Localization in 3D (TomoSAR)

Aperture Synthesis in the cross-range direction

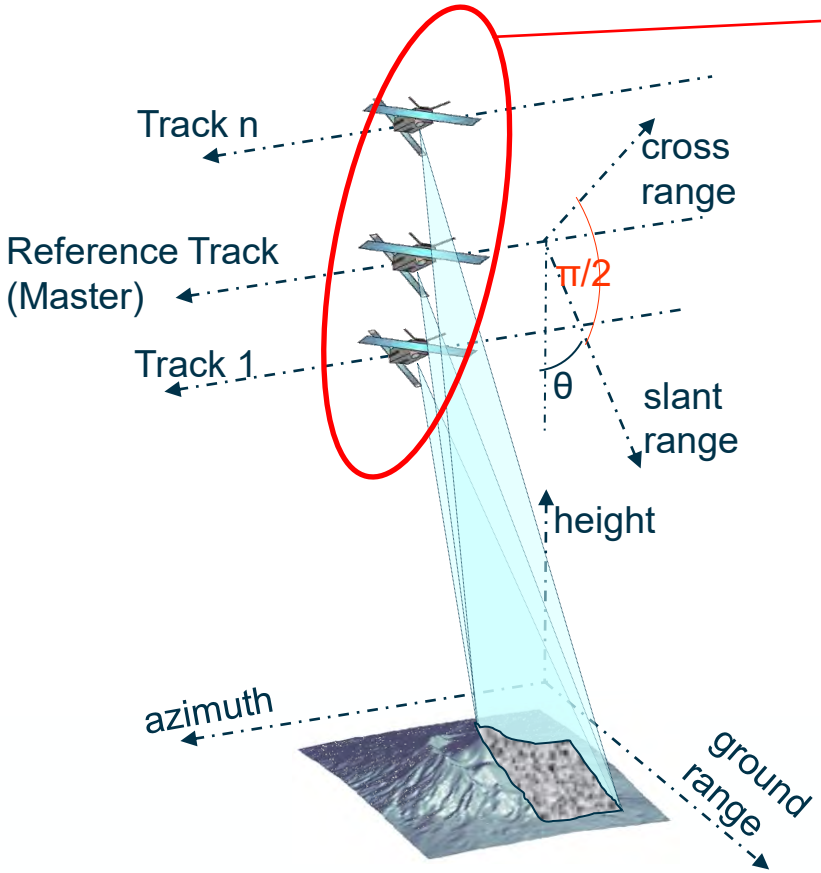

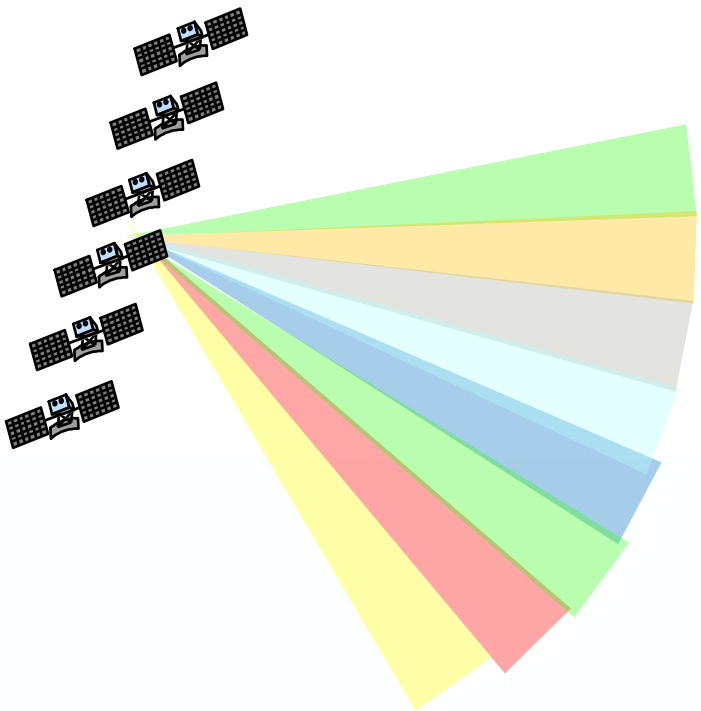

Localization in 3D (TomoSAR)

Multiple baselines ⇔ Illumination from multiple points of view

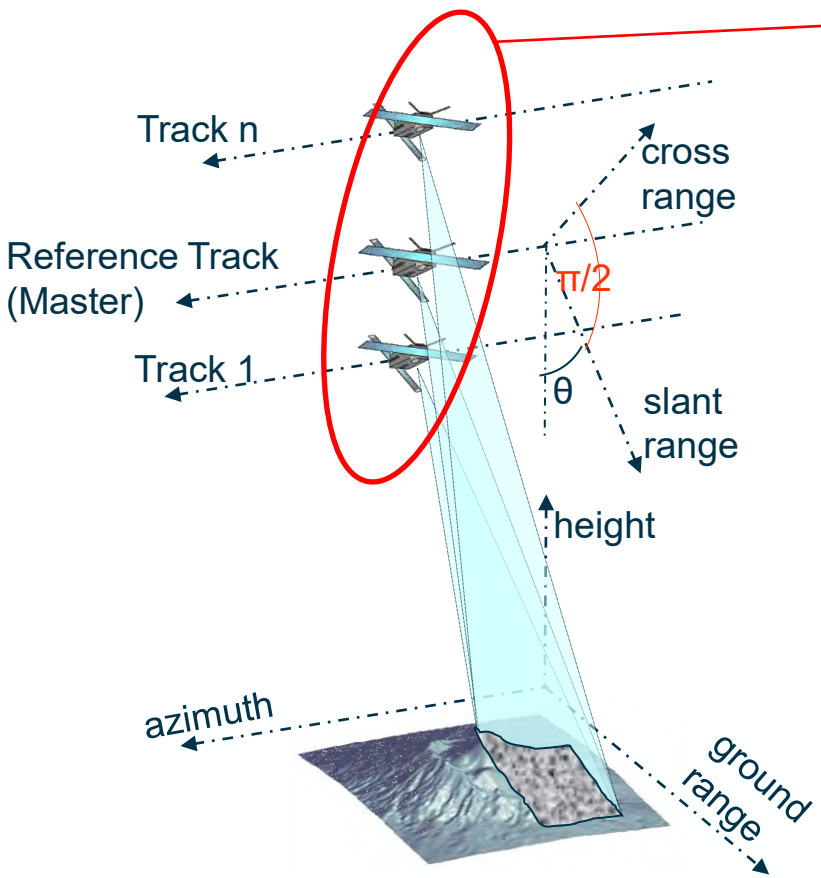

Aperture Synthesis in the cross-range direction

⇒ ***Cross-range resolution capabilities***

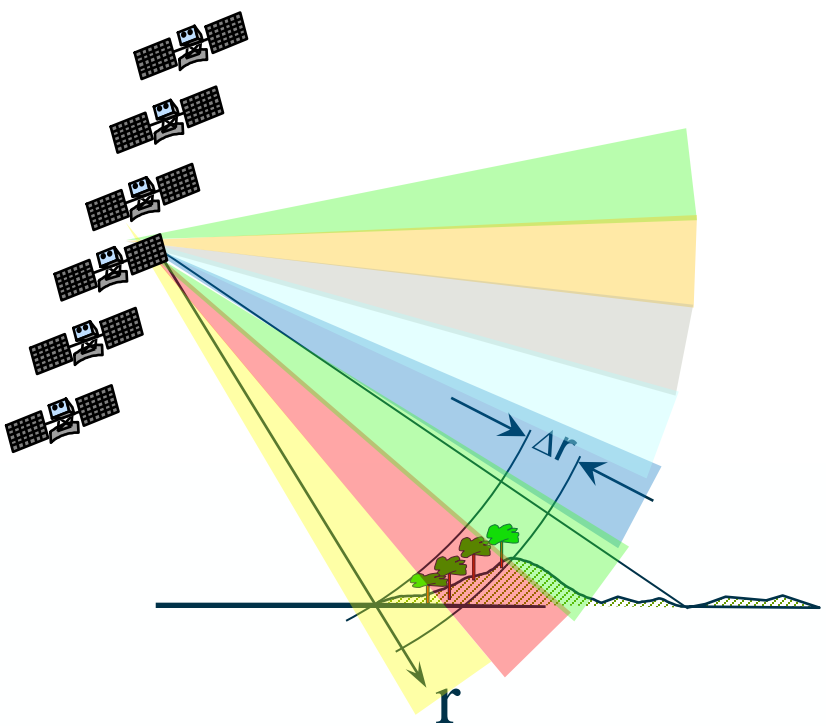

TomoSAR Resolution

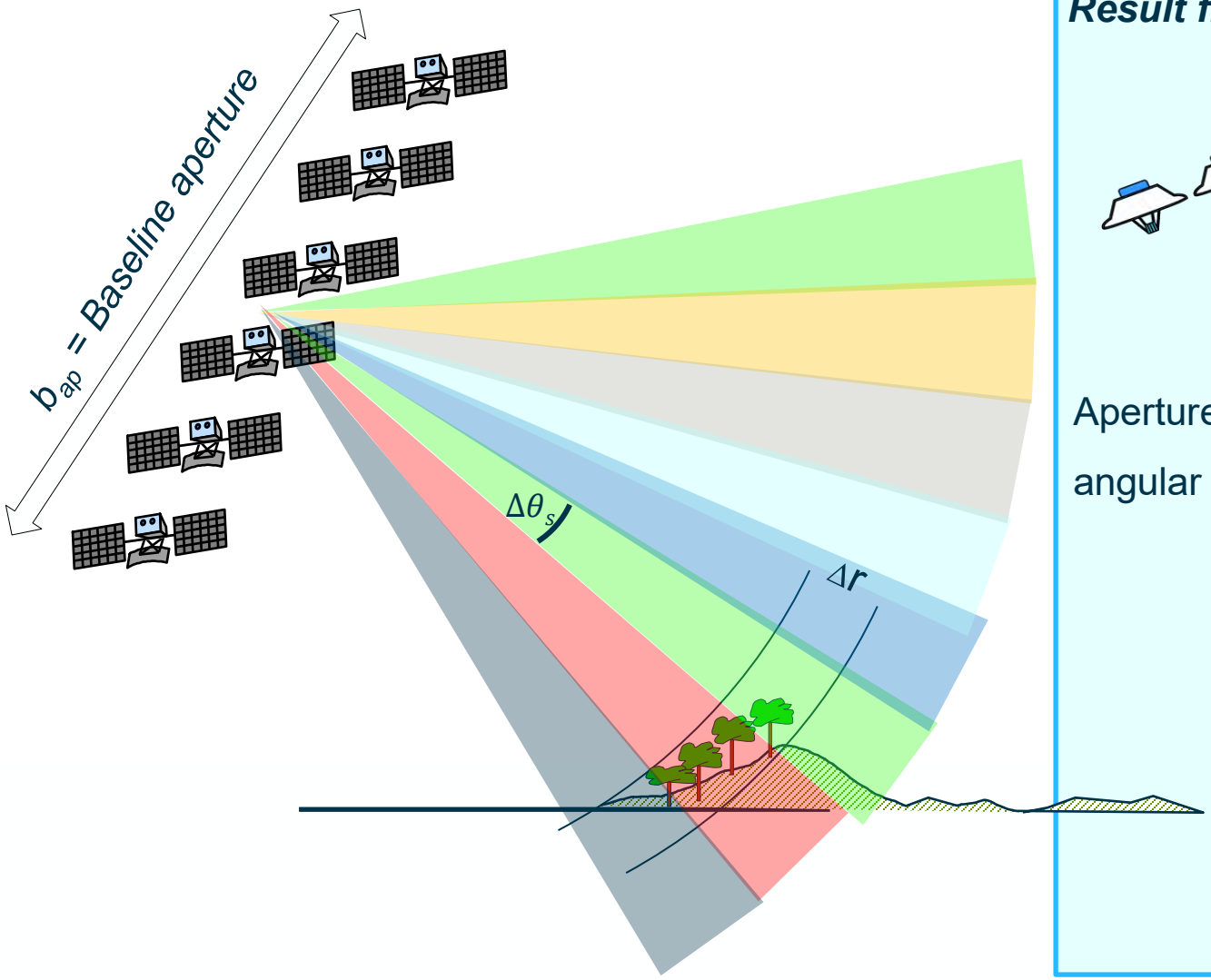

Result from array theory

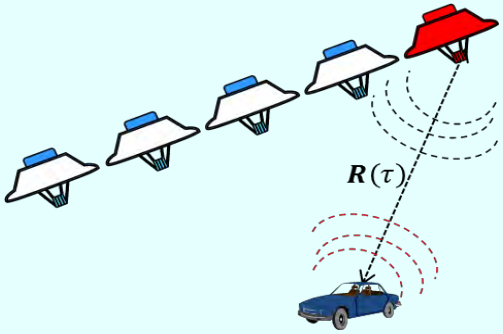

Aperture length translates to angular resolution according to

$$\Delta\theta_s \cong \frac{\lambda}{2b_{ap}}$$

TomoSAR Resolution

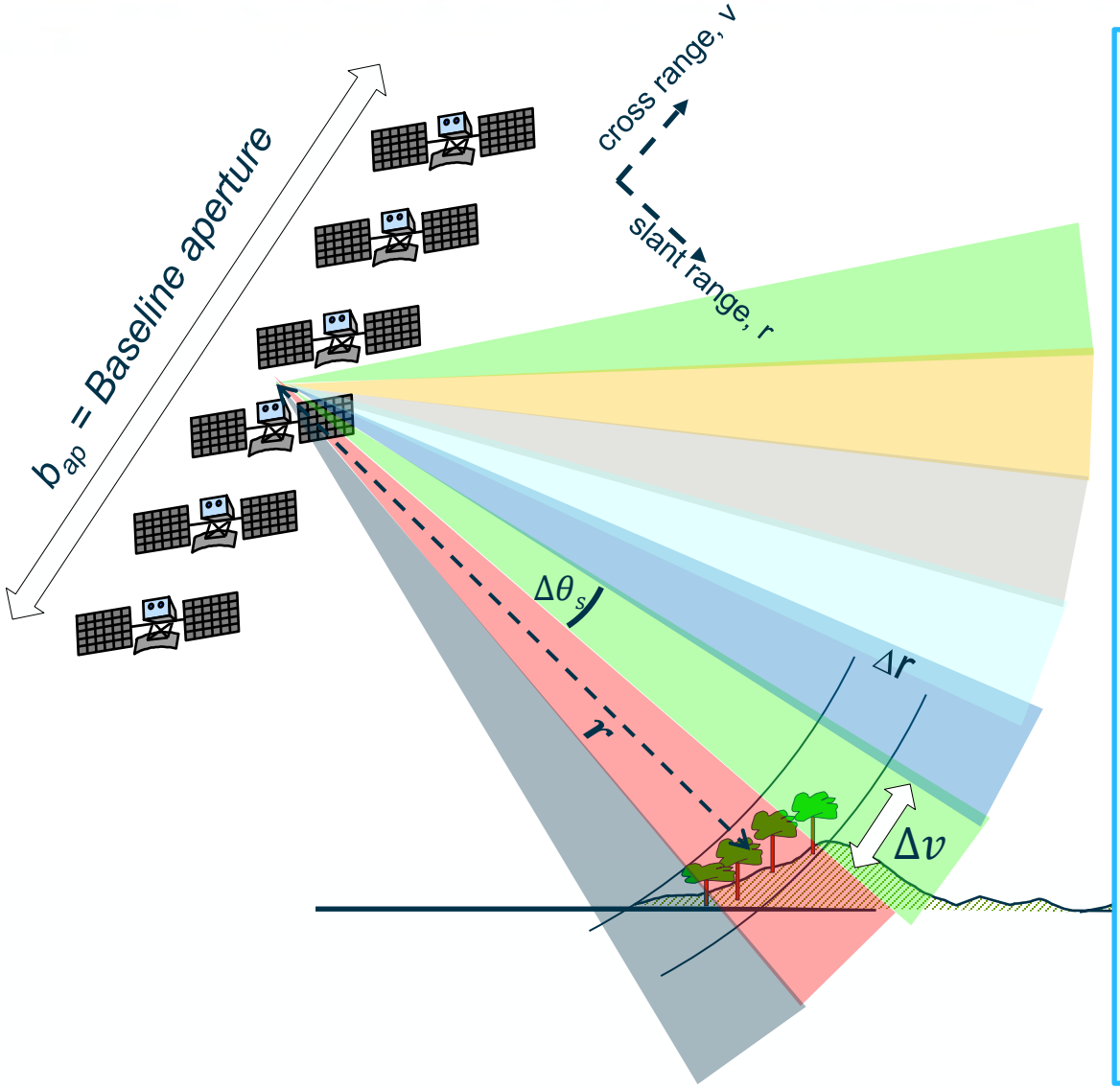

Result from array theory

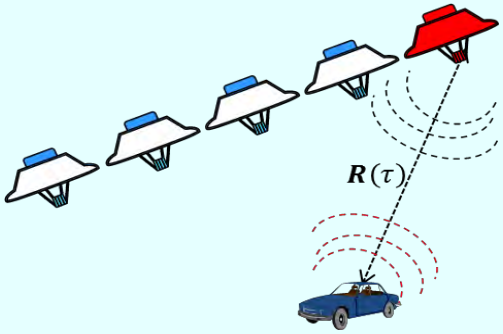

Aperture length translates to angular resolution according to

$$\Delta\theta_s \cong \frac{\lambda}{2b_{ap}}$$

Angular resolution translates into **cross-range** resolution according to

$$\Delta v \cong \Delta\theta_s \cdot r$$

TomoSAR Resolution

Resolution is determined by

- Pulse bandwidth along the slant range direction
- Synthetic aperture length in the azimuth direction
- Baseline aperture in the cross range direction

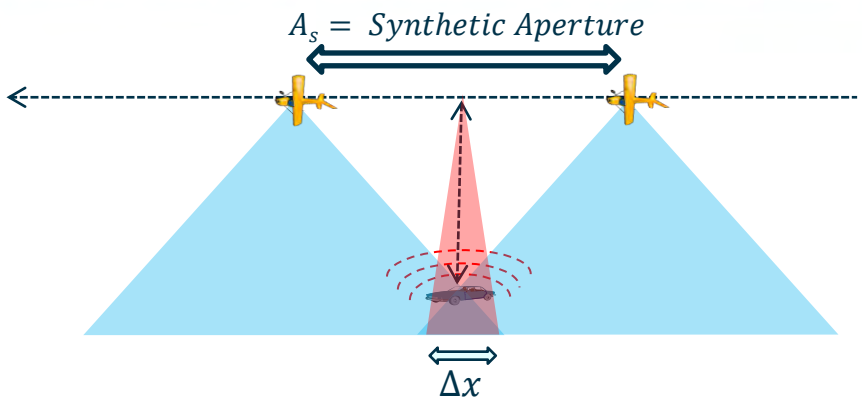

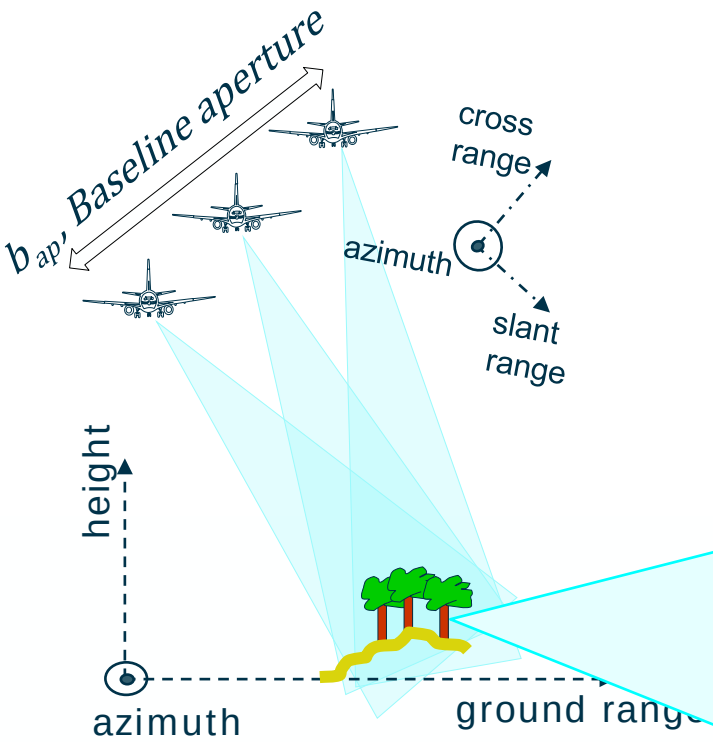

$$\Delta r = \frac{c}{2B} \qquad \Delta v = \frac{\lambda r}{2b_{ap}} \qquad \Delta x = \frac{\lambda r}{2A_s}$$

B: pulse bandwidth
λ: carrier wavelength

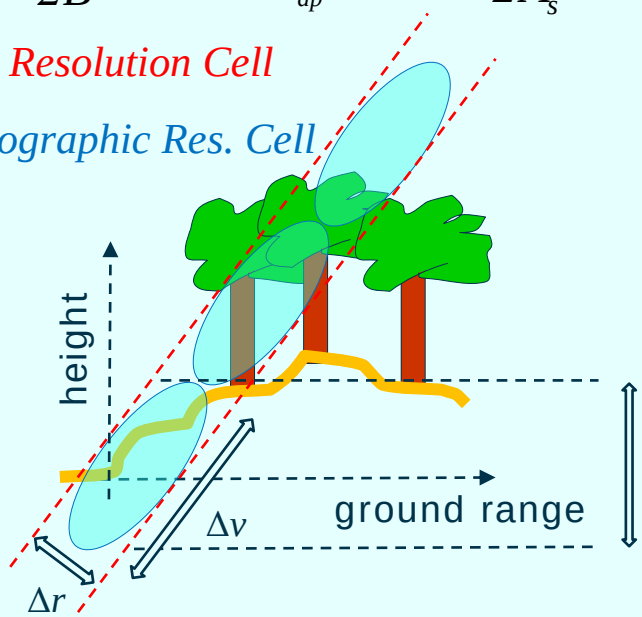

For most systems:

$\Delta v >> \Delta r, \Delta x$

$$\Delta z \cong \Delta v \cdot \sin(\theta)$$

TomoSAR Resolution

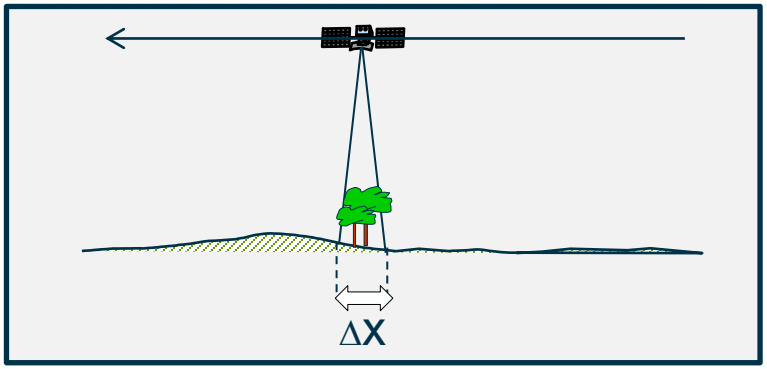

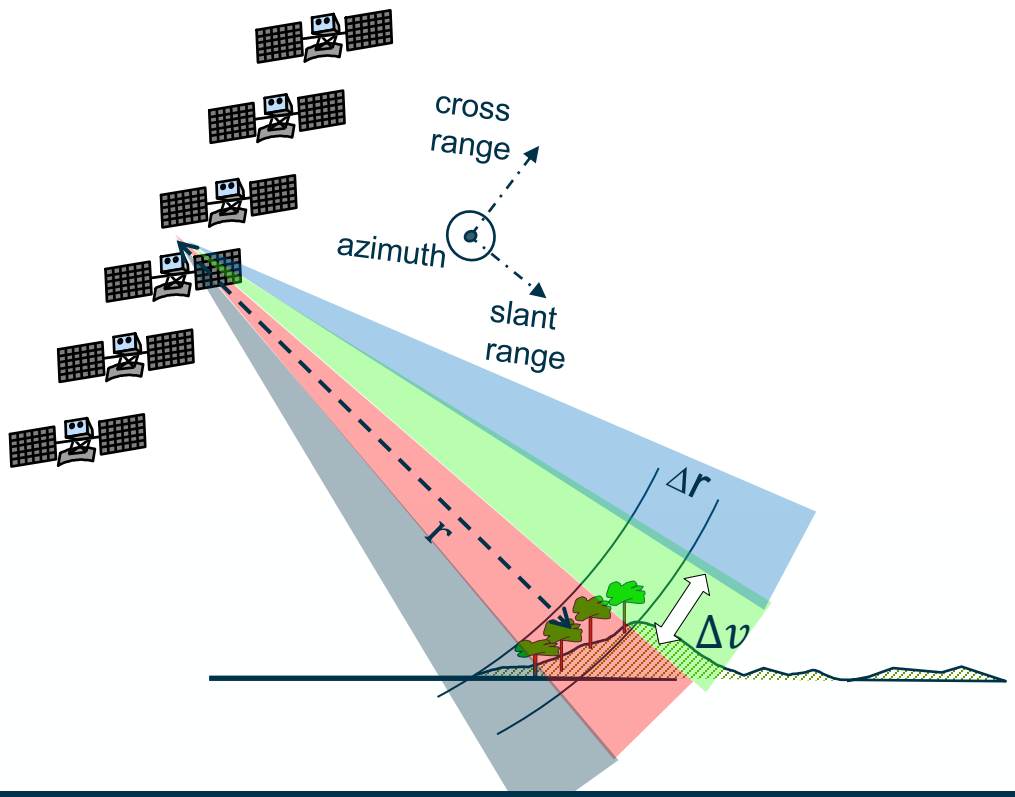

TomoSAR cube

Each voxel is associated with a range/azimuth/cross range resolution cell

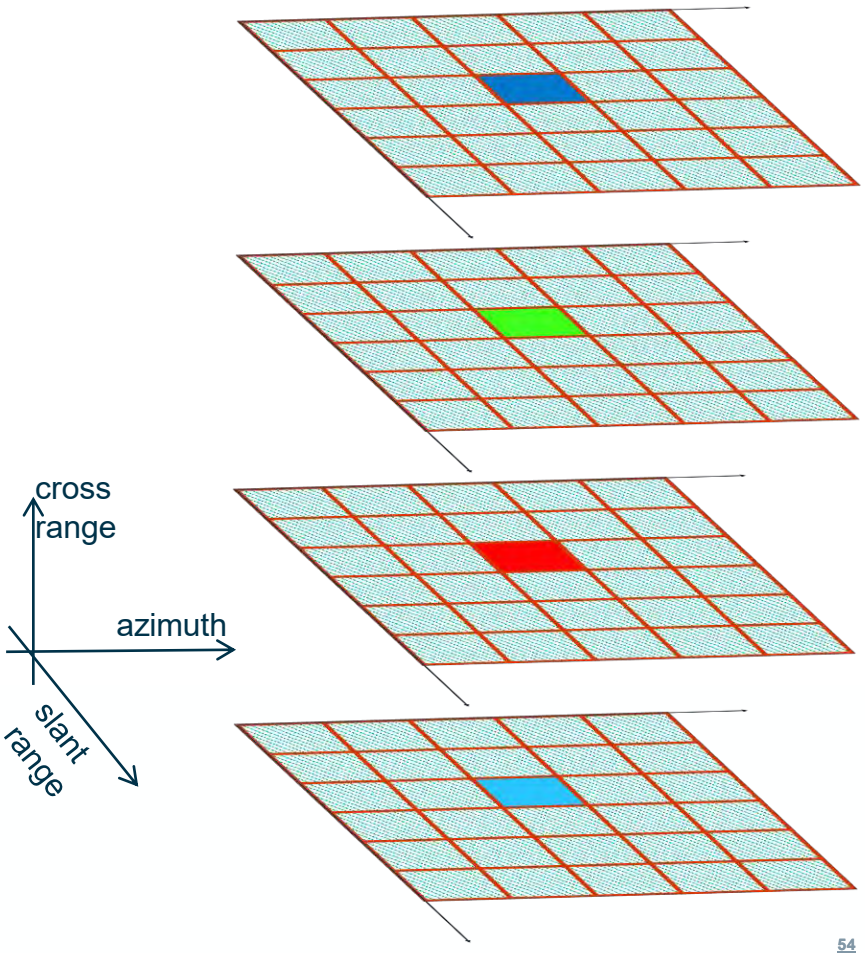

TomoSAR Processing

Mathematical model of a SAR pixel

$$I(r,x) = \int_C A(x,y,z) \cdot e^{-j\frac{4\pi}{\lambda}R(x,y,z)} dxdydz$$

$C = resolution\ cell$

SAR pixel = Integral of all contributions within the resolution cell

- Each elementary scatterer is phase-rotated according to its distance from the Radar

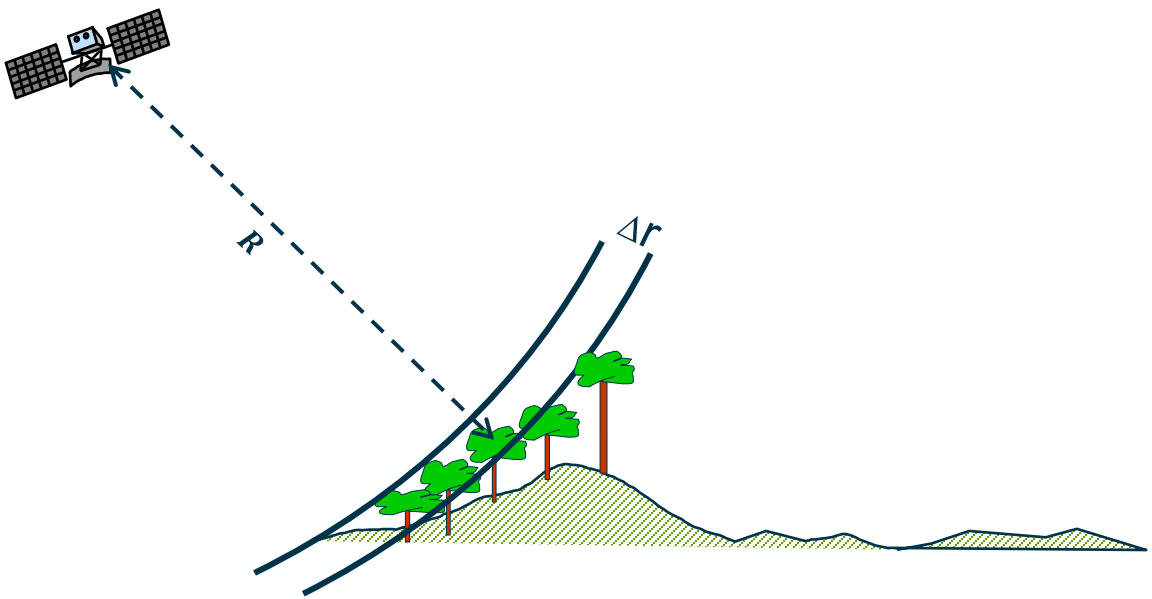

Mathematical model of a SAR pixel

$$I_n(r,x) = \int_{Cn} A(x,y,z) \cdot e^{-j\frac{4\pi}{\lambda}R_n(x,y,z)} dxdydz$$

Cn = resolution cell for the n-th view point

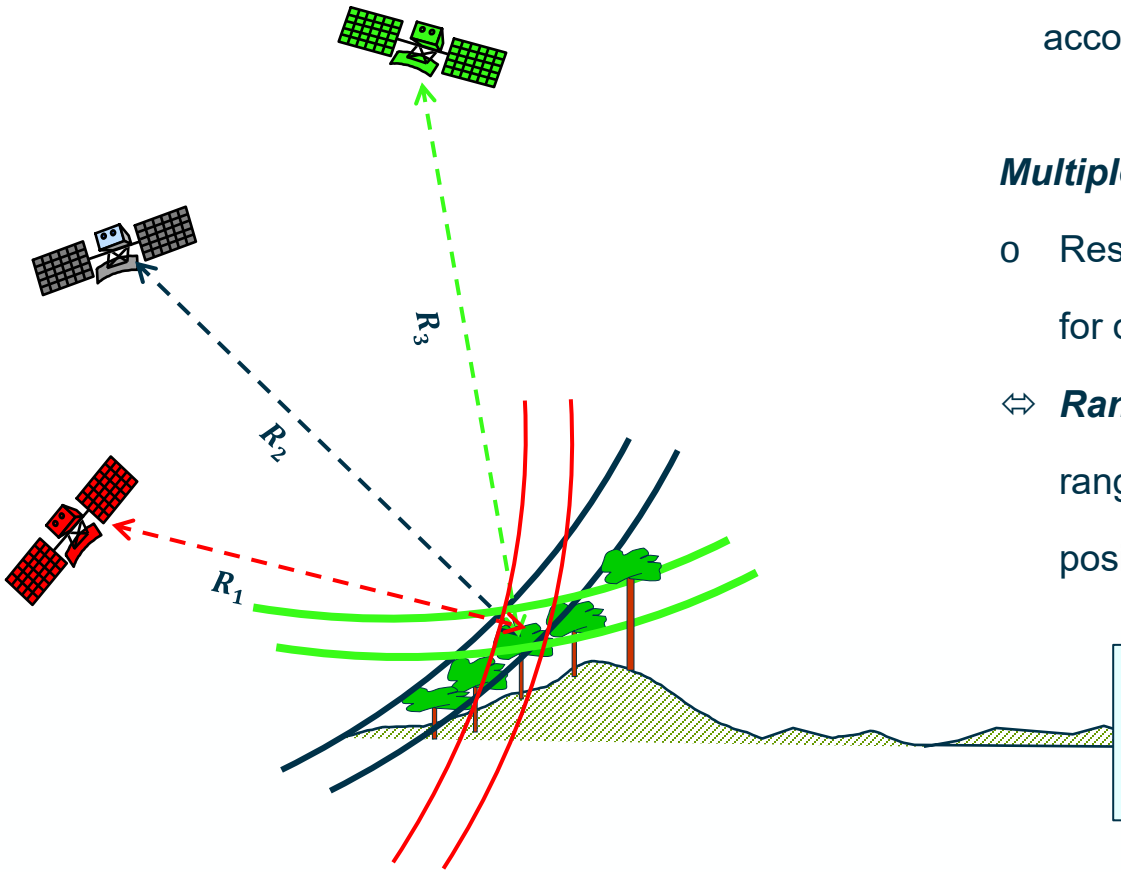

SAR pixel = Integral of all contributions within the resolution cell

- Each elementary scatterer is phase-rotated according to its distance from the Radar

Multiple baselines

- Resolution cell is oriented at different angles for different baselines

⇔ ***Range migration:*** Targets at different cross-range positions appear at different range positions for different baselines

Exact TomoSAR focusing requires 3D Back-Projection

Relaxing the model…

Hp1: range migration is negligible

⇔ *small aperture, small bandwidth, targets are distributed in a small angular sector*

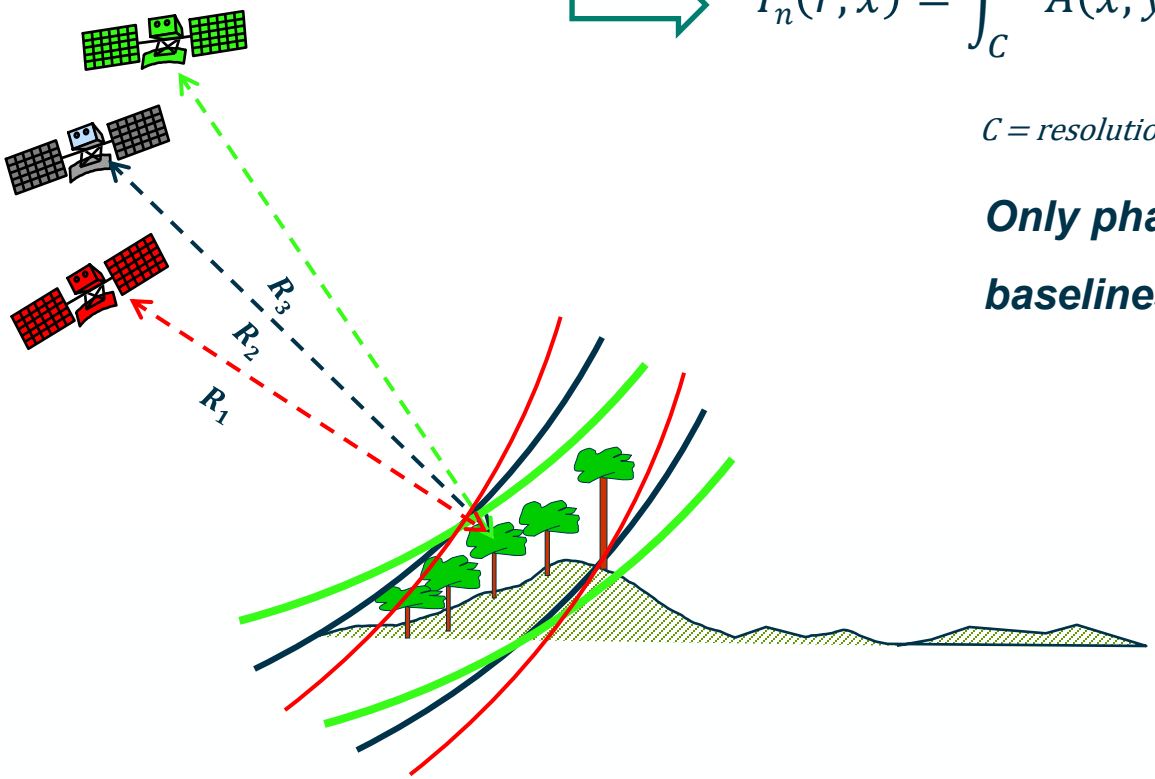

$$I_n(r,x) = \int_C A(x,y,z) \cdot e^{-j\frac{4\pi}{\lambda}R_n(x,y,z)} dxdydz$$

$C = resolution\ cell$

Only phase terms vary w.r.t. baselines

Relaxing the model…

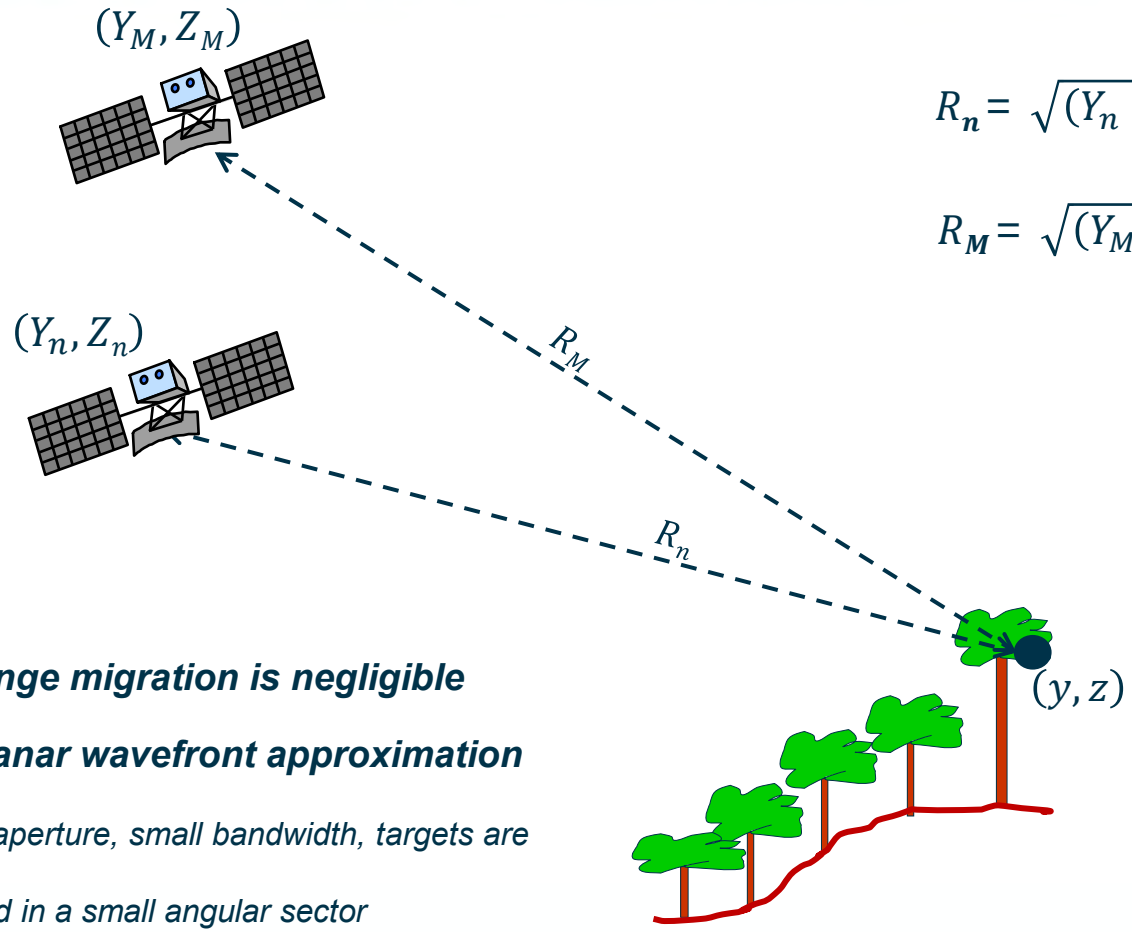

$$R_{\boldsymbol{n}} = \sqrt{(Y_n - y)^2 + (Z_n - z)^2}$$

$$R_{\boldsymbol{M}} = \sqrt{(Y_M - y)^2 + (Z_M - z)^2}$$

Hp1: range migration is negligible

Hp2: planar wavefront approximation

⇔ small aperture, small bandwidth, targets are distributed in a small angular sector

Relaxing the model…

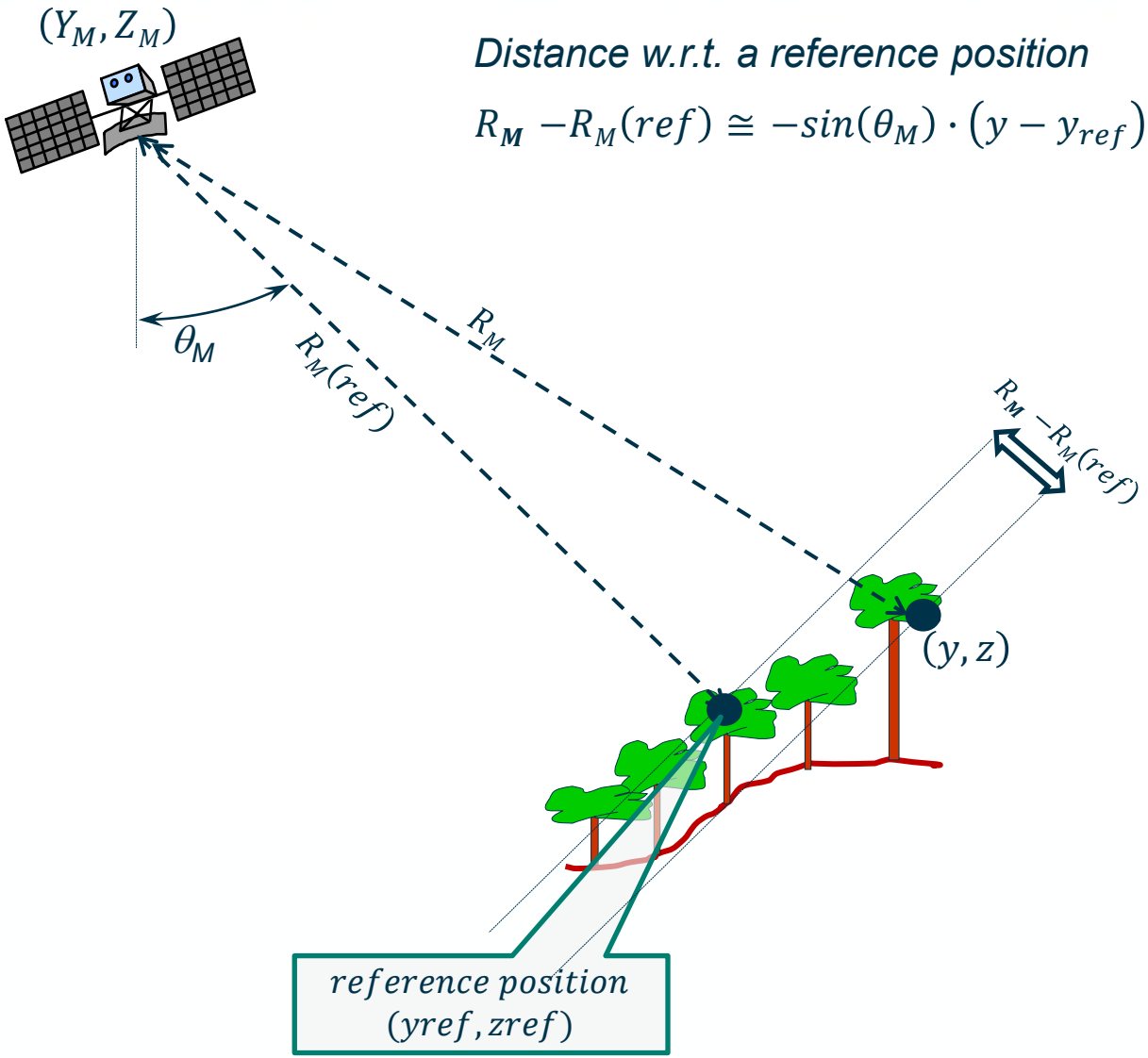

Distance w.r.t. a reference position

$$R_{\boldsymbol{M}} - R_M(ref) \cong -sin(\theta_M) \cdot (y - y_{ref}) + cos(\theta_M) \cdot (z - z_{ref})$$

Relaxing the model…

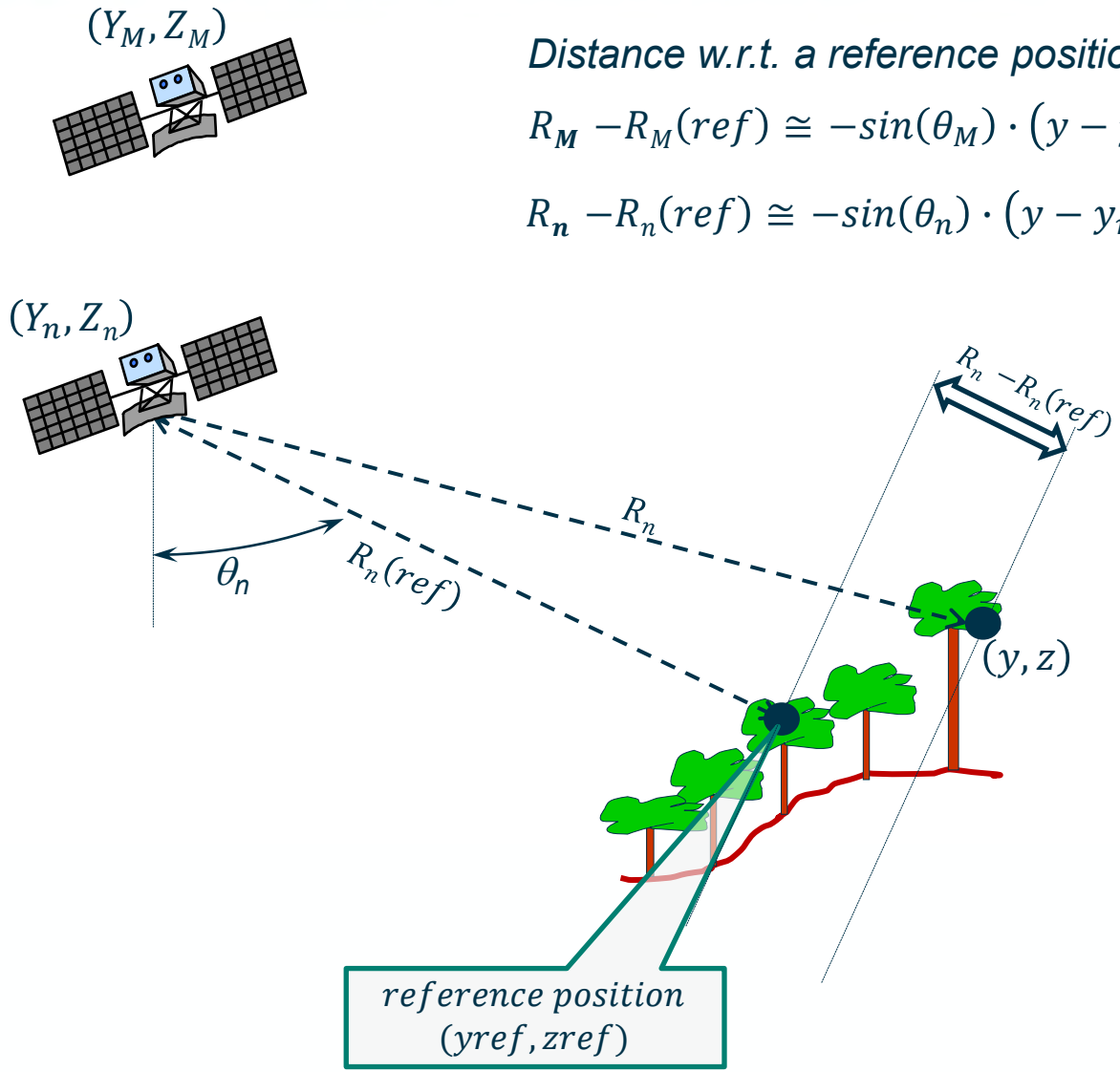

Distance w.r.t. a reference position

$$R_{\boldsymbol{M}} - R_M(ref) \cong -sin(\theta_M) \cdot (y - y_{ref}) + cos(\theta_M) \cdot (z - z_{ref})$$

$$R_{\boldsymbol{n}} - R_n(ref) \cong -sin(\theta_n) \cdot (y - y_{ref}) + cos(\theta_n) \cdot (z - z_{ref})$$

Relaxing the model…

$$R_n - R_n(ref) - \left(R_M - R_M(ref)\right)$$
$$\cong (\theta_n - \theta_M) \cdot \left[cos(\theta_M) \cdot (y - y_{ref}) + sin(\theta_n) \cdot (z - z_{ref})\right]$$

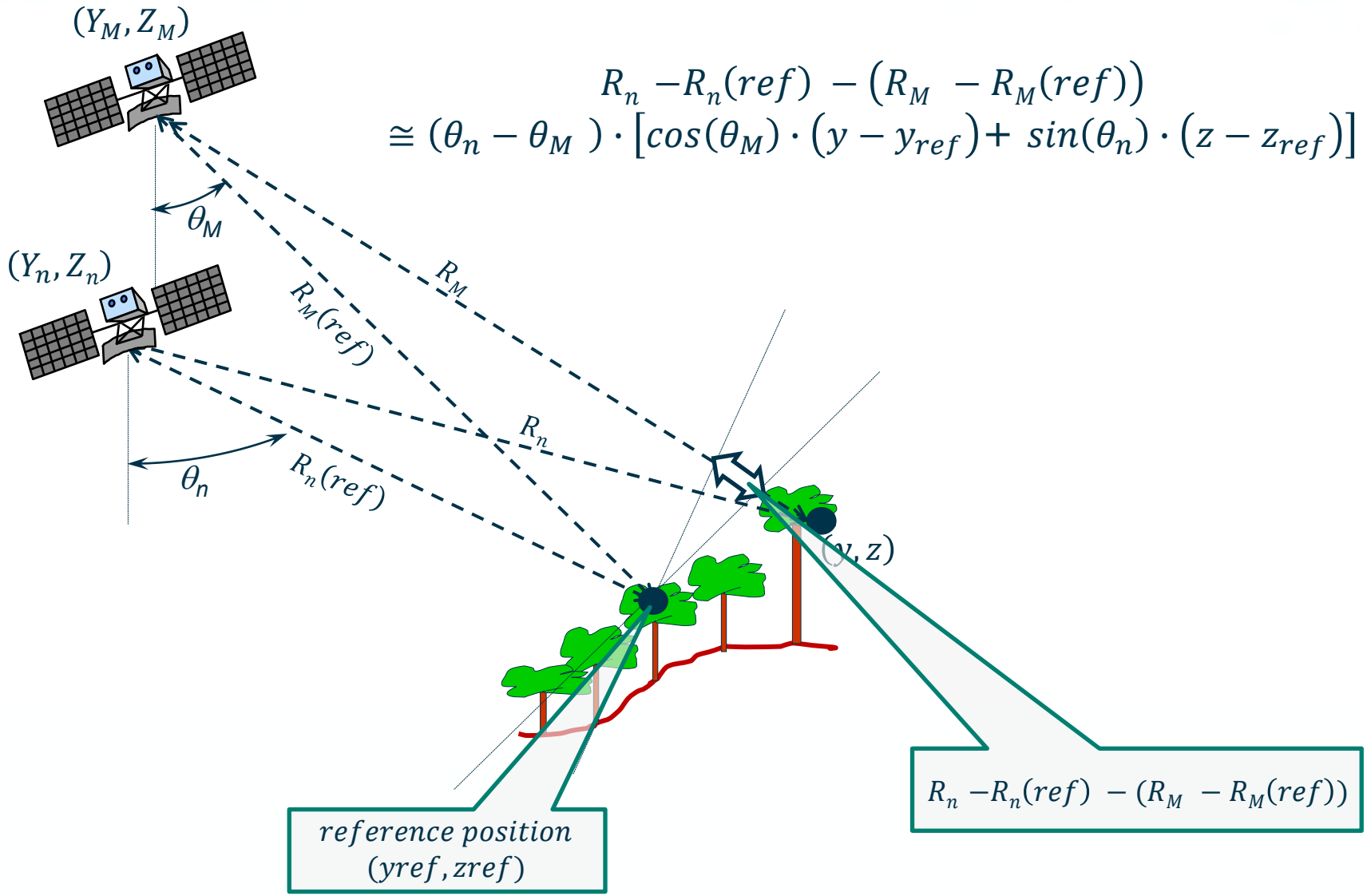

Relaxing the model…

$$R_n - R_n(ref) - \left(R_M - R_M(ref)\right)$$
$$\cong (\theta_n - \theta_M) \cdot \left[\cos(\theta_M) \cdot (y - y_{ref}) + \sin(\theta_n) \cdot (z - z_{ref})\right]$$
$$= (\theta_n - \theta_M) \cdot v$$

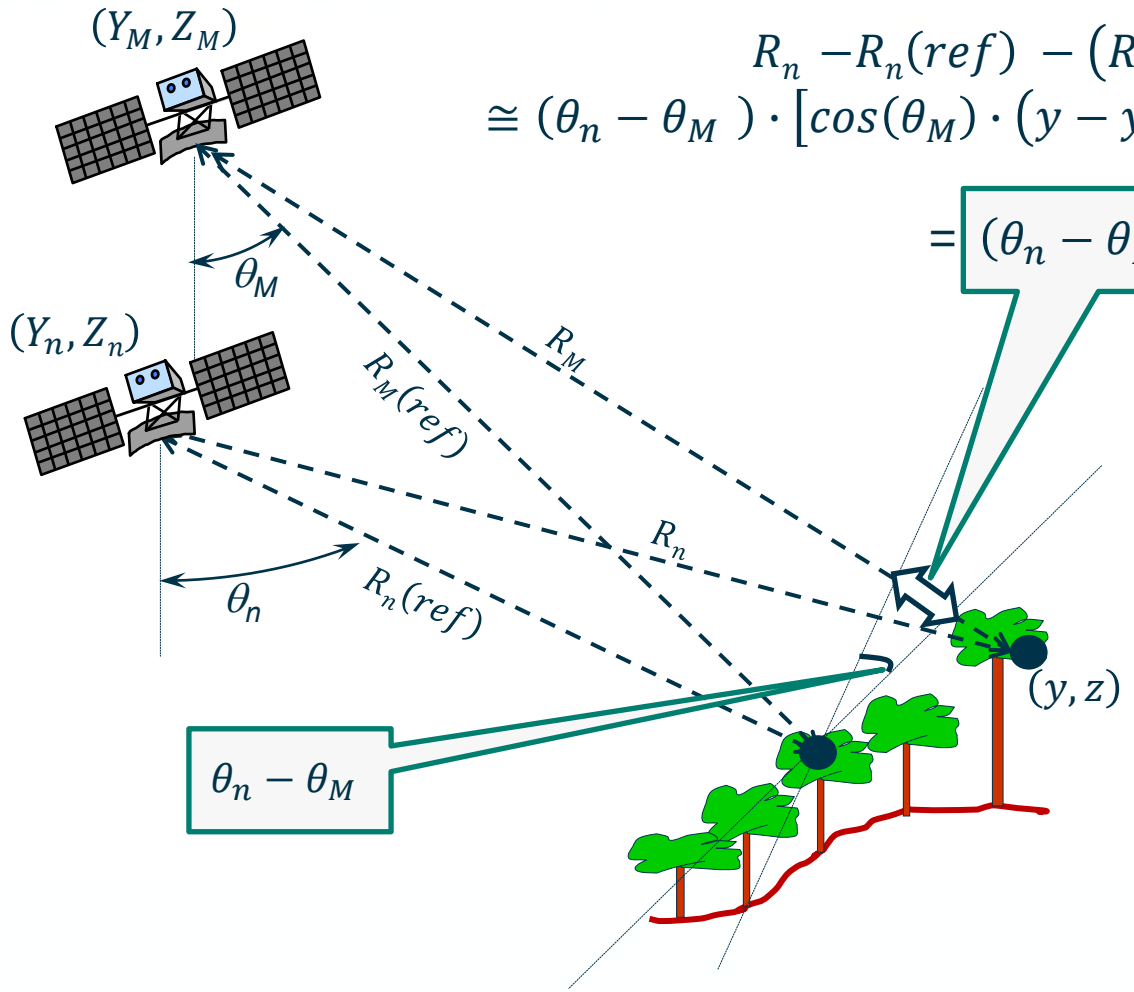

Mathematical model of a SAR pixel

b_n = **normal baseline** *of the n-th view w.r.t. the Master view*

$$b_n = (\theta_n - \theta_M\ ) \cdot R_M(ref)$$

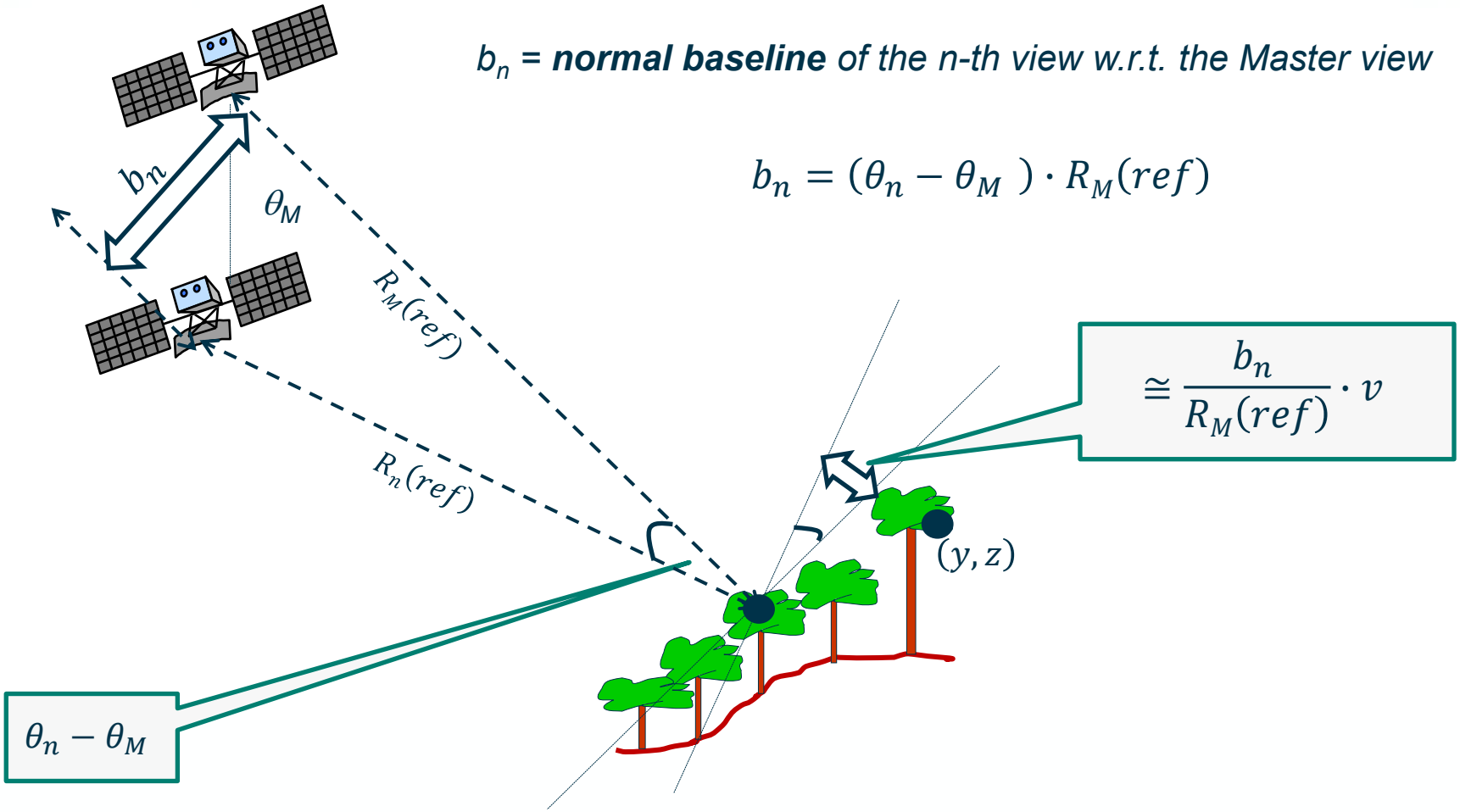

Relaxed model

$$I_n(r,x) = exp\left\{-j\frac{4\pi}{\lambda}R_n(ref)\right\} \cdot \int_C A(r',x',v)exp\left\{-j\frac{4\pi}{\lambda}r'\right\} \cdot exp\left\{-j\frac{4\pi}{\lambda}\frac{b_n}{r}v\right\}dx'dr'dv$$

Relaxed model

$$I_n(r,x) = exp\left\{-j\frac{4\pi}{\lambda}R_n(ref)\right\}\cdot\int_C A(r',x',v)exp\left\{-j\frac{4\pi}{\lambda}r'\right\}\cdot exp\left\{-j\frac{4\pi}{\lambda}\frac{b_n}{r}v\right\}dx'dr'dv$$

This term is common to all images

Relaxed model

$$I_n(r,x) = exp\left\{-j\frac{4\pi}{\lambda}R_n(ref)\right\}\cdot\int_C A(r',x',v)exp\left\{-j\frac{4\pi}{\lambda}r'\right\}\cdot exp\left\{-j\frac{4\pi}{\lambda}\frac{b_n}{r}v\right\}dx'dr'dv$$

This term is common to all images

Solving the integral w.r.t. r' and x' one gets

$$\boxed{I_n(r,x) = exp\left\{-j\frac{4\pi}{\lambda}R_n(ref)\right\}\cdot\int_C s(r,x,v)\cdot exp\left\{-j\frac{4\pi}{\lambda}\frac{b_n}{r}v\right\}dv}$$

Relaxed model

$$I_n(r,x) = exp\left\{-j\frac{4\pi}{\lambda}R_n(ref)\right\}\cdot\int_C A(r',x',v)exp\left\{-j\frac{4\pi}{\lambda}r'\right\}\cdot exp\left\{-j\frac{4\pi}{\lambda}\frac{b_n}{r}v\right\}dx'dr'dv$$

This term is common to all images

Solving the integral w.r.t. r' and x' one gets

$$\boxed{I_n(r,x) = exp\left\{-j\frac{4\pi}{\lambda}R_n(ref)\right\}\cdot\int_C s(r,x,v)\cdot exp\left\{-j\frac{4\pi}{\lambda}\frac{b_n}{r}v\right\}dv}$$

Phase offset to be removed based on knowledge of the acquisition geometry (terrain flattening)

Relaxed model

$$I_n(r,x) = exp\left\{-j\frac{4\pi}{\lambda}R_n(ref)\right\}\cdot\int_C A(r',x',v)exp\left\{-j\frac{4\pi}{\lambda}r'\right\}\cdot exp\left\{-j\frac{4\pi}{\lambda}\frac{b_n}{r}v\right\}dx'dr'dv$$

This term is common to all images

Solving the integral w.r.t. r' and x' one gets

$$I_n(r,x) = exp\left\{-j\frac{4\pi}{\lambda}R_n(ref)\right\}\cdot\int_C s(r,x,v)\cdot exp\left\{-j\frac{4\pi}{\lambda}\frac{b_n}{r}v\right\}dv$$

Phase offset to be removed based on knowledge of the acquisition geometry (terrain flattening)

s(r,x,v) = cross-range projection of target reflectivity within the SAR resolution cell at (r,x)

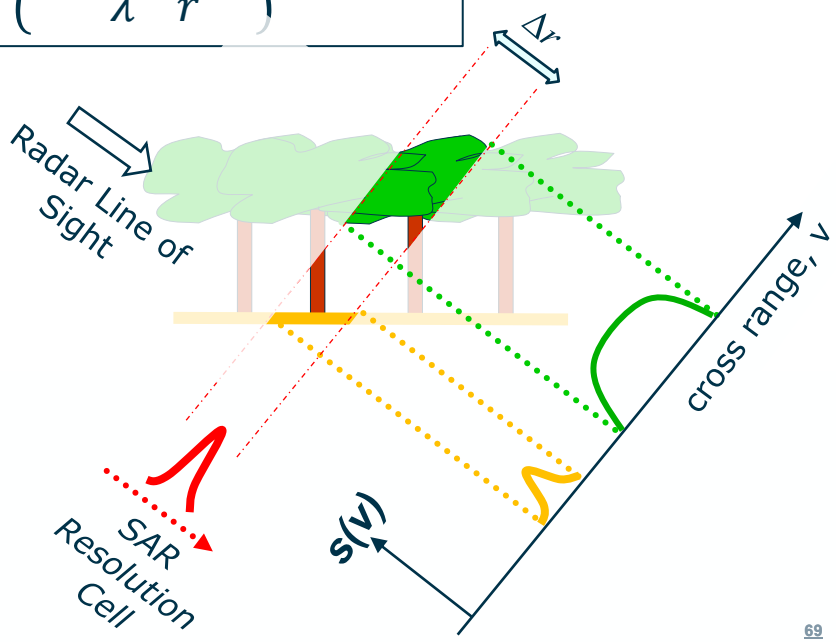

TomoSAR focusing

SAR Tomography can now be formulated according to one simple principle:

Each focused SLC SAR image is obtained as the Fourier Transform of the scene complex reflectivity projected along the cross-range coordinate

$$I_n(r,x) = \int_C s(r,x,v) \cdot exp\left\{-j\frac{4\pi}{\lambda}\frac{b_n}{r}v\right\} dv$$

$I_n(r,x)$: SLC pixel in the *n-th* image

$s(r,x,v)$: cross-range projection of target reflectivity within the SAR resolution cell at (r,x)

b_n : normal baseline for the *n-th* image

λ : carrier wavelength

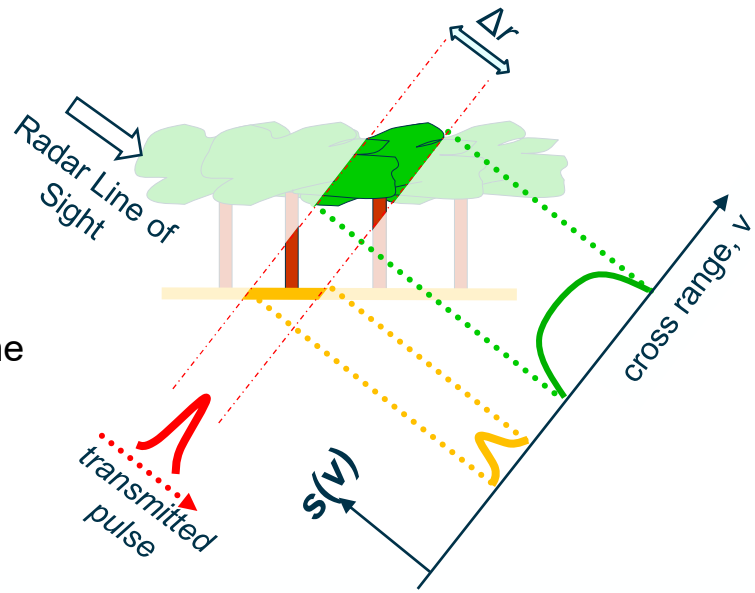

TomoSAR focusing

Each focused SLC SAR image is obtained as the Fourier Transform of the scene complex reflectivity along the cross-range coordinate

$\Rightarrow$ The cross-range distribution of the complex reflectivity can be retrieved by Fourier transforming SLC data with respect to the normal baseline

$$\hat{s}(r,x,v) = DFT\{I_n(r,x)\}$$

DFT = Discreet Fourier Transform

In other words…

$$I_n(r,x) = \int s(r,x,v)\exp\left(-j\frac{4\pi}{\lambda r}b_n v\right)dv$$

$$\Rightarrow \quad \hat{s}(r,x,v) = \sum_n I_n(r,x)\exp\left(+j\frac{4\pi}{\lambda r}b_n v\right)$$

$I_n(r,x)$ = observation

$s(r,x,v)$ = unknown

$\hat{s}(r,x,v)$ = inversion

TomoSAR focusing – examples

$$I_n(r,x) = \int_C s(r,x,v) \cdot exp\left\{-j\frac{4\pi}{\lambda}\frac{b_n}{r}v\right\} dv$$

$$\hat{s}(r,x,v) = \sum_n I_n(r,x)\exp\left(+j\frac{4\pi}{\lambda r}b_n v\right)$$

Case 1: one point target

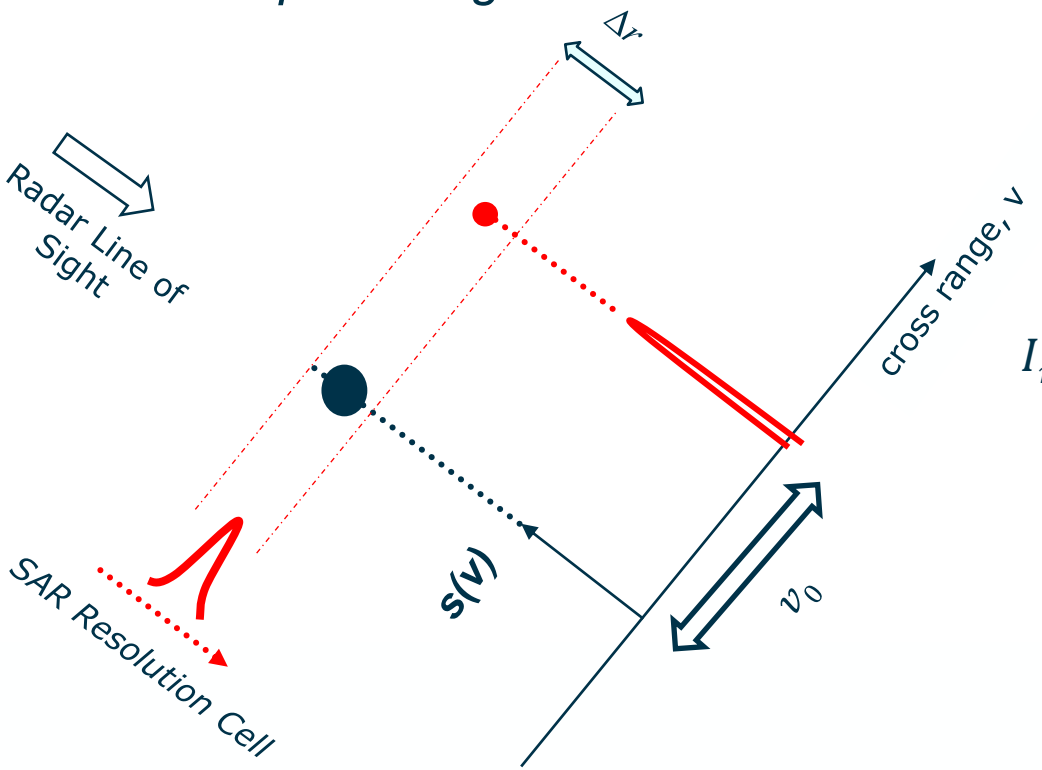

$$I_n(r,x) = s_0 \cdot exp\left\{-j\frac{4\pi}{\lambda}\frac{b_n}{r}v_0\right\}$$

● = reference position

TomoSAR focusing – examples

$$I_n(r,x) = \int_C s(r,x,v) \cdot exp\left\{-j\frac{4\pi}{\lambda}\frac{b_n}{r}v\right\} dv$$

$$\hat{s}(r,x,v) = \sum_n I_n(r,x)\exp\left(+j\frac{4\pi}{\lambda r}b_n v\right)$$

Case 1: one point target

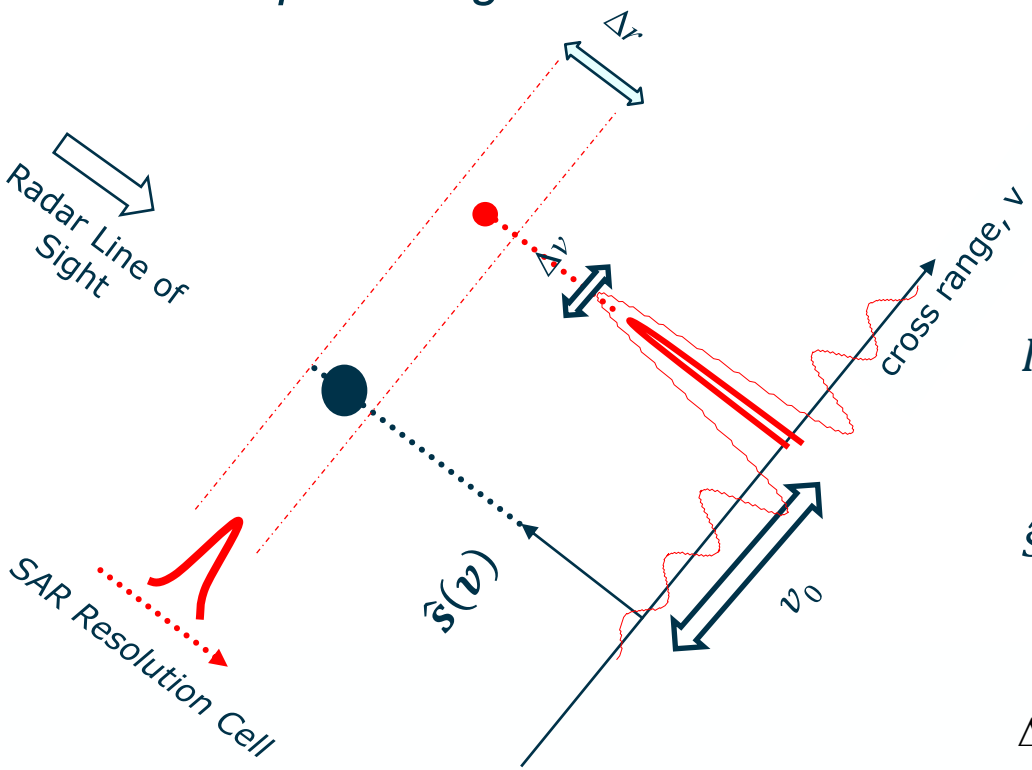

$$I_n(r,x) = s_0 \cdot exp\left\{-j\frac{4\pi}{\lambda}\frac{b_n}{r}v_0\right\}$$

$$\hat{s}(r,x,v) = s_0 \cdot sinc\left(\frac{v - v_0}{\Delta v}\right)$$

$$\Delta v = \frac{\lambda r}{2b_{ap}}$$

● = reference position

Note: Constant amplitude factors omitted

TomoSAR focusing – examples

$$I_n(r,x) = \int_C s(r,x,v) \cdot exp\left\{-j\frac{4\pi}{\lambda}\frac{b_n}{r}v\right\} dv$$

$$\hat{s}(r,x,v) = \sum_n I_n(r,x)\exp\left(+j\frac{4\pi}{\lambda r}b_n v\right)$$

Case 2: two point targets

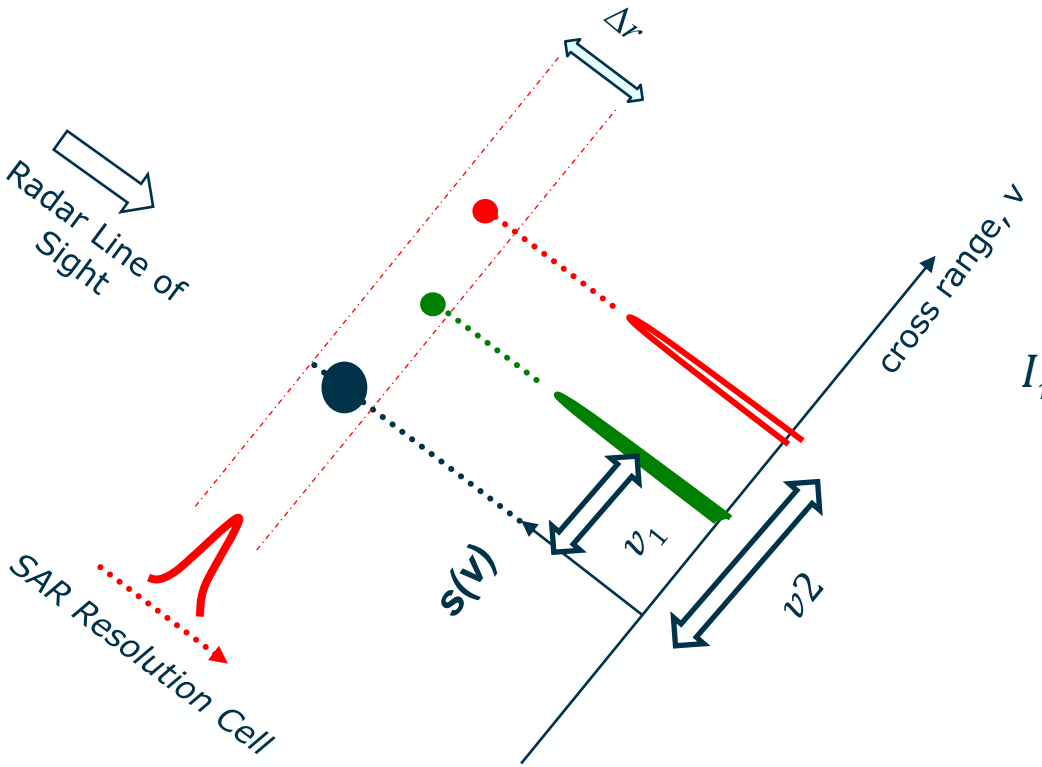

$$I_n(r,x) = \sum_{p=1}^{2} s_p \cdot exp\left\{-j\frac{4\pi}{\lambda}\frac{b_n}{r}v_p\right\}$$

● = reference position

TomoSAR focusing – examples

$$I_n(r,x) = \int_C s(r,x,v) \cdot exp\left\{-j\frac{4\pi}{\lambda}\frac{b_n}{r}v\right\} dv$$

$$\hat{s}(r,x,v) = \sum_n I_n(r,x)\exp\left(+j\frac{4\pi}{\lambda r}b_n v\right)$$

Case 2: two point targets

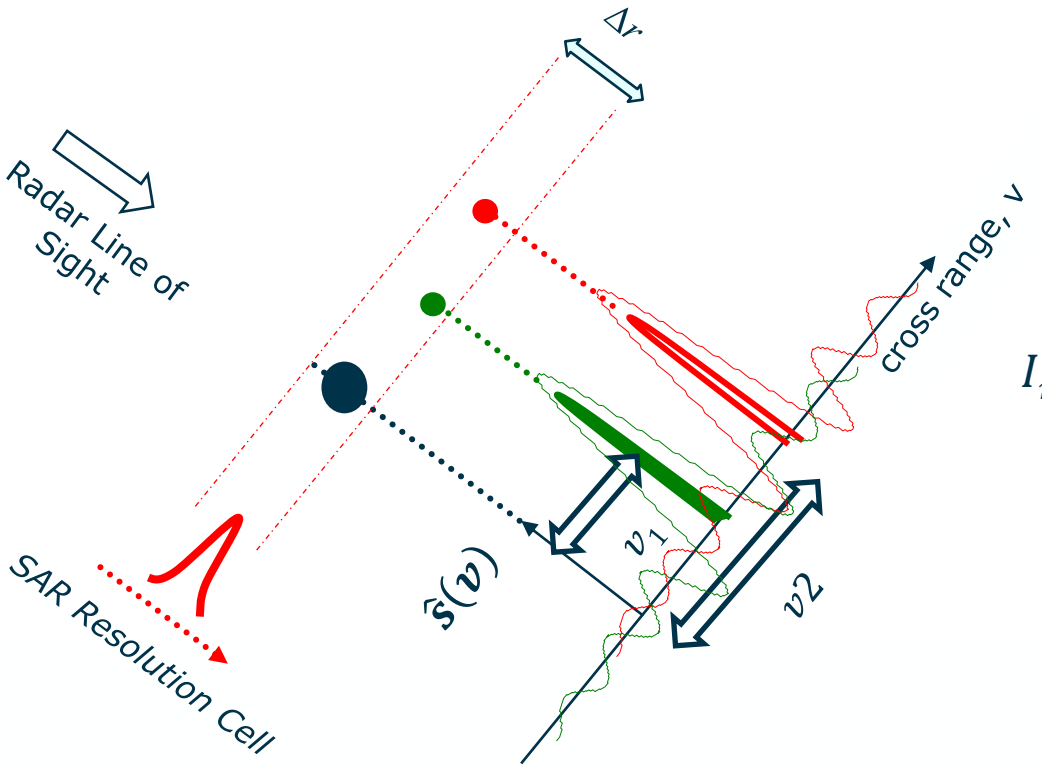

$$I_n(r,x) = \sum_{p=1}^{2} s_p \cdot exp\left\{-j\frac{4\pi}{\lambda}\frac{b_n}{r}v_p\right\}$$

$$\hat{s}(r,x,v) = \sum_{p=1}^{2} s_p \cdot sinc\left(\frac{v - vp}{\Delta v}\right)$$

● = reference position

Note: Constant amplitude factors omitted

TomoSAR focusing – examples

$$I_n(r,x) = \int_C s(r,x,v) \cdot exp\left\{-j\frac{4\pi}{\lambda}\frac{b_n}{r}v\right\} dv$$

$$\hat{s}(r,x,v) = \sum_n I_n(r,x)\exp\left(+j\frac{4\pi}{\lambda r}b_n v\right)$$

Case 3: terrain

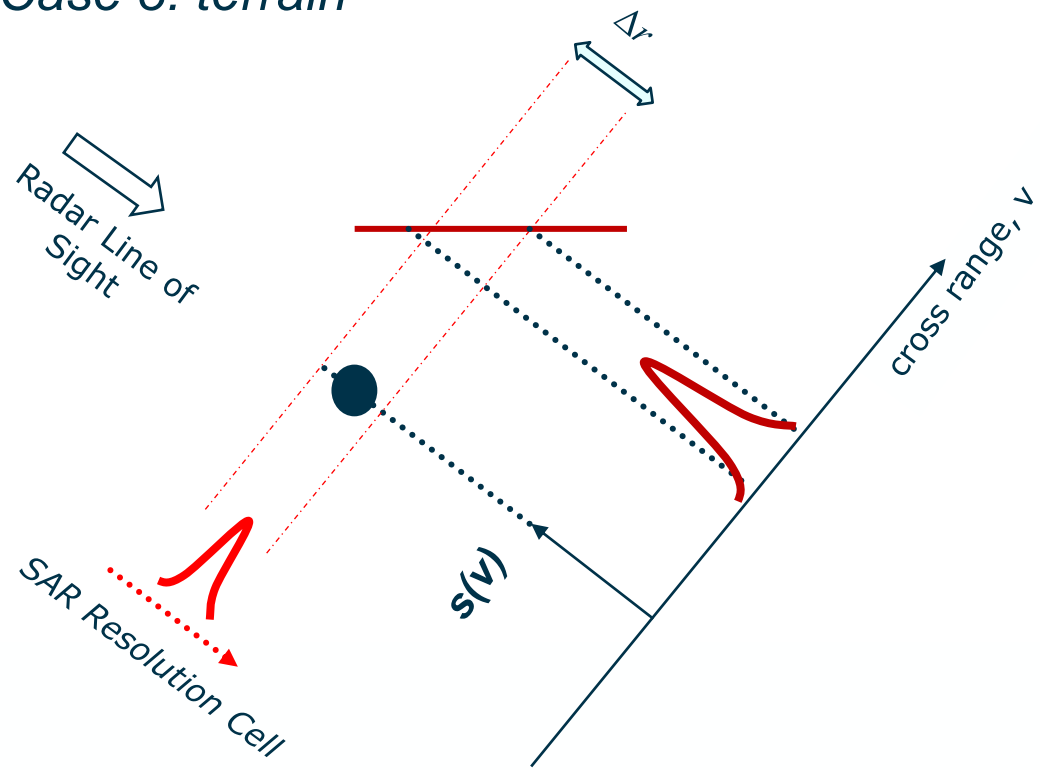

● = reference position

Terrain = extended target

⇔ *It does not project into a peak*

⇔ *Cross-range spread*

TomoSAR focusing – examples

$$I_n(r,x) = \int_C s(r,x,v) \cdot exp\left\{-j\frac{4\pi}{\lambda}\frac{b_n}{r}v\right\} dv$$

$$\hat{s}(r,x,v) = \sum_n I_n(r,x)\exp\left(+j\frac{4\pi}{\lambda r}b_n v\right)$$

Case 3: terrain

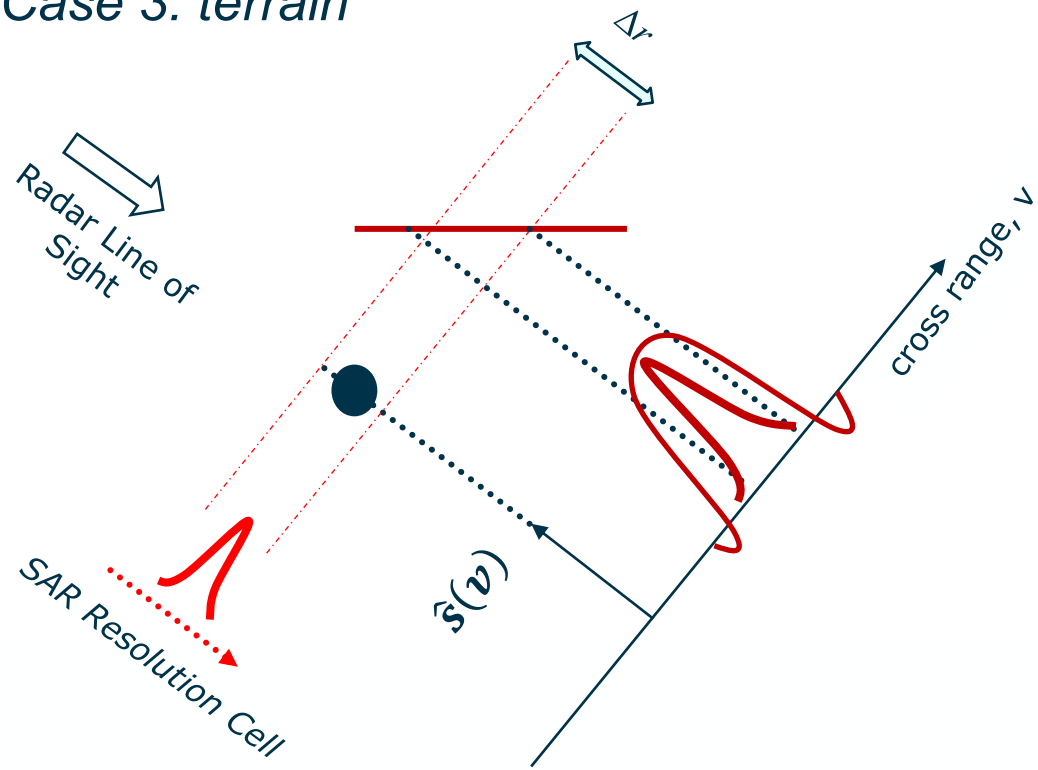

● = reference position

TomoSAR focusing – examples

$$I_n(r,x) = \int_C s(r,x,v) \cdot exp\left\{-j\frac{4\pi}{\lambda}\frac{b_n}{r}v\right\} dv$$

$$\hat{s}(r,x,v) = \sum_n I_n(r,x)\exp\left(+j\frac{4\pi}{\lambda r}b_n v\right)$$

Case 3: terrain

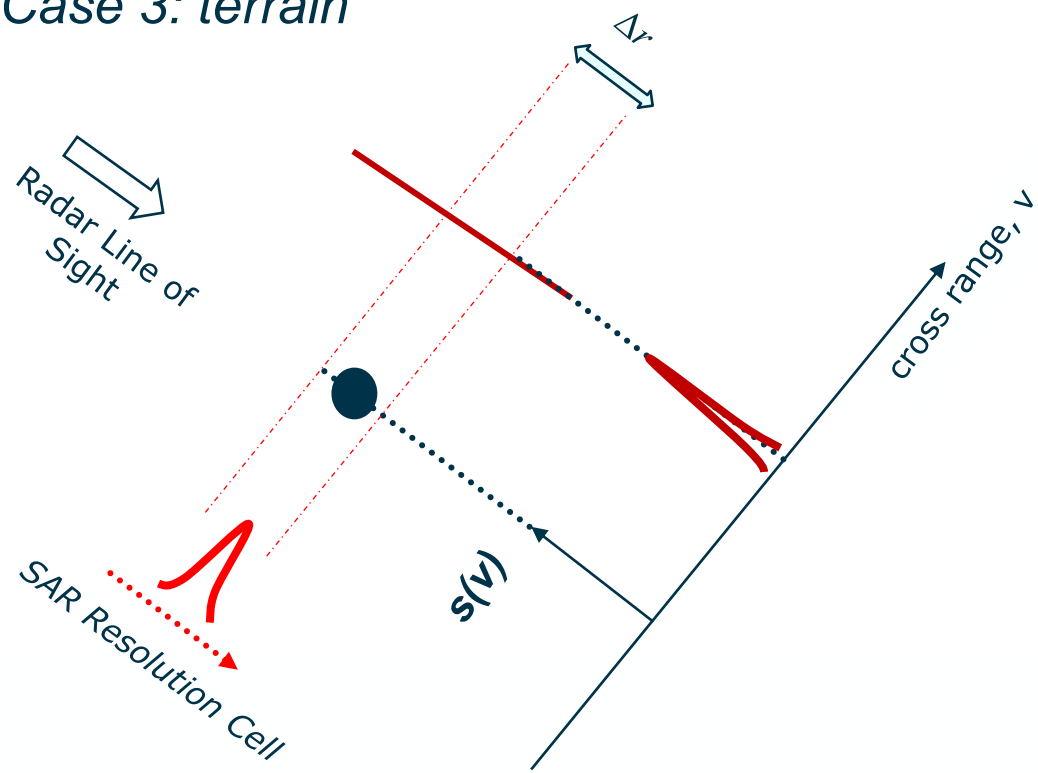

● = reference position

Terrain = extended target

⇔ *Cross-range spread depends on terrain slope*

TomoSAR focusing – examples

$$I_n(r,x) = \int_C s(r,x,v) \cdot exp\left\{-j\frac{4\pi}{\lambda}\frac{b_n}{r}v\right\} dv$$

$$\hat{s}(r,x,v) = \sum_n I_n(r,x)\exp\left(+j\frac{4\pi}{\lambda r}b_n v\right)$$

Case 3: terrain

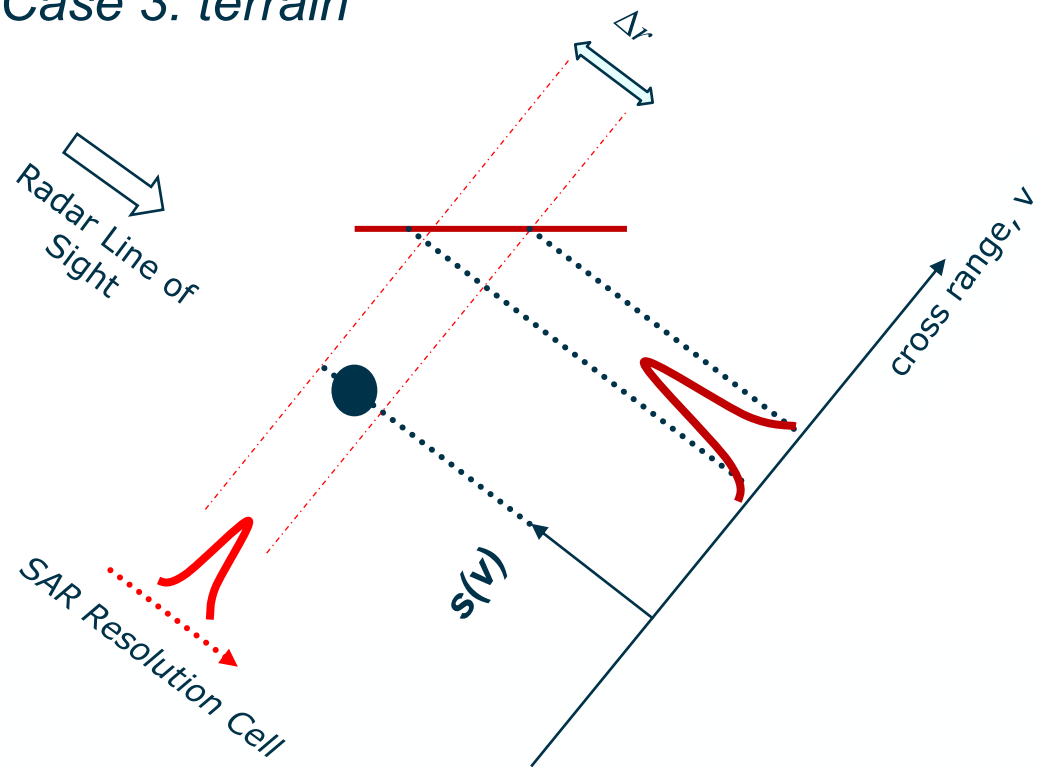

● = reference position

Terrain = extended target

⇔ *Cross-range spread depends on terrain slope*

TomoSAR focusing – examples

$$I_n(r,x) = \int_C s(r,x,v) \cdot exp\left\{-j\frac{4\pi}{\lambda}\frac{b_n}{r}v\right\} dv$$

$$\hat{s}(r,x,v) = \sum_n I_n(r,x)\exp\left(+j\frac{4\pi}{\lambda r}b_n v\right)$$

Case 3: terrain

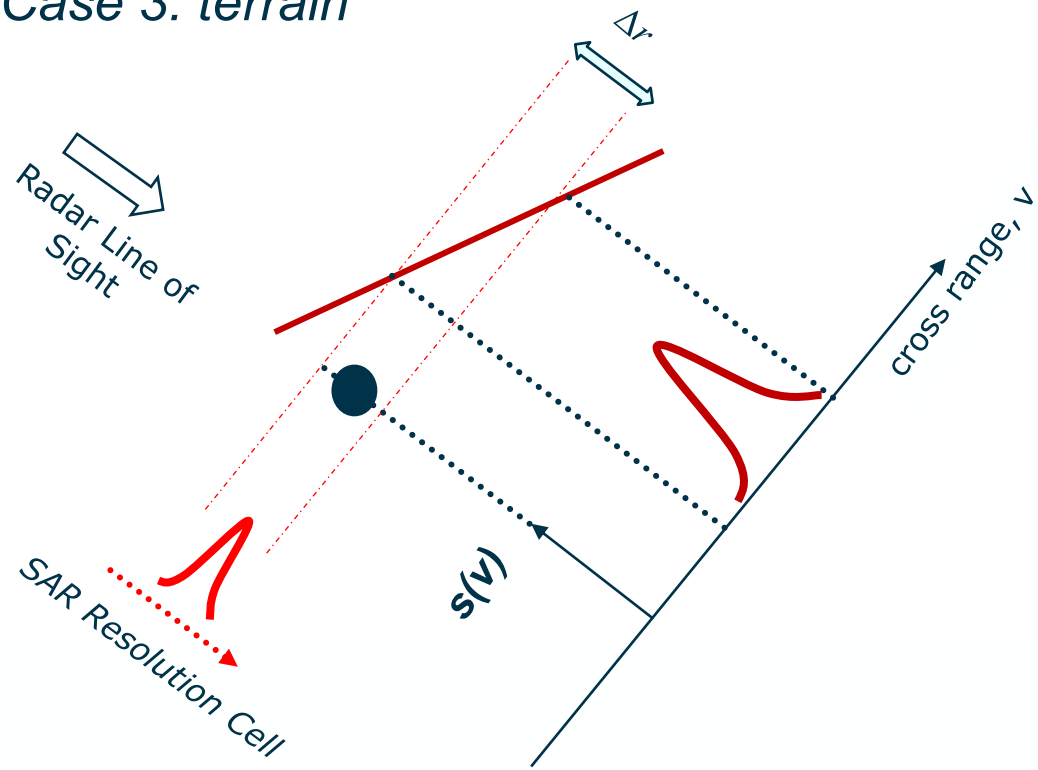

● = reference position

Terrain = extended target

⇔ *Cross-range spread depends on terrain slope*

TomoSAR focusing – examples

$$I_n(r,x) = \int_C s(r,x,v) \cdot exp\left\{-j\frac{4\pi}{\lambda}\frac{b_n}{r}v\right\} dv$$

$$\hat{s}(r,x,v) = \sum_n I_n(r,x)\exp\left(+j\frac{4\pi}{\lambda r}b_n v\right)$$

Case 4: terrain + forest

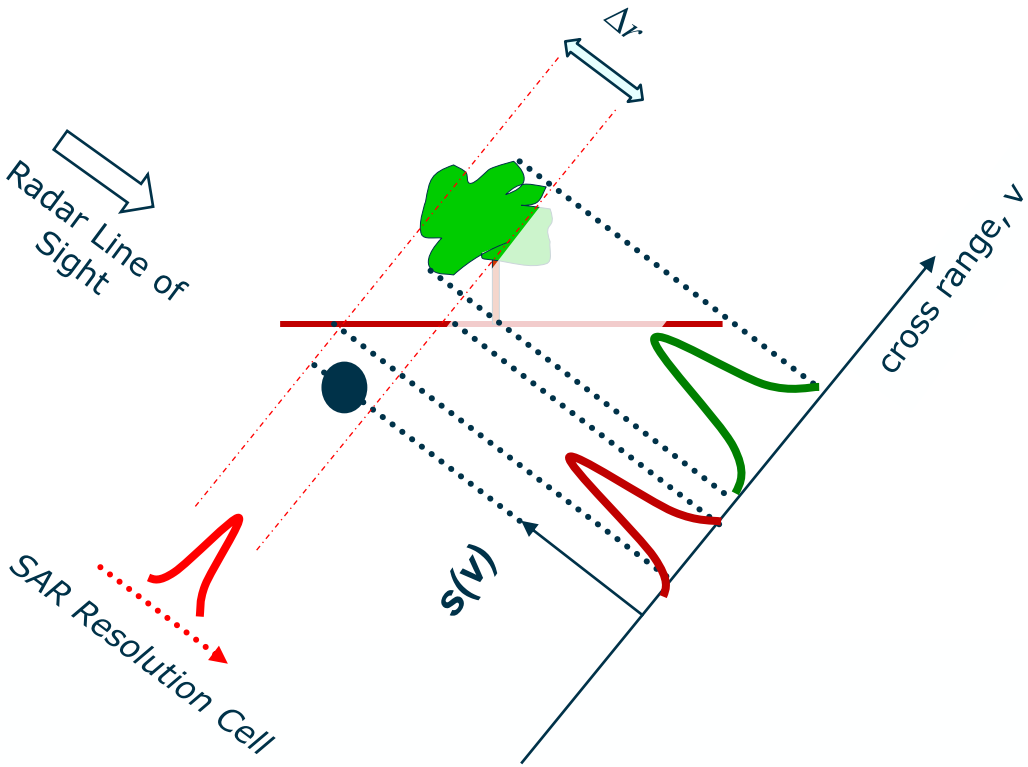

● = reference position

TomoSAR focusing – examples

$$I_n(r,x) = \int_C s(r,x,v) \cdot exp\left\{-j\frac{4\pi}{\lambda}\frac{b_n}{r}v\right\} dv$$

$$\hat{s}(r,x,v) = \sum_n I_n(r,x)\exp\left(+j\frac{4\pi}{\lambda r}b_n v\right)$$

Case 4: terrain + forest

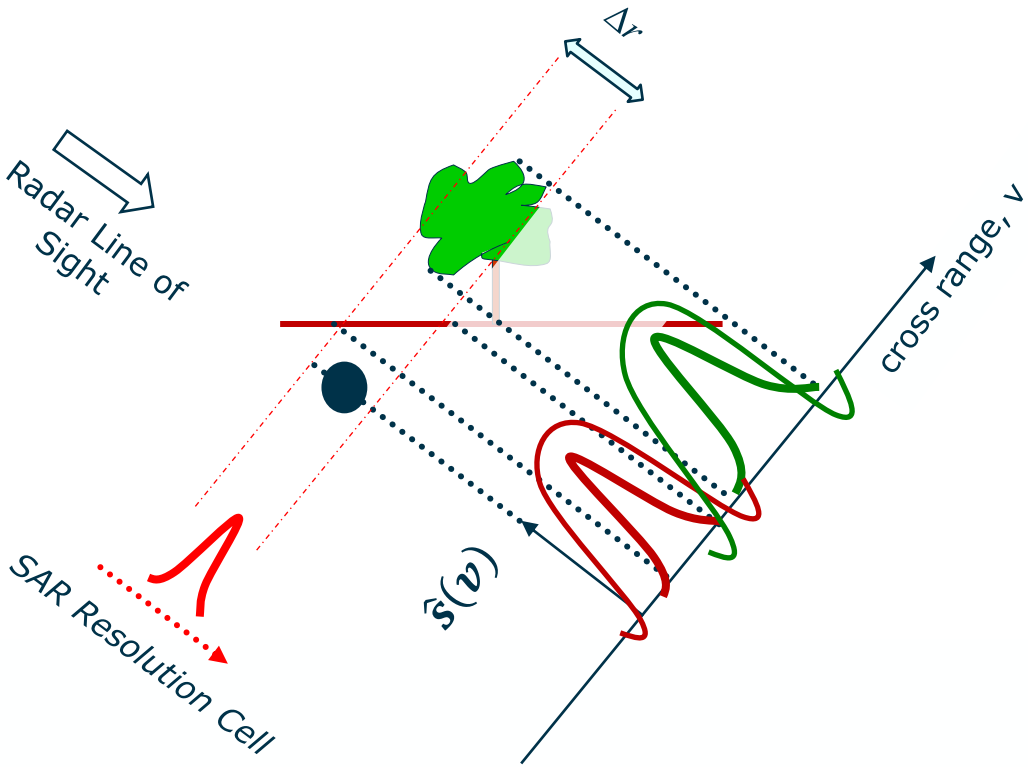

● = reference position

Ambiguity

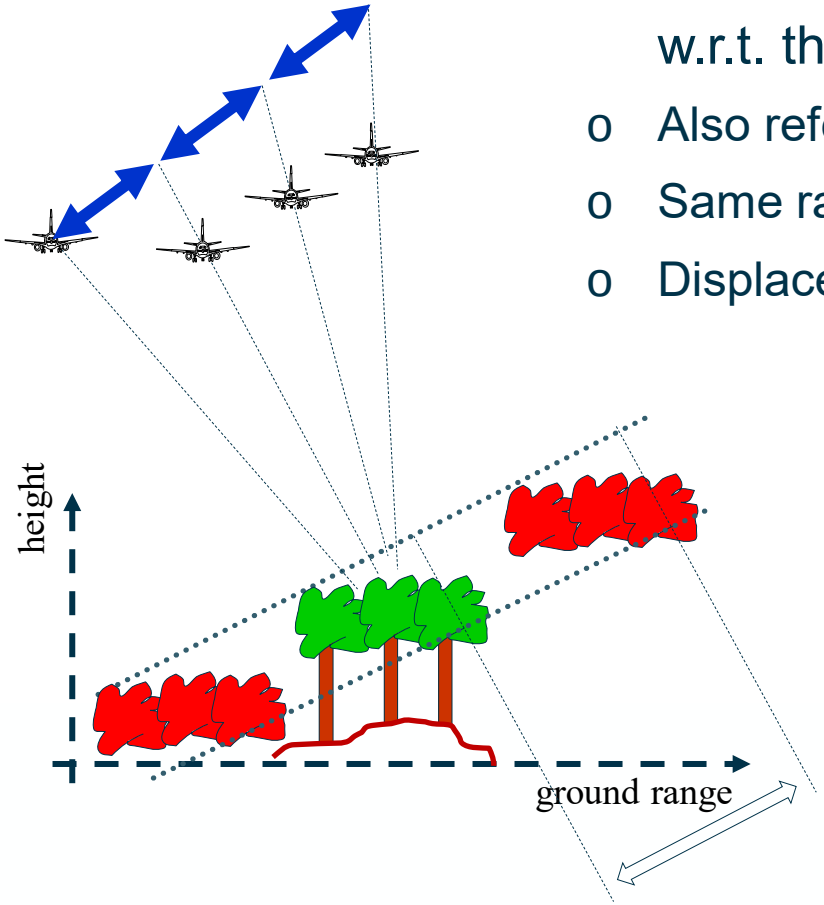

DFT produces ***periodic*** results

⇒ **Ghost** targets appearing at known position w.r.t. the real one

- Also referred to as ambiguous targets, or replicas
- Same range as the real target
- Displaced in cross-range

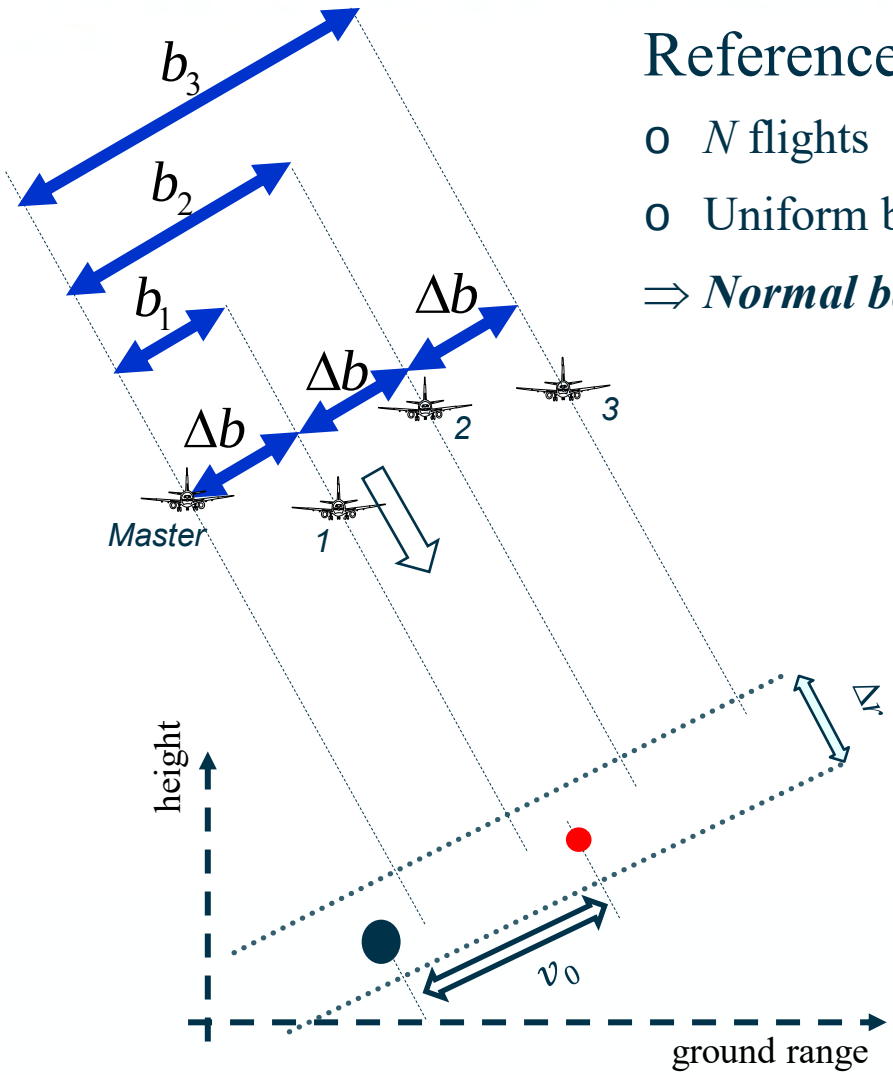

● = reference position

Reference scenario

- N flights
- Uniform baseline spacing Δb

$\Rightarrow$ ***Normal baseline for the n-th flight:*** $b_n = n\,\Delta b$

$$I_n(r,x) = s_0 \cdot exp\left\{-j\frac{4\pi}{\lambda}\frac{b_n}{r}v_0\right\}$$

$$= s_0 \cdot exp\left\{-j\frac{4\pi}{\lambda}\frac{\Delta b}{r}n \cdot v_0\right\}$$

Ambiguity

$$I_n(r,x) = s_0 \cdot exp\left\{-j\frac{4\pi}{\lambda}\frac{\Delta b}{r}n \cdot v_0\right\}$$

Phases

$$\varphi_0 = \frac{4\pi}{\lambda}\frac{\Delta b}{r}0 \cdot v_0 \qquad \varphi_1 = \frac{4\pi}{\lambda}\frac{\Delta b}{r}1 \cdot v_0 \qquad \varphi_2 = \frac{4\pi}{\lambda}\frac{\Delta b}{r}2 \cdot v_0 \qquad \varphi_3 = \frac{4\pi}{\lambda}\frac{\Delta b}{r}3 \cdot v_0$$

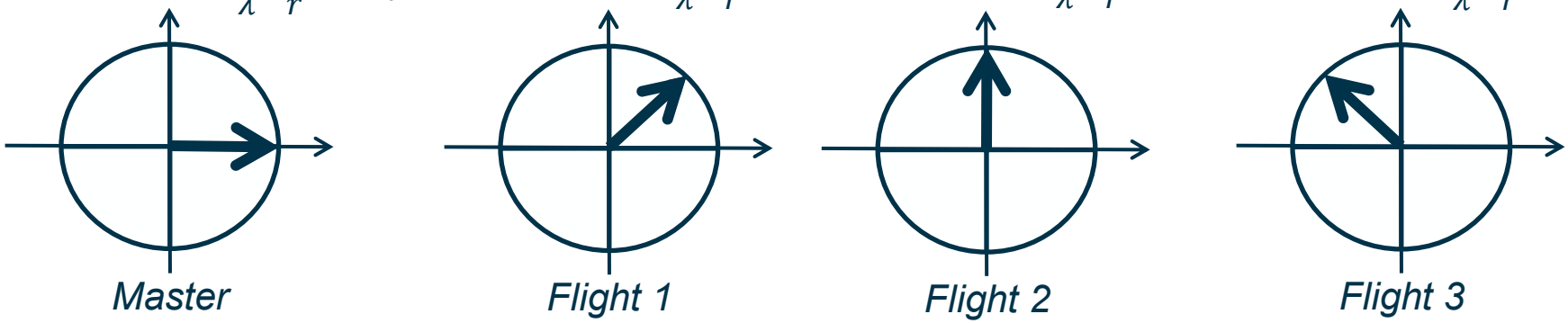

One tour = 2π

⇒ ***Different cross-range values result in the same phases for all n !!!***

Interval of ambiguity: $$v_a = \frac{\lambda r}{2\Delta b}$$

$$\frac{4\pi}{\lambda}\frac{\Delta b}{r}n \cdot (v_0 + va) = \frac{4\pi}{\lambda}\frac{\Delta b}{r}n \cdot v_0 + 2\pi n \equiv \frac{4\pi}{\lambda}\frac{\Delta b}{r}n \cdot v_0$$

Ambiguity

$$I_n(r,x) = s_0 \cdot exp\left\{-j\frac{4\pi}{\lambda}\frac{\Delta b}{r}n \cdot v_0\right\}$$

Phases

$$\varphi_0 = \frac{4\pi}{\lambda}\frac{\Delta b}{r}0 \cdot v_0$$

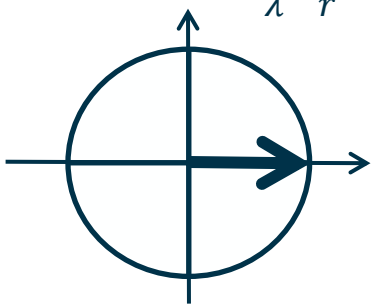

Master

$$\varphi_1 = \frac{4\pi}{\lambda}\frac{\Delta b}{r}1 \cdot v_0$$

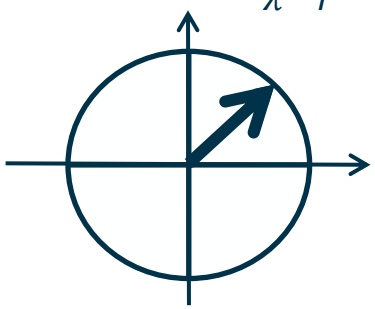

Flight 1

$$\varphi_2 = \frac{4\pi}{\lambda}\frac{\Delta b}{r}2 \cdot v_0$$

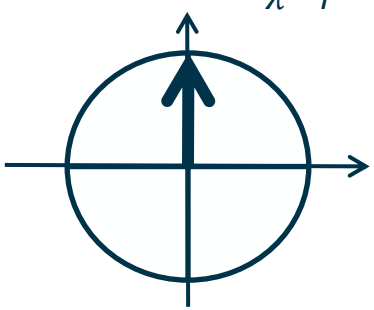

Flight 2

$$\varphi_3 = \frac{4\pi}{\lambda}\frac{\Delta b}{r}3 \cdot v_0$$

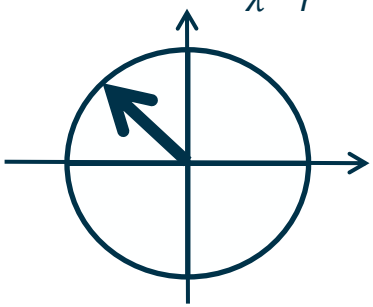

Flight 3

$$\varphi_0 = \frac{4\pi}{\lambda}\frac{\Delta b}{r}0 \cdot (v_0 + va)$$

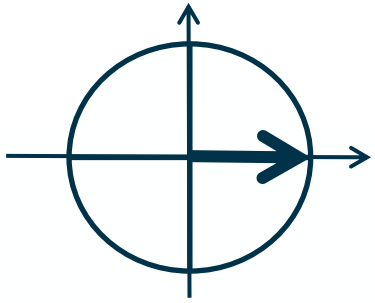

Master

$$\varphi_1 = \frac{4\pi}{\lambda}\frac{\Delta b}{r}1 \cdot (v_0 + va)$$

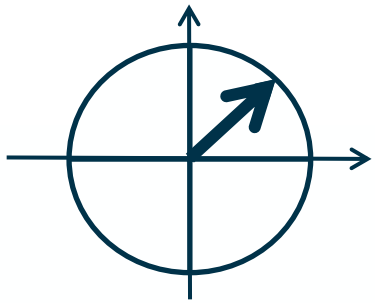

Flight 1

$$\varphi_2 = \frac{4\pi}{\lambda}\frac{\Delta b}{r}2 \cdot (v_0 + va)$$

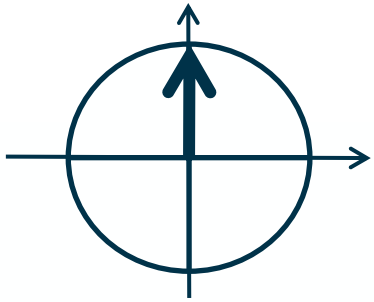

Flight 2

$$\varphi_3 = \frac{4\pi}{\lambda}\frac{\Delta b}{r}3 \cdot (v_0 + va)$$

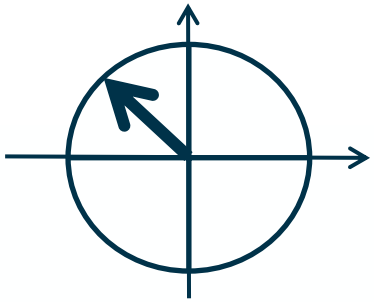

Flight 3

TomoSAR focusing – examples

$$I_n(r,x) = \int_C s(r,x,v) \cdot exp\left\{-j\frac{4\pi}{\lambda}\frac{b_n}{r}v\right\} dv$$

$$\hat{s}(r,x,v) = \sum_n I_n(r,x)\exp\left(+j\frac{4\pi}{\lambda r}b_n v\right)$$

Case 1: one point target

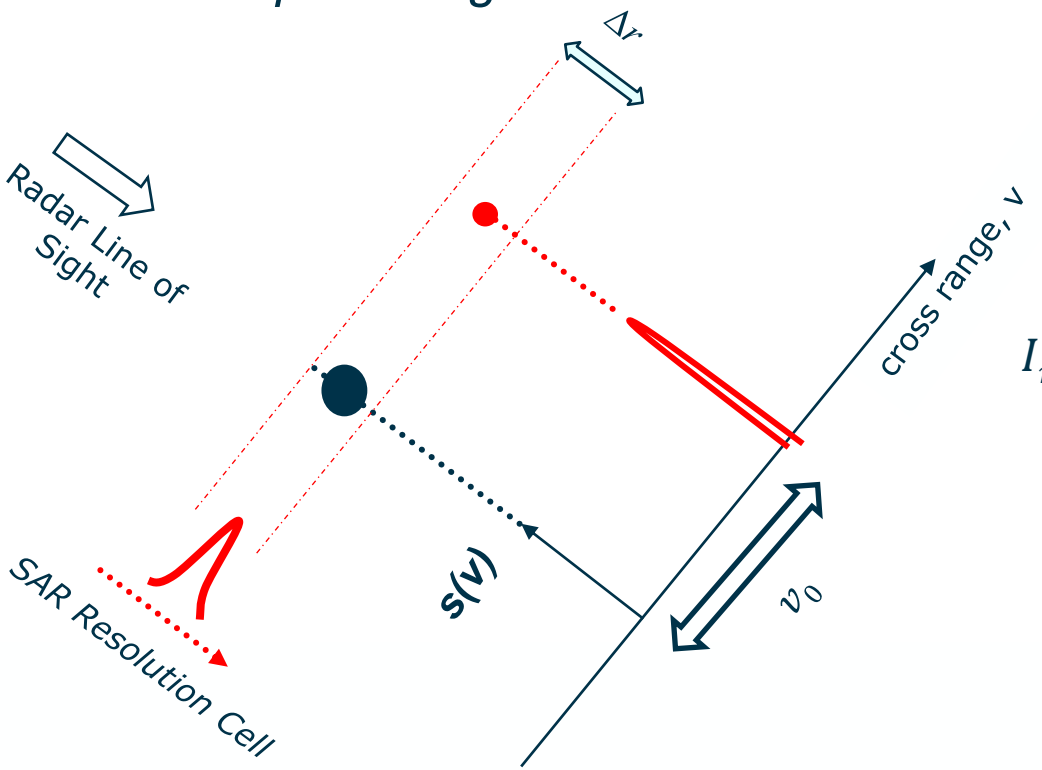

$$I_n(r,x) = s_0 \cdot exp\left\{-j\frac{4\pi}{\lambda}\frac{b_n}{r}v_0\right\}$$

● = reference position

TomoSAR focusing – examples

$$I_n(r,x) = \int_C s(r,x,v) \cdot exp\left\{-j\frac{4\pi}{\lambda}\frac{b_n}{r}v\right\} dv$$

$$\hat{s}(r,x,v) = \sum_n I_n(r,x)\exp\left(+j\frac{4\pi}{\lambda r}b_n v\right)$$

Case 1: one point target

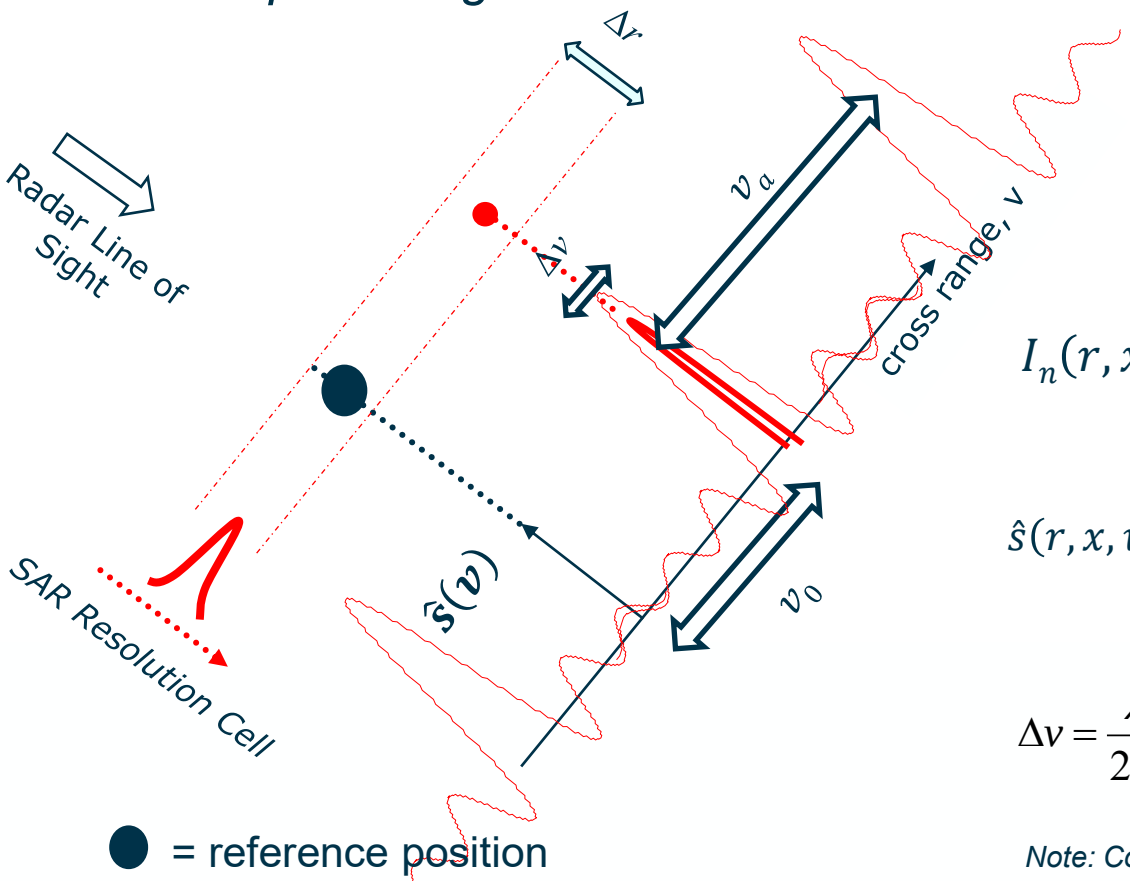

$$I_n(r,x) = s_0 \cdot exp\left\{-j\frac{4\pi}{\lambda}\frac{b_n}{r}v_0\right\}$$

$$\hat{s}(r,x,v) = s_0 \cdot \sum_{k=-\infty}^{+\infty} sinc\left(\frac{v - v_0 - kva}{\Delta v}\right)$$

$$\Delta v = \frac{\lambda r}{2b_{ap}} \qquad v_a = \frac{\lambda r}{2\Delta b}$$

Note: Constant amplitude factors omitted

Baseline design

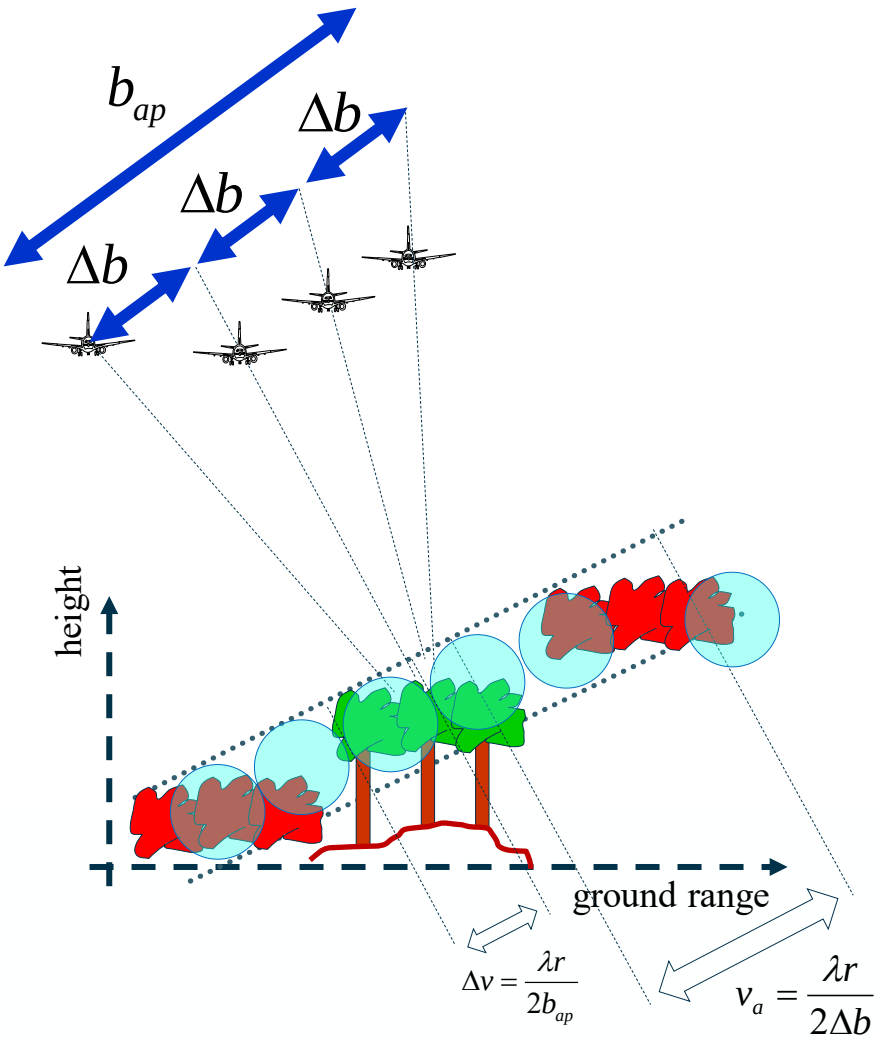

Baseline design tips

- Ambiguity ⇔ baseline spacing
- Resolution ⇔ baseline aperture

⇒ Baseline spacing: small enough to ensure that ambiguous targets stay away from the real ones

⇒ Baseline aperture: large enough to meet resolution requirement

⇒ How many passes ?

$$N \geq \frac{b_{ap}}{\Delta b} = \frac{v_a}{\Delta v}$$

Projection in height

TomoSAR forward model

$$I_n(r,x) = \int_C s(r,x,v) \cdot exp\left\{-j\frac{4\pi}{\lambda}\frac{b_n}{r}v\right\}dv$$

$I_n(r,x)$: SLC pixel in the *n-th* image

$s(r,x,v)$: cross-range projection of target reflectivity within the SAR resolution cell at (r,x)

b_n : normal baseline for the *n-th* image

λ : carrier wavelength

Change of variable from cross range to height

$$z = v \cdot \sin\theta$$

$$I_n(r,x) = \int_C s(r,x,z) \cdot exp\{-jk_z(n)z\}dz$$

k_z is usually referred to as **vertical wavenumber** or **phase to height conversion factor**

$$k_z(n) = \frac{4\pi}{\lambda r}\frac{b_n}{\sin\theta}$$

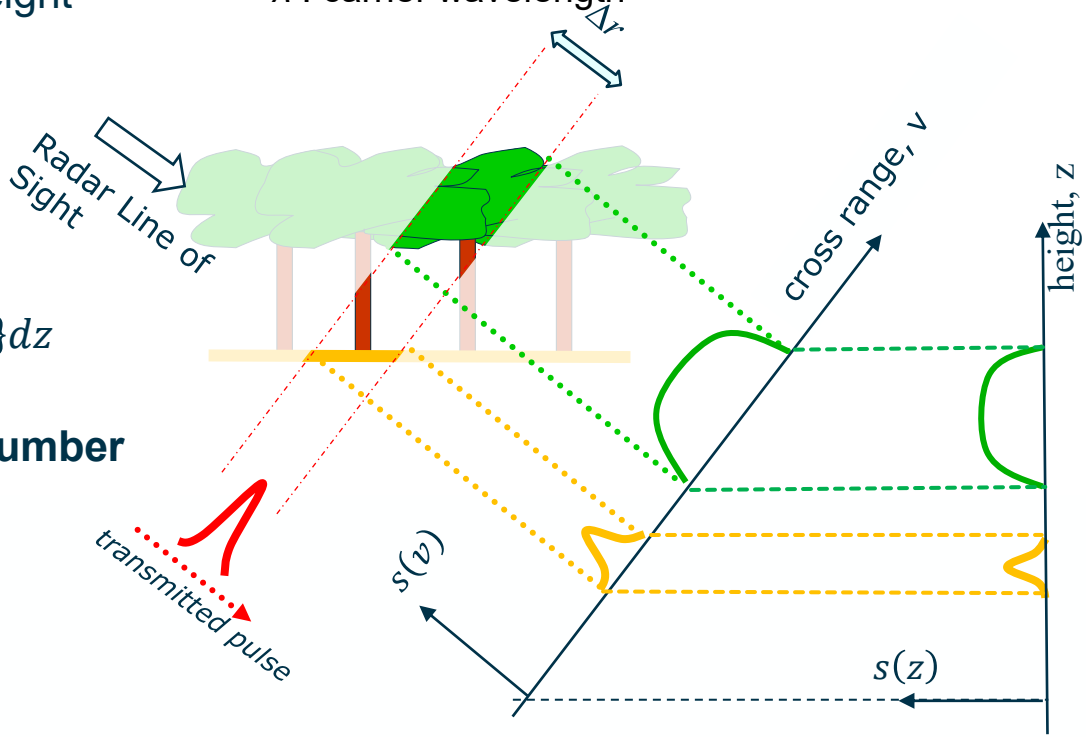

Terrain flattening

$$I_n(r,x) = exp\left\{-j\frac{4\pi}{\lambda}R_n(ref)\right\} \cdot \int_C s(r,x,v) \cdot exp\left\{-j\frac{4\pi}{\lambda}\frac{b_n}{r}v\right\} dv$$

Phase offset to be removed based on knowledge of the acquisition geometry (terrain flattening)

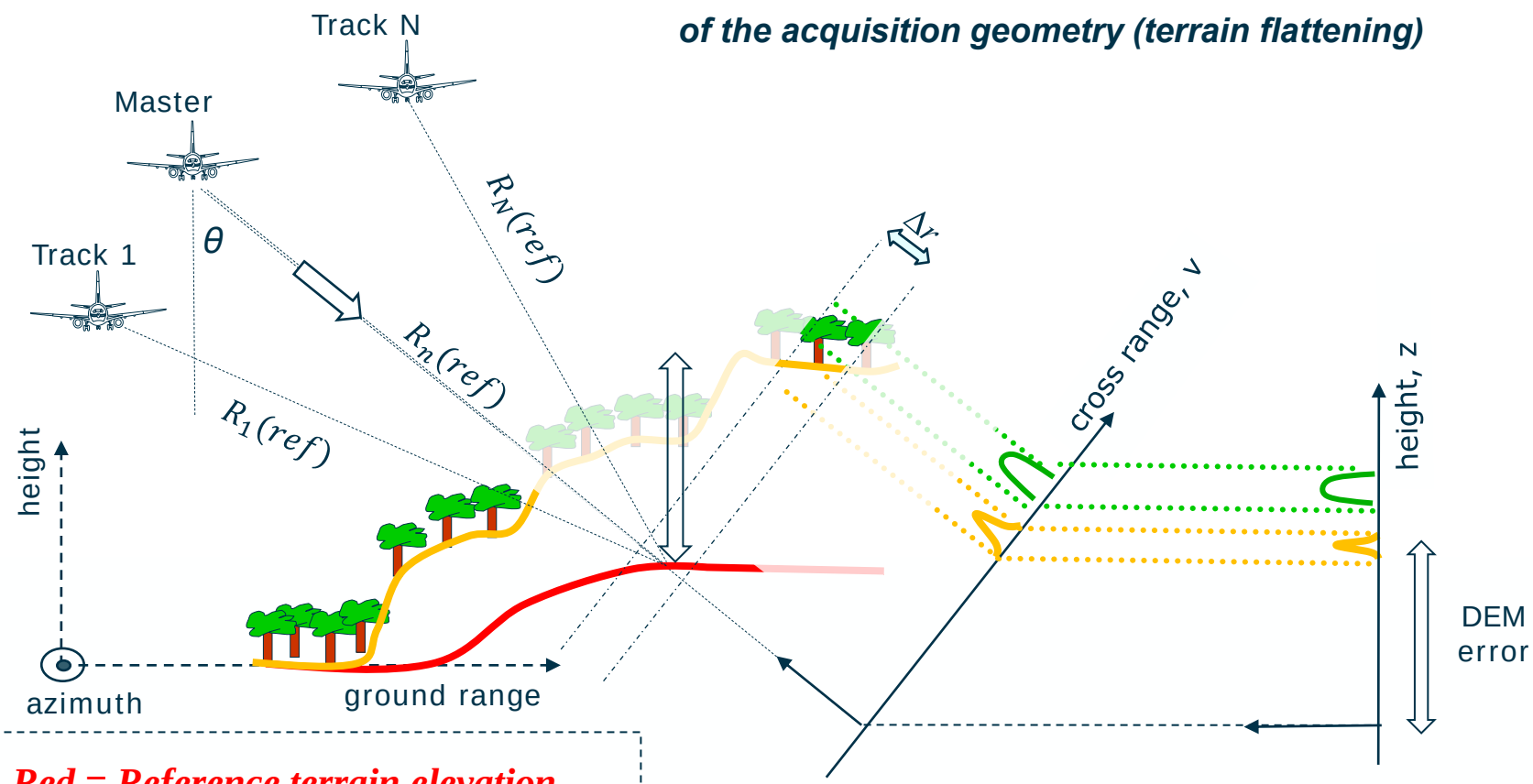

Red = Reference terrain elevation

Orange = True terrain elevation

Terrain flattening

$$I_n(r,x) = exp\left\{-j\frac{4\pi}{\lambda}R_n(ref)\right\} \cdot \int_C s(r,x,v) \cdot exp\left\{-j\frac{4\pi}{\lambda}\frac{b_n}{r}v\right\} dv$$

Phase offset to be removed based on knowledge of the acquisition geometry (terrain flattening)

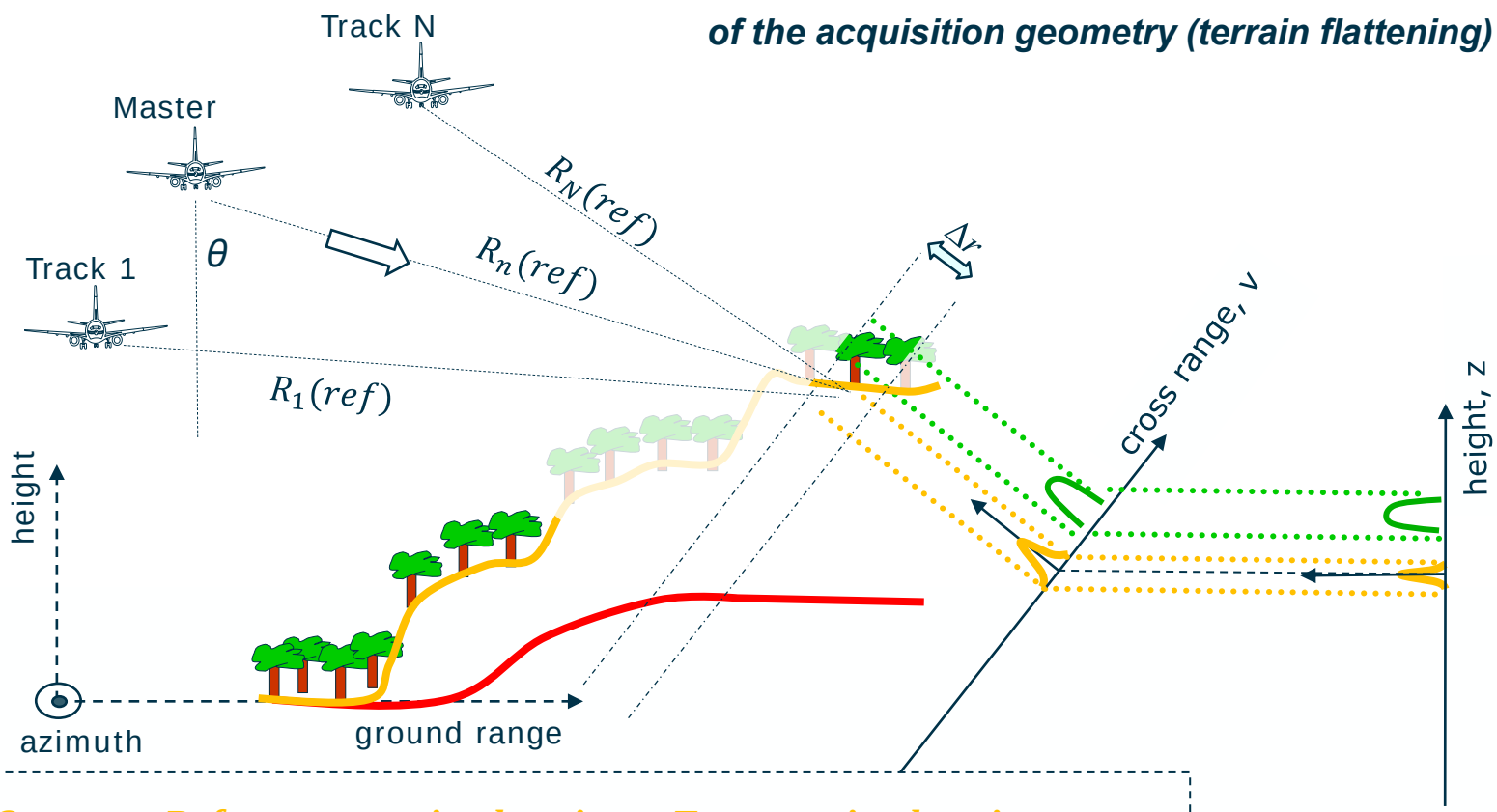

Orange = Reference terrain elevation = True terrain elevation

Current paradigm for forested areas: **retrieve the *vertical distribution of backscattered power* based on the observed *InSAR coherences***

SLC data

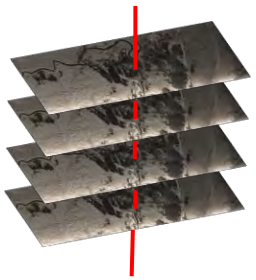

Complex data vector (Nx1)

$$\mathbf{d} = \begin{bmatrix} d_1 \\ d_2 \\ \vdots \\ d_N \end{bmatrix}$$

Coherence estimation (spatial multilooking)

$$\gamma_{nm} = \frac{\langle d_n d_m{}^* \rangle_L}{\sqrt{\langle |d_n|^2 \rangle_L \langle |d_m|^2 \rangle_L}}$$

Coherence matrix (NxN)

$$\mathbf{R} = \begin{bmatrix} 1 & \gamma_{12} & \cdots & \gamma_{1N} \\ \gamma_{21} & 1 & & \\ \vdots & & \ddots & \vdots \\ \gamma_{N1} & & \cdots & 1 \end{bmatrix}$$

TomoSAR processing

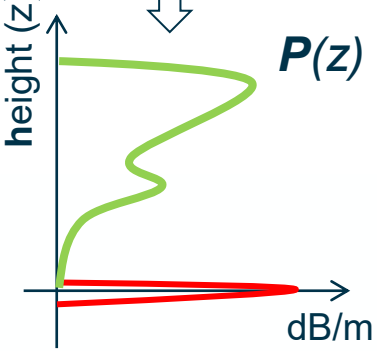

Why?

⇒ ***Improved performance by using Spectral Analysis***

- **Super-resolution** (super = finer than the limit from baseline aperture)
- **Side-lobe rejection**
- **Rejection of ambiguous targets** (using irregular baseline spacing)